Wolf Creek Cold Regions Model Set-up, Parameterisation and Modelling Summary

Centre for Hydrology Report No. 8

John Pomeroy, Centre for Hydrology, University of Saskatchewan, Saskatoon
Olga M. Semenova, State Hydrological Institute, St. Petersburg, Russia
Xing (Logan) Fang, Centre for Hydrology, University of Saskatchewan, Saskatoon
Yuri B. Vinogradov, State Hydrological Institute, St. Petersburg, Russia
Chad Ellis, Centre for Hydrology, University of Saskatchewan, Saskatoon
Tatyana A. Vinogradova, Saint Petersburg State University, Russia
Matt MacDonald, Centre for Hydrology, University of Saskatchewan, Saskatoon
Elena E. Fisher, B.V. Sochava Institute of Geography, Irkutsk, Russia
Pablo Dornes, Centre for Hydrology, University of Saskatchewan, Saskatoon
Ludmila Lebedeva, Saint Petersburg State University, Russia
Tom Brown, Centre for Hydrology, University of Saskatchewan, Saskatoon

Centre for Hydrology, University of Saskatchewan, Saskatoon, Canada and
State Hydrological Institute, Saint Petersburg, Russia.

Wolf Creek Cold Regions Model Set-up, Parameterisation and Modelling Summary

Centre for Hydrology Report No. 8

1.0 Executive Summary

Wolf Creek Research Basin is in the Upper Yukon River Basin near Whitehorse, Yukon and is representative of headwaters in the northern Coast Mountains. It was established in 1993 to better develop northern hydrological models, and related hydrological process, ecosystem and climate science. Yukon Environment maintains Wolf Creek hydrometeorological and hydrometric stations and conducts regular snow surveys in the basin. A number of hydrological models have been tested on Wolf Creek and all have had great difficulty in simulating the cold regions hydrological processes that dominate its streamflow response to snowmelt and rainfall events. Developments in understanding hydrological processes and their interaction with terrestrial ecosystems and climate at Wolf Creek have lead to the development of the Cold Regions Hydrological Model (CRHM) by a consortium of scientists led by the University of Saskatchewan and Environment Canada. CRHM comprehensively incorporates the blowing snow, intercepted snow, sublimation, melt energetics, infiltration to frozen soils, organic terrain runoff and other cold regions hydrological phenomenon and discretizes the catchment on a hydrological response unit basis for applying water and energy balance calculations. The model is intended for prediction of ungauged basins with parameter selection from physically measurable properties of the river basin or regional transference of calibrated values. In Russia, a long tradition of cold regions hydrological research has led to the development of the Hydrograph model by the State Hydrological Institute, St. Petersburg. The Hydrograph model contains several promising innovations regarding the formation and routing of runoff, discretizes the basin using hydrological response units and addresses some (but not all) cold regions hydrological processes. Hydrograph parameter selection is made from both physically measured properties and those that are calibrated, but the calibrations can be easily regionalized.

Test simulations of runoff processes using CRHM and Hydrograph for Wolf Creek Research Basin was undertaken using data archives that had been assembled and cleaned up in a related project by the University of Saskatchewan. The test simulations are a demonstration of model capabilities and a way to gain familiarity with the basin, its characteristics and data and to better compare model features. Data available included a GIS database of basin characteristics (topography and vegetation distribution) and the hydrometeorological and hydrometric observational dataset from Yukon Environment. Basin physical parameters were selected from the extensive field research literature available on Wolf Creek. Both CRHM and Hydrograph were set up on Wolf Creek and parameterised for forest, alpine and shrub tundra hydrology zones; CRHM was also set up for the Granger Sub-basin of Wolf Creek to test the alpine and shrub tundra hydrology parameterisations in detail. CRHM was run without parameter calibration and was able to reproduce the basic patterns of snow accumulation, melt and runoff with reasonable water balance reproduction in all environments. This was the first complete physically-

based simulation of a cold regions water cycle (blowing snow, intercepted snow, melt, infiltration to frozen soils, runoff) conducted in the Yukon. With calibration the CRHM runs could be further improved and with more basin information the routing aspects can be run using physical characteristics of the basin. Hydrograph was set up with some manual parameter calibration from streamflow where parameters were relatively unknown. This was the first application of Hydrograph to the Canadian North and certain similarities were noticed between Yukon and east Siberian hydrology. The sub-surface hydrology presented a formidable unknown in parameterising the model. Hydrograph performed well in initial simulations of the basin hydrograph for multi-year runs. Several issues with observational data quality created substantial uncertainty in evaluating the model runs.

The results presented in this report should be considered to be preliminary, given the incompleteness of the data required to run the model with directly observable parameters. Both modelling groups will continue to refine the information to take advantage of the best characteristics of the CRHM and Hydrograph models, namely their ability to use parameters that are obtained directly from field observations. The next steps in this project are to use the models in a complementary manner for process representation, parameter estimation and routing so that hydrological modelling can be developed and improved for the Upper Yukon Basin. It is essential that this research be supported to develop over a longer term than this short scoping study, so that the benefits of collaboration between the Canadian and Russian groups with Wolf Creek as the nexus, can be fully realised into a suite of improved cold regions hydrological models that can be run with confidence over large and small basins in the North.

1.1 Background

The Wolf Creek Research Basin was established in 1993 to carry out water related studies. Since that time the project has evolved into an integrated, multidisciplinary research project which includes studies of climate and climate change, vegetation, forestry, fisheries and wildlife. Ongoing research activities have continued over the years with more than 30 separate research and monitoring projects completed or under way by numerous universities and government agencies. The research basin has a number of hydrometeorological stations distributed through three distinct ecosystems (boreal forest, subalpine taiga and alpine tundra). The diversity of the watershed, combined with the available long term comprehensive hydrometeorological data, is responsible for the popularity of Wolf Creek as a site to carry out cold regions research by scientists from across Canada and abroad. The data availability and diversity also makes Wolf Creek an ideal location for watershed modeling activities. Yukon Water Resources is in the process of updating its flood forecasting model for the upper Yukon River basin. This is required due to increases in flooding in recent years associated with climate warming and increased glacier melt. The objectives of the study are to adapt a cold regions hydrological model for the upper Yukon River basin. Two cold regions models have been set up and parameterised for use at Wolf Creek - the Cold Regions Hydrological Model (CRHM) developed by the University of Saskatchewan and the Hydrograph model developed by the State Hydrological Institute in St. Petersburg, Russia. CRHM contains detailed cold region process descriptions whilst Hydrograph has parametric descriptions of many cold regions processes. Routing components of CRHM have been tested on basins of 400 km^2 or less whilst Hydrograph routing has been tested on very large basins. The ultimate objective of the project is to combine aspects of Hydrograph routing routines and CRHM physics, initially run at Wolf Creek and ultimately upscale to the upper Yukon River basin, to be used for flow forecasting and climate change assessments. An additional goal of this work is to communicate the history and recent developments in modelling activities in Wolf Creek and their role in helping to address gaps in knowledge that will help water managers take effective actions, as well as assist decision makers in responding to climate change.

1.2 Objectives

The objectives of this study are to summarize hydrological modelling work undertaken to date in Wolf Creek, and then to set up and parameterise the CRHM and UHM models at Wolf Creek and assess the capabilities and uncertainties of the respective models.

1.3 Structure of Report

1.0 Executive Summary
- 1.1 Background
- 1.2 Objectives
- 1.3 Structure

2.0 Hydrological Modelling Relevant to Wolf Creek
- 2.1 Cold Regions Hydrology and Hydrological Processes
- 2.2 Review of Hydrological Modelling
- 2.3 Modelling Review Conclusions
- 2.4 Modelling Review References

3.0 Cold Regions Hydrological Model Description and Tests in Wolf Creek
- 3.1 Preparing the Cold Regions Hydrological Model for Wolf Creek
- 3.2 Initial Tests of CRHM in Wolf Creek
- 3.3 Conclusions for CRHM Tests
- 3.4 CRHM Modelling References

4.0 Introduction to the Hydrograph Model
- 4.1 Model Description
- 4.2 Results
- 4.3 Conclusions
- 4.4 Hydrograph Modelling References

5.0 Conclusions

6.0 Complete References for Wolf Creek Hydrology

2.0 Hydrological Modelling Relevant to Wolf Creek

This section is a brief review of hydrological modelling work undertaken to date in Wolf Creek in the context of hydrological modelling with a special emphasis on cold regions hydrology and modelling issues. The review discusses the key modelling studies conducted and their major findings, as well as the role of past and current modelling work in advancing our understanding of changing hydrological regimes in the broader Yukon River system. The report starts by reviewing the literature pertinent to cold regions hydrology focusing on the description of the hydrological processes controlling snow-cover ablation and snowmelt runoff, and on the simulation techniques that have been done to date. It then details the Cold Regions Hydrological Model as relevant to Wolf Creek and makes conclusions on the results of recent modelling in the basin. A final reference list of all hydrology studies pertaining to Wolf Creek is appended to the back of the report.

2.1 Cold Regions Hydrology and Hydrological Processes

Wolf Creek is a cold regions basin, typical of many in northern Canada. The northern part of Canada and other high latitude regions are characterised by their extreme seasonal radiation regimes, with negative radiation balances in the winter period, that combined with freezing temperatures and snowfall as the principal component of the annual precipitation, results in snow-covers that often last over half year (Woo et al., 2005). These snow dominated environments have a strong influence on the generation and dynamics of snowmelt runoff and on atmospheric processes as a result of energy balance considerations. Therefore, an improved understanding of the snow related processes during the snow, frozen soil, and permafrost hydrology is essential not only for scientific interests but also for practical aspects such as water management and for the quantification of the potential changes under future global warming scenarios.

2.1.1 Snow accumulation processes

A detailed understanding of the seasonal and spatial variations of snow accumulation within a basin is substantial for the winter water budget and is a key issue to reduce uncertainties in modelling snow-cover ablation and snowmelt runoff. Estimation of snowfall is particularity challenging. The properties and characteristics of fallen snow change as a function of energy fluxes, wind, moisture, water vapour, and pressure (Singh and Singh, 2001). Measurements of snowfall precipitation are strongly affected by wind. Therefore, windshields are usually set up around the snow gauges to improve snow deposition. The standard snow gauge used in Canada was the MSC Nipher Shielded Snow Gauge System. This gauge consists in a hollow metal cylinder, 560 mm long and 127 mm in diameter, surrounded by a solid shield with the shape of an inverted bell. This instrument, designed to collect solid and liquid precipitation, proved to be a very reliable gauge. However, since it should be manually operated, its application in northern cold regions was restricted to locations with safe accessibility. Further, the installation of these gauges within a basin was usually limited to open areas which resulted in inaccurate estimates of the spatial variability of the snow-cover. Since the determination of an adequate precipitation data is an essential factor in the calculation of the mass balance for a given basin, efforts to reduce the uncertainty in the spatial variability of the snow

accumulation patters have been focused in the identification of land use or landscape units where basin snow surveys are conducted (Woo and Marsh, 1978). Similar approaches were used in the arctic and subarctic research programs such as in Trail Valley Creek and Wolf Creek where extensive snow transects in representative landscape units are regularly surveyed by measuring snow depth and density.

Snow accumulation is a scale dependent process. At large or regional scales the spatial variability of snow-cover is affected by latitude, elevation, orography, and the presence of large water bodies. At mesoscales (100 m to 10 km), patterns in snow accumulation are governed by topography (i.e. relief features) and vegetation cover, whereas at microscales variations in air flow patterns and interception are responsible for the spatial variability in the accumulation patterns (Pomeroy and Gray, 1995). Differences in snow accumulation are the result of interception, sublimation, and redistribution processes (Gray and Pomeroy, 1995).

In open environments such as alpine and tundra areas, thinner end-of-winter snow-covers are expected in low vegetated, and exposed windswept areas as result of the redistribution of snow by wind given the relatively low surface roughness of these areas. Conversely, deeper snow-covers are observed in sheltered sites due to the presence of leeward slopes, topographic depressions and denser and taller shrub areas that reduce snow transport processes facilitating the deposition of the blowing snow. Estimation of the blowing snow, transport, and sublimation effects over the accumulation period for open environments led to the development of the Prairie Blowing Snow Model (PBSM; Pomeroy et al., 1993). This model uses a physically-based approach to calculate transport and sublimation rates for blowing snow given measurements of air temperature, humidity and wind speed. Applications of this model are described in Pomeroy and Li (2000). Distributed numerical simulations of snow transport and sublimation using a simplified version of PBSM at the landscape scale in a low-arctic tundra environment (Essery et al., 1999) showed the importance of the inclusion of sublimation to accurately simulate late-winter accumulations. Essery and Pomeroy (2004a) also showed for the same environment that distribution of vegetation was a key factor in describing snow-cover patterns, as shrubs act as trapping blowing snow from open areas. They found that the amount of snow held by shrubs was proportional to the shrub height until a given threshold determined by the supply of snow decreasing its spatial variability. Similarly, an increase in shrub density led to a decrease in the spatial variance of the snow accumulation pattern. Since topographic effects were less dominant, presumably due to the low relief, aggregated simulations successfully described the control of the vegetation on snow redistribution.

Forest environments on the other hand, show a spatially more homogeneous snow accumulation pattern. Boreal forests mainly consist of evergreen coniferous trees that intercept a large proportion of annual snowfall. This intercepted snow may sublimate or release to the ground. Field observations from boreal forests showed that 30% to 45% of annual snowfall sublimates as a result of its exposure as intercepted snow (Pomeroy and Gray, 1995; Pomeroy et al., 1998a; Lundberg and Halldin, 2001). Sublimation reduces the snow available for accumulation. Compared with snow on the ground, snow

sublimates quicker in forest canopies because of greater absorption of short-wave radiation by the canopy and a higher exposure to turbulent-exchange forces (Lundberg et al., 2004). Forest canopy is important in controlling the interception-sublimation process (e.g. Kuz'min, 1960; Pomeroy and Gray, 1995; Pomeroy et al., 2002). Hedstrom and Pomeroy (1998) and Pomeroy et al. (1998a) showed that an increase in the leaf area index (LAI) resulted in a decreasing snow accumulation. Observations showed that interception efficiency of the canopy is particularly sensitive to snowfall amount, canopy density and time since snowfall. Thus, interception efficiency decreases with increasing snowfall, time since snowfall, and initial canopy snow load. Base on those observations, a physically based model was developed to calculate snowfall interception from meteorological data and forest properties (Hedstrom and Pomeroy, 1998).

These results also suggested that differences between forest stands and clear-cuts are due to interception and sublimation processes in the forest canopy rather than redistribution of the snow intercepted in the canopy. Results from several boreal forest stands (Pomeroy et al., 2002) showed that the ratio of forest to clearing snow accumulation declined from values near 1 to near 0.5 as LAI and canopy increased. Pomeroy et al. (1998b) and Faria et al. (2000) found that the snow accumulation mass follows a log normal distribution within forests stands and that pre-melt variance of SWE within boreal forest stands increases with increasing canopy density. In conclusion, since most of the forested catchments are covered by a mosaic of clearings and stands of varying density, the knowledge of the variations in the seasonal and spatial patterns of snow accumulation and the relation between distributions of forest properties such as LAI and snow accumulation, are essential for catchment-scale predictions of snow accumulation and melt.

2.1.2 Snow ablation processes

Snowmelt is the most significant hydrological in arctic and subarctic environments process since spring snowmelt freshet is usually the largest runoff event of the year. The snowmelt period is characterised by complex and dynamic processes resulting in rapid changes in albedo, turbulent fluxes, internal snow energy, and surface temperature as the snow-cover is depleted. These changes have drastic effects on the surface-atmosphere exchanges (Pomeroy et al., 1998b). Most studies of arctic and subarctic snowmelt hydrology have focused upon process descriptions including dynamics of snowpack percolation (e.g. Marsh and Woo, 1984a and b), canopy interception and sublimation (e.g. Pomeroy et al., 1999), canopy effects on radiation (e.g. Sicart et al., 2004; Bewley et al., 2007), snow advection (e.g. Liston et al., 1995, Neumann et al., 1998), infiltration, soil storage and runoff (e.g. Kane et al., 1991; Carey and Woo, 1999; Carey and Quinton, 2005). Recent research however, has been focusing in the substantial variability of the snow ablation processes and interactions with the landscape, and their effects on snowmelt runoff (e.g. Marsh and Pomeroy, 1996; Pomeroy et al., 2003; Janowicz et al., 2004, Pomeroy et al., 2006, McCartney et al., 2006).

The typical approach used to calculate snow melt energy of a snow-pack at point scales is based on the reference to a unit control volume (Male, 1980). Thus, the energy available for melt, Q_M ($W \cdot m^2$) is:

$$Q_M = K^* + L^* + Q_E + Q_H + Q_D + Q_G - \frac{dU}{dt} \quad (1)$$

where K^* is the net shortwave radiation to snow ($W \cdot m^2$), L^* is the net longwave radiation to
snow ($W \cdot m^2$), Q_E is the latent heat flux from the surface due to sublimation ($W \cdot m^2$), Q_H is the sensible heat flux to the atmosphere ($W \cdot m^2$), Q_D is the energy transported to the snowpack by precipitation ($W \cdot m^2$), Q_G is the conducted heat flux from the ground ($W \cdot m^2$), and dU/dt is the change of internal energy of the snowpack over time t.

The melt rate dM/dt of the dry snow mass M ($kg \cdot m^2$) is governed by the available snowmelt energy flux and interactions between liquid in the snowpack, sublimation, and mass of precipitation (Pomeroy et al., 2003) and can be expressed as:

$$\frac{dM}{dt} = \frac{Q_F - Q_M}{\lambda_f} - \frac{Q_E}{\lambda_s} + d \quad (2)$$

where Q_F is the energy associated with freezing of liquid in the snowpack, λ_f and λ_s are the latent heat of fusion and sublimation respectively ($J \cdot kg^{-1}$), and d is the mass of deposited snow and rain equal to precipitation rate p ($kg \cdot m^2 \cdot s^1$) minus blowing snow erosion ($\nabla \cdot T$), expressed as the divergence,∇, of the horizontal transport rate, T, ($kg \cdot m^1 \cdot s^1$).

Melt can occur when the snowpack, induced by energy inputs, warms to the isothermal condition (°C=0). Once the snowpack is isothermal, additional energy inputs will result in phase change from solid to liquid. However, melt can also occur in cold snowpacks when surface meltwater drains through the cold interior snowpack via preferential flow paths (Marsh and Woo, 1984 *a* and *b*; Marsh and Pomeroy, 1996). Limitation to this approach arise as a result of highly variable processes governing the available snow melt that violate the assumptions behind the snowmelt energy calculations such as uniform surface and large fetch requirements for steady-state.

As discussed in the previous section, several studies described the importance of the premelt snow-cover conditions in governing the rate of snowmelt. Pomeroy et al. (2004) described the implications of the spatial distribution of snow-cover and melt rates that need to be considered for an appropriate description of the snow-cover depletion in subarctic environments. In agreement with Faria et al. (2000), they found that the log-normal frequency distribution may be used to describe pre-melt spatial distribution of SWE in a complex tundra terrain. Although, a slope class differentiation was suggested. Within-class variability of pre-melt SWE was further grouped into windswept tundra and sheltered tundra-forest regimes. However in all sites, the log-normal fit of observed SWE degraded progressively during melt as a result of the spatially variable melt rate. Observations showed that the spatial variability and covariability between initial SWE and melt rates is scale and landscape dependent. At small scales (<100 m) negative correlation between initial SWE and melt rate was observed in those areas where shrubs were exposed above snow. This negative association was not observed in forest or dipper drifted snow over short vegetation. Similarly, at medium scales a negative correlation

was also found between adjacent landscape units likely due to the differential insolation and accumulation regimes between plateaus and slopes. At larger or basin scales, the association between landscape-class initial SWE and melt rate turned positive due to the variability in snow redistribution and interception processes amongst the different landscapes (i.e. forest, shrub tundra, and alpine). Thus, the combined effect of low SWE and melt rate in alpines areas, larger SWE and melt rates in shrub areas, and low SWE and melt rates in forest areas, resulted in most of the studied years in an positive association with an initial deceleration and later acceleration of snow cover area (SCA) compared with a monotonic snow depletion.

Studies stressing the importance of the spatial variability of the available snow melt energy in arctic and subarctic environments have highlighted the effects of topography, vegetation, local advection, and importance of the initial conditions on the dynamic of the snowmelt processes. Marks et al. (2001, 2002) showed that in mountain catchments, vegetation and topography could account for patterns of snow deposition, sublimation, melt, and runoff generation. They conclude that snow drift areas represent only a small portion of mountain catchments, but hold a significant portion of catchment SWE; and that windswept areas may account for a large part of catchment area, but hold relatively little catchment SWE. Pomeroy et al. (2003) re-examined the snowmelt calculations to slopes and found substantial differences in energetics and rates of snow ablation over shrub–tundra surfaces of varying slope and aspect. Incoming solar radiation on north facing (NF) and south facing (SF) slopes varied with cloudiness conditions. On sunny days, the values on the SF were substantially higher that on the NF, whereas smaller differences were observed on cloudy days, showing thus that cloudiness plays a dominant role driving the spatial variability of melt. These differences in solar radiation on NF and SF slopes initially caused small differences in net radiation in early melt. However, as shrubs and bare ground emerged due to faster melting on the SF slope, the albedo differences resulted in large positive values of net radiation to the SF, whilst the NF fluxes remained negative.

The presence of shrubs was demonstrated to have important influences on controlling both snow accumulation and ablation regimes (Liston et al., 2002). Observations and modelling results in blowing snow transport in arctic and subarctic environments showed that in general the greatest accumulations in shrub tundra were associated to the presence of nearby open areas acting as a source of snow transport and due to exposure nature of shrubs that reduced the aerodynamics roughness rather than the density or high of the shrubs, the e (Pomeroy and Gray, 1995; Essery and Pomeroy, 2004a). Pomeroy et al. (1997) found that shrub tundra accumulated four to five times more snow than sparsely vegetated tundra. Sturm et al. (2001) showed that the presence of tall shrubs influences the surface albedo over the melt season and increases snowmelt rates. Pomeroy et al. (2006) described the importance of shrub exposure in governing snowmelt energy; in general, shrub exposure enhanced melt energy due to greater longwave and sensible heat fluxes to snow.

McCartney et al. (2006) observed that the high snow accumulation in tall shrubs in Wolf Creek basin plays a key role in controlling the timing of the snowmelt streamflow regime.

The effects on snowmelt rates and extinction of solar radiation due to shrub canopy were examined by Bewley et al. (2007). They developed a model to simulate the effective transmission and reflectance of shortwave radiation from a discontinuous shrub canopy over a melting snowpack. The inclusion of shaded canopy gaps improved the diurnal simulation of shortwave transfer with respect to simple radiative transfer models. Results were consistent with available observations while there are still uncertainties in the validity of the areal albedo and transmissivity values due to the lack of observation at larger scales.

2.1.3. Snowmelt runoff

Snowmelt runoff is often the dominant streamflow event in arctic and subarctic environments. In northern mountain areas surface energetics vary with receipt of solar radiation, vegetation cover, and initial snow accumulation. Therefore the timing of snowmelt is controlled by aspect, presence of shrubs or forest, and redistribution of winter snow by wind.

Several factors control the runoff generation processes in northern cold regions (Carey and Quinton, 2005):
(1) snowmelt runoff is the dominant hydrological event,
(2) the presence of permafrost restricts deep drainage due to near-surface water tables (Quinton and Marsh, 1999; Carey and Woo, 2001a),
(3) infiltration into frozen soils can potentially impede or reduce vertical soil drainage modifying the contribution of runoff water to stream flow (Janowicz, 2000; Gray et al., 2001, McCartney et al., 2006),
(4) the presence of an organic layer overlaying the mineral soils increase the subsurface flow when water tables reside within this upper soil layer (Quinton et al., 2000; Carey and Woo, 2001a);
(5) the presence of soil pipes provides a preferential bypass flow mechanism that could led to higher subsurface flows (Carey and Woo, 2000), and
(6) the presence of earth hummocks increases the time for runoff water to reach the stream due to the tortuosity of the inter-hummock channels (Quinton and Marsh, 1998).

The effects of meltwater percolation on the timing and volume of water availability for runoff were studied in different landscapes in an arctic environment (Marsh and Pomeroy, 1996). It was demonstrated using a the percolation model of Marsh and Woo (1984b) that the meltwater percolation through the snowpack controls the timing of the meltwater release being available for infiltration to frozen soil or runoff approximately six days after the start of melt. The initial release of meltwater first occurred on the shallow upland tundra sites, whereas there was a delay of nearly two weeks in the deep snow drifts. Variability in the initial snow-cover conditions and between landscapes resulted in differential delays. Thus, the delays between the initiation of melt and arrival of meltwater at the base of the snowpack varied from 6 days for 0.45 m deep snow at tundra sites, to 10 days for 1.85 m deep snow at drift sites. Spatially, the lag between melt and runoff showed a gradual behaviour. For example, for 19 May of the 1993 snowmelt season, the tundra areas (70 % of the basin) were fully contributing meltwater,

the shrub tundra areas (22% of the basin) were partially contributing meltwater, while the drift areas (8% of the basin) were not contributing any meltwater.

Runoff generation differs widely between the slopes; there is normally no spring runoff generated from SF slopes as all meltwater evaporates or infiltrates. In contrast, on NF slopes usually capped by an organic layer and underlain by permafrost, vertical drainage quickly led to saturation of the frozen organic layer since the high ice-content at the organic-mineral interface prevents deeper drainage. This impounded infiltration within the organic layer results in surface runoff in rills and gullies, and subsurface runoff along pipes and within the matrix of the organic soil (Carey and Woo, 1999).

Snowmelt infiltration into frozen mineral soils is a complex process where heat and water transport in soils is governed by soil temperature, antecedent conditions, and the amount and rate of meltwater release (Gray et al., 2001). Granger et al. (1984) distinguish frozen soils into three broad categories according to their infiltration potential:
(1) restricted, where water entry is impeded by surface conditions. Infiltration is thus negligible and melt goes directly to runoff,
(2) limited, where infiltration is governed primarily by the SWE and the frozen water content of the top 30 cm of soil, and
(3) unlimited, where gravity flow dominates meltwater infiltration.
In this case runoff is negligible, so infiltration equals SWE. For limited infiltrability, cumulative infiltration is expressed as a function of saturation moisture content at the soil surface, total soil saturation (water and ice) and average soil temperature for the 0.4 m soil layer at the start of infiltration, and a factor representing the infiltration opportunity time. Applications of this parametric correlation approach for estimating snowmelt infiltration into frozen soils showed an reasonable agreement between observed and modeled values in level forest, subarctic and prairie soils (Zhao and Gray, 1999; Janowicz, 2000; Gray et al., 2001).

Organic soils on the other hand, often facilitate infiltration due to their high porosity and low winter moisture content. However the different combination of organic and mineral materials results in different flow mechanisms. Typically northern soils are capped by an organic layer. This layer tends to be thicker over permafrost sites such as north-facing slopes and valley bottoms. During snowmelt, meltwater infiltrates and percolates the frozen organic layer. Deep percolation is limited at the organic-mineral interface as a result of the low porosities and trasmissivities of the mineral soils, resulting in a perched saturated zone that prompts lateral flow (Carey and Woo, 1999).

Overland flow and lateral or subsurface flow in the organic layer are collectively termed as quick flow. This hillslope runoff can include flow in rill and gullies, along soil pipes, and within the organic matrix (Carey and Woo, 2000). Slopes with a continuous and thicker organic cover experience little or no overland flow due to both a large water storage capacity and an eventual frozen or unfrozen infiltration rate which exceeds the rate of input from snowmelt or rainfall (Quinton and Marsh, 1999). In this case, subsurface flow dominates resulting in higher water table levels in the organic layer near the stream, whereas in the upslope areas the water table often falls into the low

conductivity mineral soils. Thus, estimation of subsurface flow from organic-covered hillslopes underlain by permafrost requires that the elevation of the saturated layer be known, since the saturated hydraulic conductivity of the organic material decreases exponentially with depth (Quinton et al., 2000). Lateral flow in the organic soil predominates early in the thaw period while the water table still remains in the organic soil. Following this period, water movement tends to be mainly vertical, between the ground surface and the underlying mineral sediment (Quinton et al., 2005). A special case of lateral flow in arctic environments is the preferential subsurface flow from hillslopes through peat-filled inter-hummock channels. Quinton et al. (2000) found that flow is conveyed predominately through the peat of the inner-hummock areas due to the large contrast in hydraulic conductivity with the mineral hummocks. Quinton and Marsh (1999) also suggested that hillslope runoff response and contributing area change according to the location of the water table. Higher water tables led to rapid flow and larger source areas since contributing area extends to upland sites, whereas low water levels typically located in the lower peat layer, reduce the source area to only near stream zones resulting in slow flows due to the low transmissivity of the lower peat layer.

McCartney et al. (2006) illustrated the variability of snowmelt and melt-water runoff for different landscapes units in a small subarctic mountain basin. They found substantial variability in the accumulation prior to the onset of melt, being the vegetation areas those with the largest SWE values. Melt was controlled by topography, since melt started first in southerly slopes at lower elevations. Melt rates between the different landscape units did not vary substantially, however faster melt were observed on those with steeper aspect. Runoff rates for each landscape unit on the other hand exhibited a complex pattern as a result of the combination of different melt rates and soil properties, whereas runoff volumes were primarily controlled by the initial SWE. Thus, soils with thinner organic layer showed a restricted infiltration when melt was rapid resulting in high runoff rates. Conversely, soils capped with an organic layer stored all the melt water when melt rates were slow allowing percolation in the mineral soils that resulted in lower runoff rates.

2.2 Review of Hydrological Modelling

2.2.1 Classification of Hydrological Models

Although there are several ways of classifying hydrological models (Chow et al., 1988; Singh, 1995; Abbot and Resfgaard, 1996), modelling approaches may be distinguished by three main characteristics (Grayson and Blöschl, 2001):
(1) the nature of the basic algorithm (empirical, conceptual, and physical or process-based),
(2) the approach to input or parameter specification (stochastic or deterministic), and
(3) the spatial representation (lumped or distributed).

Empirical models are derived from data; therefore they are not based on scientific laws describing physical processes. Since the model structure relies on a give range of data, their applicability and validity is limited to this range of data. Conceptual models are based on a theoretical understanding of the hydrological processes. They generally use physical laws but in a highly simplified form. Conceptual models contains parameters that may have physical significance, however most of the parameter are conceptual and hence the definition of their values relies entirely on calibration. A typical example of a conceptual rainfall runoff model makes use of the linear reservoir and channel concept such as the SLURP model (Kite and Kouwen, 1992). Physically based models on the other hand use scientific laws to describe hydrological processes.

Typically the process representation and inputs of hydrological models are deterministic where based in physical laws the same inputs and model parameterisation generate the same model output. Stochastic models includes some random component that limits the exact model prediction, therefore it is often associated to a given probability and usually delimited by confidence intervals.

Lumped models in their more simplified version deal with a catchment as a single unit. They relate precipitation inputs to discharge outputs without any consideration of the spatial patterns of the hydrological processes and basin characteristics. Therefore, they cannot capture the lateral or horizontal redistribution of moisture in soils and in the drainage network. Conversely, distributed models explicitly account for the spatial patterns of process response. Well known examples of distributed hydrological models are the TOPMODEL (Beven and Kirkby, 1979; Beven et al., 1995; Beven, 1997), the SHE model (Abbot et al., 1986, Resfgaard and Storm, 1996), the SWAT model (Arnold et al., 1998), and the WATFLOOD model (Kouwen, 1988). However, these models use different approaches for process representation. For example, while TOPMODEL uses a conceptual approach based on a detailed topographic description, the SHE model integrates a 3D groundwater model, a 2D diffusive wave approximation for the overland flow and a 1D full dynamic component of the river flow.

2.2.2 Snowmelt modelling

In the last 40 years, many snowmelt models have been developed with several purposes and applications such as global circulation models, snow monitoring, snow physics, and

avalanche forecasting (Etchevers et al., 2004). Snowmelt models generally fall into two categories: temperature index models and energy balance models.

Temperature index models have been the most common approach for snowmelt modelling mainly due to their low input data requirement, the wide availability of air temperature data, and their generally good model performance despite their simplicity (Beven, 2001). The temperature index or degree day approach assumes an empirical relationship between air temperature and snowmelt. The basic formulation developed by Anderson et al. (1973) is given by:

$$\begin{aligned} M &= MF\,(T_a - T_b), && T_a > T_b \\ M &= 0, && T_a \le T_b \end{aligned} \tag{3}$$

where M is the snowmelt depth (mm/h), MF is the melt factor or rate of melt per degree unit time ($mm°C^{-1}h^{-1}$), T_a is the air temperature (°C), and T_b is the base temperature at which snow begins to melt (°C). Examples of temperature index models are the HBV model (Bergström, 1976), the SRM model (Martinec and Rango, 1986), the UBC model (Quick and Pipes, 1977), and the SWAT model (Fontaine et al., 2002).

Physically based snowmelt models are based upon energy balance of the snowpack (equation 1). Since snowmelt involves the change of phase of ice to liquid water, the energy balance equation is the main physical framework for modelling snowmelt and implies the application of the energy equation to a 'control volume' of snow. There are several variants of this parametric energy balance approach (e.g. Kustas et al. 1994; Liston and Elder, 2006). The main difficulties in predicting snowmelt using the energy budget approach are the variations of the terms in equation (1) over time (at diurnal, synoptic and seasonal timescales) and space (Ferguson, 1999). Net shortwave radiation is generally the dominant source of heat, particularly on clear days and largely exceeds the long wave loss at night. It varies greatly according to sun angle, cloud cover, and topographic effects. Sensible heat increases with wind speed and is particularly important when snow cover is patchy and heat is advected over the snowpack from warmer snow-free areas (Morris, 1989; Marsh and Pomeroy, 1996). Latent heat can vary greatly at diurnal and synoptic scales, with both positive and negative values, but its net effect is generally much smaller than radiant or sensible heat. Ground heat flux is small and usually negligible.

Difficulties in the application of the energy balance approach arise when distributed simulations of snow-cover are needed. Differences in snow accumulation regimes between environments generate very heterogeneous snow-packs which results in a gradual depletion of the snow-cover. This is even more manifest in mountain environments because the initial snowpack tends to be deeper at higher elevations whereas the melt energy tends to be lower, so that snow persists for a long time in the higher parts of the basin. Thus, in modelling snowmelt over a watershed, the reductionist approach of applying a 'point' model at many points on a fine grid often results impractical. Snow cover depletions curves (SDCs) are used as a way to describe the spatial distribution of the snow-cover. They summarises the percent areal coverage of the

snow-pack with the average snow depth at a given time. In this approach, the amount of melt is multiplied by the snow-covered area to estimate the total input of water to a basin. Historically, SDCs were based on the temperature index approach (e.g. Anderson, 1973; Martinec, 1985; Brubaker et al., 1996) by relating snow-covered area to accumulated melt or degree days and usually applied to large areas such as elevation zones or entire watersheds. Examples of application of SDCs to physically based and distributed models includes the landscape based approach (Donald et al., 1995) and as way of parameterisation of subgrid variability (Luce et al., 1999).

The spatial distribution of snow-covered area is a key input to atmospheric and hydrologic models. During snowmelt, there is a significant change in snow albedo between a snow-covered area and an area of exposed vegetation that leads to large differences in surface net radiation and thus to large differences in surface sensible and latent energy fluxes that interact with the atmosphere. Therefore, when snow models are implemented as part of a land-surface scheme coupled to an atmospheric model for numerical weather prediction or climate modelling, they have to represent the influences of snow on the albedo of the surface and exchanges of heat and moisture between the surface and the atmosphere (Essery and Etchevers 2004). Snow models and land-surface models have increased greatly in sophistication over recent years, and the number of parameters that have to be specified for their operation has increased accordingly. The Project for Intercomparison of Land Surface Parameterization Schemes (PILPS; Henderson-Sellers et al. 1995) had shown that different parameter set and model structures among LSS models give significantly different surfaces fluxes. Particularly, in Phase 2(d) of the PILPS project the representation of the snow in LSS models was evaluated (Slater et al., 2001). PILPS 2(d) found that all LSS models were able to reproduce interannual variations of accumulation and ablation patterns, but that significant differences in timing of the complete ablation of snow between the models were observed. Problems in representing amounts of energy incident on the portion of the grid assigned as snow, especially during ablation events at early stages of the snow season, were the cause of substantive divergences during the snow season due to internal feedback processes. Similarly, the Snow Model Intercomparison Project (SnowMIP) found a wide range of capabilities in simulating snow water equivalent (SWE) at a point during the accumulation and melt periods between the models (Etchevers et al., 2004).

Modelling approaches in arctic environments includes the derivation snow-cover areal depletion curves from satellite observations to distribute the SWE (Déry et al., 2004 and 2005). Despite its simplicity this method has the limitation that is given by the spatial and temporal resolution of the satellite images which is better suited for larger scale studies. Physically based modelling studies showed the effects of the spatial variability of the incident solar and turbulent fluxes radiation in controlling snowmelt even in relatively low relief (Pohl et al., 2005a and 2006). Comparison between simulations using uniform and distributed snow and melt showed that the uniform approach was unable to reproduce the observed snow-cover depletion whereas the distributed approach provided a realistic and gradual snow-cover ablation (Pohl and Marsh, 2006). Pohl et al. (2005b) using a distributed land surface hydrological model with a vegetation based spatial representation were able to simulate mean SWE and basin runoff in a open tundra environment, whereas

less satisfactory results were seen in a energetically more complex shrub tundra environment. Improvement to the landscape representation was conducted by Davison et al. (2006) by incorporating topographic effects such as wind-swept tundra and drift snow classes.

2.2.3 Scaling issues

In this report the definitions proposed by Blöschl and Sivapalan (1995), the term 'scale' which refers to a characteristics length or time and the term 'scaling' that denotes a change in scale, are adopted. Moreover, upscaling means transferring information from smaller to larger scales (i.e. aggregating) whereas downscaling refers to the opposite transference of information, where the information is disaggregated from large to small scales.

In general the scale at which the data is collected is different from the scale at which predictions are needed. Measurements are made to get information about the natural processes; however these data will not exactly reproduce the natural variability of the processes mainly due to instrument error and the spatial dimensions of the instruments. Hence, patterns of the data will differ from the true natural patterns. Precipitation, for example, is measured at widely space points typically with fine resolution. Even at an experimental watershed, spacing between gauges may be on the order of 5 to 10 km. In order to capture the diurnal pattern of heating and cooling on the surface temperature, which can be a strongly nonlinear process, climate information is needed on time scales of at least one to few hours. Interpolation of monthly precipitation appears reasonable in some studies, but hourly or even daily precipitation cannot be reasonably interpolated from widely spaced precipitation gages (Johnson and Handson, 1995). Similar problems almost certainly exist for temperature and longwave radiation. Wind data, so critical to blowing snow and turbulent heat transfers, is even rarer than precipitation data.

Typically, the modelling or working scale is a compromise solution between process representation and the model application. Since more often than not the modelling scale is different than the process scale (i.e. scale that the natural phenomena exhibit) and much larger than the observation scale (i.e. scale at which observations are sampled), scaling techniques are needed to bridge this gap (Blöschl and Sivapalan, 1995). Thus, interpolation and aggregation/disaggregation techniques are the more common methods used. Interpolation techniques estimate patterns from points (i.e. changes of scale in terms of spacing) whereas aggregation methods involve the combination of a number of point values in space to form one average value (i.e. change of scale in terms of support) which correspond to an increase in support scale. Disagregation methods on the other hand, are the opposite transformation and estimate patterns from spatial average values.

Hydrological models are sensitive to scaling issues. The typical modelling approach is to apply the same model structure in several basins whereas the parameters, empiric or not, are varied in the calibration process. This means that the model structure is general but not the parameters. Therefore, a change in scale might involve a change in the parameter values, in particular if these parameters are related to local conditions such as climate and physiography (Bergström and Graham, 1998).

2.2.4 Aggregation methodologies

Heterogeneity in the landscape has forced hydrologists to conceptualise the physics and seek effective parameter values (Pietroniro and Soulis, 2003). Distributed hydrological models use aggregation methods to account for landscape variability and processes representation; however a critical point in the application of these models is the choice of element size. In general increasing the level of discretisation increases the accuracy of the simulation, but there should be a level beyond which the model performance can not we increased (Wood et al., 1988). In addition the smaller the grid size in which the catchment is divided the larger is the volume of information needed and the associated computational time.

A typical method for representing landscape heterogeneity is the grid-based approach (e.g. Système Hydrologique Européen, SHE). In this case, the basin is split into a number of usually square elements linked to channel reaches. Each grid is the computational element and has a specific surface elevation given by a digital elevation map. This approach has the potential to assign distributed filed of meteorological data and the capability of predicting a variety of distributed processes at each element grid. However, predictions are grid-scale dependent. Refsgaard (1997) concluded, after comparing finer and coarser grids, that simulations based on 1000 m or larger grid size while still accurate may require recalibration of the parameters. In distributed hydrological models the assumption of areas with similar hydrological behaviour is a common method for reducing model complexity. The Representative Elementary Area (REA) approach defined by Wood et al. (1988), assumes that the size of the areal elements is defined by considering that the processes at smaller scales are hydrologically insignificant for modeling purposes. Wood et al. (1988) carried out an empirical averaging experiment to assess the impact of scale. They averaged simulated runoff over small subcatchments, aggregating the subcatchments into larger catchments, and repeating the averaging process. After ranking the runoff volumes and plotting the average runoff versus area, they found that after approximately 1 km^2 the curves flatted out with increasing area. Since different correlation lengths and spatially invariant precipitation did not significantly change this result, they concluded that the REA was strongly influenced by topography. Even though the concept of universal REA is attractive for modelling purposes (e.g. grid based models), it had been demonstrated that the size for a model element is dependent on the processes being represented and the type of climate, terrain and vegetation where the model is being applied (Blöschl at al., 1995, Woods et al., 1995). These results show that there is no evidence for one universal size of REA and that the size of REA depends on many factors, including storm duration and variability, flow routing and infiltration characteristics. It is therefore apparent that the size of the REA will be specific to a particular catchment and particular application.

The complexities of the environment and data availability have seen many researchers favour aggregated computational units. The main reason for that is to reduce the increasing computational time, especially for larger basins and finer spatial resolution, and the number of parameters to be determined. Hydrological Response Units (HRUs) are one of the more common aggregation approaches where the model units are defined

according to the hydrological behaviour. These units can be related to landscape units and are characterized from an understanding of the hydrological processes and land use point of view. Therefore HRUs are usually defined by overlapping maps of different characteristics, such as soils, slope, aspect, vegetation cover, etc. (Flügel, 1995; Beven, 2000). Grouped Response Units (GRUs; Kouwen et al.,(1993) are an alternative for describing spatial variability, where areas with similar land cover, soils, etc., are grouped with no requirement for grids or sub-basins to be hydrologically homogenous. Kuchment et al. (1996) used a finite-element schematization in a physically based rainfall runoff model for representing the main channel network and landscape mosaic. By combining topographic, soil, and land use maps they divided de basin into 445 finite elements, giving an average area for a single element of about 7.5 km^2 and providing 99 finite elements along the river network, but still preserving the general pattern of steep and gentle slopes. Effective parameters were found through calibration. Another methodology is Representative Elementary Watershed (REW; Reggiani and Schellekens, 2003) defined as the smallest elementary unit into which a watershed can be discretised being still representative of other sub-entities of the watershed. The REW was assumed to be composed of five sub-regions: the unsaturated zone, saturated zone, concentrated overland flow zone, saturated overland flow zone and channel zone. The main difference with the traditional approaches (i.e. point mode equations) is that the governing equations derived from the REW approach are applicable directly at the catchment scale, and hence they have been derived in a comprehensive manner for the whole catchment or REW, as opposed to being derived separately for different processes (Lee et al., 2005). Although the REW approach is proposed as an alternative method, its application is still limited.

The major disadvantage in models using aggregation methods based in similarities (e.g. HRUs, GRUs), is the way in which each unit is considered to by spatially homogeneous. In general, within the computational element the physics is conceptualised and effective parameter values are used to account for subgrid variability.

There are several methods currently used to attempt to include subgrid heterogeneity into distributed modelling efforts. One includes replacement of the most important dependent variables in the governing equations by probability distribution functions (pdfs). Becker and Braun (1999) applied areal distribution functions of soil water holding capacity to represent spatial heterogeneities distinguishing between agricultural and forested HRUs. However, they concluded that additional scaling laws are required for describing lateral flows between landscapes. Faria et al. (2000) examined the forest canopy influence on snow-cover depletion. They found that the frequency distribution of SWE under boreal canopies fit a log-normal distribution; and the highest canopy density had the most variable snow water equivalent. The relationships between the spatial distributions of SWE and melt energy promoted earlier depletion of the snow cover than if the melt energy were uniform, with the strongest effect in heterogeneous or medium density canopies. Another examples include the explicit incorporation of parameterisation of subgrid variability through the use of a depletion curve into the snowmelt model was made by Luce et al. (1999) and Luce and Tarboton, (2004). Analogous conclusions were described by Pomeroy et al. (2004), where one of the major scaling problems in applying point-scale equations over large areas is the spatial association between driven variables

and/or parameters, which can result in spatial correlations and covariance amongst the terms of a physically based equation. A different approach is the up-scaling of point-scale hydrologic conservation equations to the computational grid areas. They mainly seek to scale the governing equations so that they accurately represent the phenomena at the larger modelling scale. It is based on the 'coarse-graining' approach which states that mechanisms important in one scale are not important in either a much larger or much smaller scale (e.g. Kavvas et al 1998; Kavvas, 1999).

2.2.5 Parameter Estimation

One of the consequences of using sophisticated hydrological models or a detailed spatial model discretization is the increase in the number of model unknown parameters with their associated uncertainties that when propagated through the model, increase the bounds the predictive uncertainty (Atkinson et al., 2003). Applicability of physically based modelling approaches, which in theory would enable the parameters to be derived from field measurements, has been restrained by heterogeneity of process responses and unknown scale-dependence of parameters. Prior information is thus limited and it is recognised that models and/or parameters must be identified through inverse modelling (Kavetski et al., 2003).

Calibration of hydrological models is intended to estimate model parameters that allow the model to closely match the observed behaviour of the real system it represent (Gupta et al., 1998). Traditionally the calibration of hydrological models has been performed manually by trial-and-error against streamflow observations. The trial-and-error method implies a manual parameter adjustment by running a number of model simulations. Due to its limitations (e.g. subjectivity and time consuming processes), research into automatic calibration procedures based on the increasing computer power has led to the use of different automatic parameter optimisation approaches. These approaches are based in general; on optimise (i.e. minimise or maximise, as appropriate) the value of an objective functions, which are numerical measures of the difference between observed and simulated data (Sorooshian and Gupta, 1995). Automatic parameter optimisation has the advantages, compared with manual calibration, that it is faster since it is computer based, is less subjective and the confidence of the model simulation can be explicitly stated. On the other hand, the difficulty in defining the best objective function or criterion to be optimised, the difficulty in finding the global optimum when many parameters are involved, the mutually dependency of, and the impossibility to distinguish between the different error sources are the main disadvantages of automatic calibration methods (Refsargaard and Storm, 1996).

The calibration procedure also has to deal with different types of uncertainties. For instance, the model parameter values can be determined directly from direct measurement, however in many situations the parameters are conceptual representations that do not exist in reality. Therefore, sources of uncertainty can be due to random or systematic errors in the input data and recorded data used for comparison with the simulated output, errors associated to the use of optimal parameter values and errors due to an incomplete or biased model structure. In addition, Duan et al. (1992) illustrated that, even when simple model structure are used and input data error is minimal, the

parameter estimation problem is not trivial. It is constrained by many regions of attraction, many local optima, rough response surfaces with discontinuous derivatives, poor and varying sensitivities of the response surface and non linear parameter interaction.

2.2.6 Regionalisation of model parameters

Regionalisation methods imply the transference of model parameters from a basin that is expected to behave similarly to the basin of interest. The similarity measure can be based on spatial proximity, basin attributes, or similarity indices Blöschl (2005). There are several regionalisation techniques, however nearly all the studies follow the same approach (e.g. Blöschl and Sivapalan, 1995; Abdulla and Lettenmaier, 1997; Fernandez et al. 2000; Littlewood 2003). Typically, regionalisation techniques involve the definition of relationships between calibrated model parameters and basin attributes. The most common methods are the bi-variate and multivariate regression methods between parameters and basin attributes, and the definition of cluster or groups of basins in hydrologically homogeneous areas where *a priori* defined parameters can be applied. The difficulty is that the relationships are likely to be weak due to parameter equifinality since many parameter sets might produce similar simulations. For example, Kuczera and Mroczkowski (1998) suggested that the problem of parameter identifiability in conceptual catchment models (where parameters do not exist in nature) is due to the existence of multiple optima and high correlation amongst model parameters. This makes the regionalisation of conceptual model parameters in ungauged basins virtually impossible.

Hydrological regionalisation studies have so far shown limited success and in general depend on the degree of similarity between the basins and on the type of the data used in the regional analysis (Littlewood, 2003). Fernandez et al. (2000) addressed this issue by performing a regional calibration approach where parameters were identified by both minimising model biases and maximising goodness of fit of relationships between parameters and basin characteristics. Regional calibration techniques were also performed by Hundecha and Bárdossy (2004) using a semi distributed conceptual model in 95 sub-basins of the Rhine basin where the coefficients of the relationships between basin attributes and parameters were calibrated rather than the model parameters, however a limitation of these methods could be the large number of coefficients to be calibrated. Alternatively, Parajka et al. (2007) proposed an iterative regional calibration method as a solution to the dimensionality of the calibration problem where local information such as streamflow data was combined with regional information such as an a priori distribution of the model parameters from gauged basins in the area in one objective function. Götzinger and Bárdossy (2007) showed that regionalisation methods using conditions imposed on the parameters by basin characteristics in distributed conceptual models were the ones that performed best due to the reduction of parameter space. Merz and Blöschl (2004) after comparing several regionalisation methods in 308 Austrian basins found that methods based on spatial proximity performed better than regression methods based on basin attributes. Goswami et al. (2007) demonstrated that the regionalisation of rainfall-runoff model parameters which were calibrated against regional pooling of streamflow data of twelve basins in France was the one that

performed best amongst three methods involving calibration, concluding that the assessment of regional homogeneity and analysis of data are very important for regionalisation approaches using calibration methods. In any case, regionalisation is of restricted utility in northern Canada because of the sparse streamgauging network and can only work where physically based parameters are regionalised over large areas.

2.3 Modelling Review Conclusions

Modelling studies on Wolf Creek have recently included SLURP, WATFLOOD, WATCLASS, MESH and CRHM which range from conceptual to physically based models. For proper application to a cold regions environment like Wolf Creek physically based models are preferred. Due to their reduced parameter complexity, HRU models are also preferred. In Canada, currently the CRHM model uses both physically based and HRU methods suitable for cold regions and it should be further evaluated in the basin. Other models from Russia and other countries with cold regions hydrology should also be evaluated.

2.4 References Specific to Hydrological Modelling

Abbott, M. B., Bathurst, J. C., Cunge, J. A., O'Connell, P. E. and J. Rasmussen. 1986. An introduction to the European Hydrological System - Systeme Hydrologique Européen "SHE", 1: History and philosophy of a physically-based distributed modelling system. *J. Hydrol.*, **87**, 45-59.

Abbot, M. B. and J. C. Refsgaard. 1996. Distributed Hydrological Modelling. Kluwer Academic Publishers.

Abdulla, F. A. and D. P. Lettenmaier. 1997. Development of regional parameter estimation equations for a macroscale hydrologic model. *J. Hydrol.*, **197**, 230-257.

Anderson, E. A. 1973. National Weather Service River Forecast System—Snow accumulation and ablation model. NOAA Tech. Memo. NWS Hydro-17, U.S. National Weather Service. (Available from NOAA/NWS, Office of Hydrology, 1325 East-West Highway, Silver Springs, MD 20910).

Arnold, J. G., Srinivasan, R., Muttiah, R.S., and J. R. Williams. 1998. Large area hydrologic modeling and assessment. Part 1: model development. *J. American Water Resour. Asso*., **34**, 73-89.

Atkinson, S. E., Sivapalan, M., Wood, R. A, and N. R Vinley. 2003. Dominant physical controls on hourly flow predictions and the role of spatial variability: Mahurangi catchment, New Zealand. *Adv. Water Resour.*, **26**, 219-235.

Backer, A. and P. Brown. 1999. Disaggregation, aggregation and spatial scaling in hydrological modelling. *J. Hydrol.*, **217**, 239-252.

Bergström, S., 1976. Development and application of a conceptual runoff model for Scandinavian catchments. (Department of Water Resources Engineering, Lund Institute of Technology/University of Lund, Bulletin Series A, No. 52, 134 pp.).

Bergströn, S. and L. P. Graham. 1998. On the scale problem in hydrological modelling. *J. Hydrol*., **211**, 253-265.

Beven K. J. and M. Kirkby.1979. A physically based variable contributing area model of basin hydrology. *Hydrol. Sci. Bull.*, **24**, 43-69.

Beven, K. J. and A. Binley. 1992. The future of distributed models. Model calibration and uncertainty prediction. *Hydrol. Process.*, **6**, 279-298.

Beven, K. J. 1997. Distributed hydrological modelling: Application of the TOPMODEL concept. J. While & Sons.

Beven, K. J. 2001. Rainfall-runoff modelling. The primer. Willey, Chichester, UK, pp: 372.

Beven, K. J. 2001. How far can we go in distributed hydrological modelling? *Hydrology and Earth System Sciences*, **5**, 1–12.

Beven, K. J., Lamb, R., Quinn, P., Romanowicz, R., and J. Freer. 1995. TOPMODEL. In: *Computer Models of Watershed Hydrology*. Singh, V.T. (Ed.), Water Resources Publications, pp: 627-688.

Bewley, D., Pomeroy J. W., and R. L. H. Essery. 2007. Solar radiation transfer through a sub-arctic shrub canopy. *Arct. Alp. Res.*, **39**, 365–374.

Blöschl, G. and M. Sivapalan. 1995. Scale issues in hydrological modelling - a review. *Hydrol. Process.*, **9**, 251-290.

Blöschl, G., Grayson, R. B., and M. Sivapalan. 1995. On the representative elementary area (REA) concept and its utility for distributed-runoff modelling. *Hydrol. Process.*, **9**, 313-330.

Blöschl, G. 1999. Scaling issues in snow hydrology. *Hydrol. Process.*, **13**, 2149-2175.

Blöschl, G., 2005. Rainfall-runoff modeling of ungauged catchments. In: *Encyclopedia of Hydrological Sciences*. Anderson, M.G. (Ed). John Wiley, Chichister, U.K., 2061-2080.

Boyle, D. P., Gupta, H. V., and S. Sorooshian. 2000. Toward improved calibration of hydrologic models: Combining the strengths of manual and automatic methods. *Water Resour. Res*., **36**, 3663-3674.

Brubaker, K., Rango, A., and W. Kustas. 1996. Incorporating radiation inputs into the snowmelt runoff model. Hydrol. Process.,**10**, 1329-1343.

Carey, S. K. and M. K. Woo. 1999. Hydrology of two slopes in subarctic Yukon, Canada. *Hydrol. Process*., **13**: 2549–2562.

Carey, S. K and M. K. Woo. 2000. The role of soil pipes as a slope runoff mechanism, subarctic Yukon, Canada. *J. Hydrol.*, **223**, 206–222.

Carey, S. K and M. K. Woo. 2001a. Slope runoff processes and flow generation in a subarctic, subalpine environment. *J. Hydrol.*, **253**, 110–129.

Carey, S. K. and M. K. Woo. 2001b. Spatial variability of hillslope water balance, wolf creek basin, subartic region. *Hydrol. Process*., **15**, 3113-3132.

Carey, S. K. and W. L. Quinton. 2005. Evaluating runoff generation during summer using hydrometric, stable isotope and hydrochemical methods in a discontinuous permafrost alpine catchment. *Hydrol. Process*., **19**, 95-114.

Chow, V. T., Maidment, D. R., and L. W. Mays. 1998. Applied Hydrology. McGraw-Hill, New York, US, pp: 585

Crawford N. H. and R. K. Linsley. 1966. Digital simulation in hydrology: Stanford Watershed Model IV. Stanford Univ., Dept. Civ. Eng. Tech. Rep. 39. pp

Davison, B., Pohl, S., Dornes, P., Marsh, P., Pietroniro, A., MacKay, M., 2006. Characterizing snowmelt variability in a land surface hydrologic model. *Atmosphere Ocean*, **44**, 271-287.

Déry, S. J., Crow, W. T., Stieglitz, M., and E. F. Wood. 2004. Modeling snow-cover heterogeneity over complex arctic terrain for regional and global climate models. *J. Hydromet.*, **5**, 33-48.

Déry, S. J., Salomonson, V. V., Stieglitz, M., Hall, D. K., and I. Appel. 2005. An approach to using snow areal depletion curves inferred from MODIS and its application to land surface modelling in Alaska. *Hydrol. Process.*,**19**, 2755-2774.

Donald, J. R., Soulis, E. D., Kouwen, N., and A. Pietroniro, 1995. Snowcover depletion curves and satellite snowcover estimates for snowmelt runoff modelling. *Water Resour. Res.*, **31**, 995-1009.

Dornes, P. F., Pomeroy, J. W., Pietroniro, A., Carey, S. K., and W. L. Quinton. 2006. The use of inductive and deductive reasoning to model snowmelt runoff from northern mountain catchments. In: Proc. iEMSs Third Biennial Meeting "Summit on Environmental Modelling and Software". Voinov, A., Jakeman, A. J., and A. E. Rizzoli

(Eds). International Environmental Modelling and Software Society, 9-13 July, Burlington, VT, USA. CD Rom. http://www.iemss.org/iemss2006/sessions/all.html.

Dornes, P. F., Pomeroy, J. W., Pietroniro, A., Carey, S. K., and W .L. Quinton. 2008a. Influence of landscape aggregation in modeling snow-cover ablation and snowmelt runoff in subarctic mountainous environment. *J. Hydrol. Sci.*, **53**, 1-15.

Dornes, P. F., Pomeroy, J. W., Pietroniro, A., and D. L. Verseghy. 2008b. Influence of landscape aggregation in modeling snow-cover ablation and snowmelt runoff in subarctic mountainous environment. *J. Hydrometeor.*, **9**, 789–803.

Dornes, P. F., Tolson, B., Davison, B., Pietroniro, A., Pomeroy, J. W., and P. Marsh. 2008c. Regionalisation of Land Surface Hydrological Model Parameters in Subarctic and Arctic Environments. *J. Phys. Chem. Earth* (in press)

Dozier, J. and J. Frew. 1990. Rapid calculation of terrain parameters for radiation modeling from digital elevation data. IEEE Transactions in Geoscience and Remote Sensing, **28**, 963-69.

Duan, Q., Sorooshian, S, and V. K. Gupta. 1992. Effective and efficient global optimization for conceptual rainfall-runoff models. *Water Resour. Res.*, **28**, 1015-1031.

Duan, Q., Sorooshian, S, and V. K. Gupta. 1994. Optimal use of the SCE-UA global optimization method for calibrating watershed models. *J. Hydrol.*, **158**, 265-284.

Essery, R., Li, L., and J. Pomeroy. 1999. A distributed model of blowing snow over complex terrain. *Hydrol. Process*., **13**, 2423-2438.

Essery, R. and J. Pomeroy. 2004a. Vegetation and topographic control of wind-blown snow distributions in distributed and aggregated simulations for an arctic tundra basin. *J Hydromet.*, 5, 735-744.

Essery, R. and J. Pomeroy. 2004b. Implications of spatial distributions of snow mass and melt rate for snow-cover depletion: theoretical considerations. *A. Glaciol*., **38**, 261-265.

Essery, R. and P. Etchevers. 2004. Parameter sensitivity in simulations of snowmelt. *J. Geophys. Res.*, 109, D20111, doi:10.1029/2004JD005036.

Etchevers, P., Martin, E., Brown, R., Fierz, C., Lejeune, Y., and 18 others. 2004. Validation of the surface energy budget simulated by several snow models (SnowMIP project). *Ann. Glaciol.*, **38**, 150-158.

Faria, D. A., Pomeroy, J. W., and R. L. H. Essery. 2000. Effect of covariance between ablation and snow water equivalent on depletion of snow-covered area in a forest. *Hydrol. Process.*, **14**, 2683-2695.

Ferguson, R. I. 1999. Snowmelt runoff models. *Prog. Phys. Geog.*, **23**, 205-227.

Fernandez, W., Vogel, R. M., and A. Sankarasubramanian. 2000. Regional calibration of a watershed model. *Hydrol. Sci. J.*, **45**, 689-707.

Flügel, W. A. 1995. Delineating hydrological response units by geographical information system analyses for regional hydrological modeling using PRMS/MMS in the drainage basin of the river Bröl, germany. *Hydrol. Process*., **9**, 423-436.

Foster, J., Liston, G., Koster, R., Essery, R., Beher, H., Dumenil, L., Verseguy, D., Thompson, S., Pollard, D. and J. 1996. Snow cover and snow mass intercomparisons of general circulation models and remotely sensed datasets. *J. Climate*, **9**, 409-426.

Fontaine, T.A., Cruickshank, T.S., Arnold, J.G., and R.H. Hotchkiss. 2002. Development of a snowfall-snowmelt routine for mountainous terrain for the soil water assessment tool (SWAT). *J. Hydrol.*, **262**, 209–223.

Freeze R. A. and R. L Harlan. 1969. Blueprint for a physically-based digitally simulated, hydrologic response model. *J. Hydrol.*, **9**, 237–258.

Giesbrecht, M. A. and M. K. Woo. 2000. Simulation of snowmelt in a sub-arctic spruce woodland: 2. Open woodland model. *Water Resour. Res.*, **36**, 2287–2295.

Goswami, M., O'Connor, K. M., and K. P. Bhattari. 2007. Development of regionalisation procedures using a multi-approach for flow simulation in an ungauged catchment. *J. Hydrol.*, **333**, 517-531.

Götzinger, J. and A. Bárdossy. 2007. Comparison of four regionalization methods for a distributed hydrological model. *J. Hydrol.*, **333**, 374-384.

Granger, R. J., Gray, D. M., and G. E. Dyck. 1984. Snowmelt infiltration to frozen prairie soils. *Canadian J. Earth Sci.*, **21**, 669–677.

Gray, D. M. and D. H. Male. 1981. Handbook of Snow: Principles, processes, Management and Use. Pergamon Press, Toronto, Canada, pp: 776.

Gray, D. M. and P. G. Landine. 1988. An energy-budget snowmelt model for the Canadian Prairies. *Can. J. Earth Sci.*, **25**, 1292-1303.

Gray, D. M., Toth, B., Pomeroy, J. W., Zhao, L., and R. J. Granger. 2001. Estimating areal snowmelt infiltration into frozen soils. *Hydrol. Process*.,**15**, 3095–3111.

Grayson R. and G. Blöschl. 2001. Spatial modelling of catchment dynamics. In: *Spatial Patterns in Catchment Hydrology. Observations and modelling*. Grayson R. and G. Blöschl (Eds). Cambridge University Press, UK, pp: 404.

Gupta, H. V., Sorooshian, S., and P.O. Yapo. 1998. Toward improved calibration of hydrologic models: multiple and noncommensurable measures of information. *Water Resour. Res,* **34**, 751-763.

Gupta, H. V., Sorooshian, S., Hogue, T. S. and D. P. Boyle. 2003. Advances in the automatic calibration of watershed models. In: *Calibration of Watershed Models, Water Science and Application Series* 6. Duan Q., Gupta H. V., Sorooshian S., Rousseau A. N., and R. Turcotte (Eds.). American Geophysical Union. Washington, US, pp. 9–28.

Hedstrom, N. R. and J. W. Pomeroy. 1998. Measurements and modelling of snow interception in the boreal forest. *Hydrol. Process*., **12**, 1611-1625.

Henderson-Sellers, A., Pitman, A. J., Love, P. K., Irannejad P., and T. H. Chen, 1995. The Project for Intercomparison of Land Surface Schemes (PILPS): Phases 2 and 3. Bull. *Amer. Meteor. Soc.*, **73**, 489-503.

Hundecha, Y. and A. Bárdossy. 2004. Modeling of the effect of land uses changes on runoff generation of a river basin through parameter regionalisation of a watershed model. *J. Hydrol.*, **292**, 281-295.

Janowicz, J.R. 2000. Spatial variability of snowmelt infiltration to frozen soil within the Yukon boreal forest. *Proceedings AWRA Conference on Water Resources in Extreme Environments*, Anchorage, Alaska, May 1-3, 2000. Edited by D.L. Kane, 121-127.

Janowicz, J. R., Gray, D. M., and J. W. Pomeroy. 2002. Characterisation of snowmelt infiltration scaling parameters within a mountainous subarctic watershed. In: *Proceedings 59th Eastern Snow Conference*. Stowe, USA, pp: 67–81.

Janowicz, J.R., Hedstrom, N., Pomeroy, J.W., Granger, R., and S.K. Carey 2004. Wolf Creek Research Basin water balance studies. In, (eds Kane, D.L. and D. Yang) *Northern Research Basins Water Balance*, IAHS Publ. No. 290, IAHS Press, Wallingford. 195-204.

Johnson, G. L. and C. Handson. 1995. Topographic and atmospheric influences on precipitation variability over mountainous watershed. *J. Appl. Meteor.*, **34**, 68-87.

Kane D. L., Hinzman L. D., Benson C. S., and G. E. Liston. 1991. Snow hydrology of a headwater arctic basin. 1. Physical measurements and process studies. *Water Resour. Res.*, **27**, 1099-1109.

Kavetski, D., Frank, S. W., and G. Kuczera. 2003. Confronting input data uncertainty in environmental modelling. In: *Calibration of Watershed Models, Water Science and Application Series* 6. Duan Q., Gupta H. V., Sorooshian S., Rousseau A. N., and R. Turcotte (Eds.). American Geophysical Union. Washington, US, pp. 49–68.

Kavvas, M. L, Chen, Z. Q., Tan, L., Soon, S. T., Terakawa, A., Yosohitani, J., and K. Fukami. 1998. A regional-scale land surface parameterization based on areally-averaged hydrological conservation equations. *Hydrol. Sci. J.*, **43**, 611-631.

Kavvas, M. L. 1999. On the coarse-graining of hydrological processes with increasing scales. *J. Hydrol*., **217**, 191-202.

Kite, G. W. and N. Kouwen. 1992. Watershed modelling using land classifications. *Water Resour. Res.*, **28**, 3193-3200.

Kouwen, N. 1988. WATFLOOD: A microcomputer-based flow forecasting system based on real-time weather data. *Can. Water. Resour. J.*, **13**, 62-77.

Kuczera, G. and M. Mroczkowiski. 1998. Assesment of hydrological parameter uncertainty and the worth of multiresponse data. *Water Resour. Res.*, **34**, 1481-1489.

Kustas W. P, Rango, A., and R. Uijlenhoet. 1994. A simple energy budget algorithm for the snowmelt runoff model. *Water Resour. Res.*, **30**, 1515–1527.

Kuchment, L. S. and A. N. Gelfan. 1996. The determination of the snowmelt rate and the meltwater outflow from a snowpack for modelling river runoff generation. *J. Hydrol.*, **179**, 23-26.

Kuchment, L. S., Deminov, V. N., Naden, P. S., Cooper, D. M., and P. Broadhirst. 1996. Rainfall-runoff modelling of the Ouse basin, North Yorkshire: an application of a physically based distributed model. *J. Hydrol.*, **181**, 323-342.

Kuz'min, P.P. 1960. Formirovanie Snezhnogo Pokrova i Metody Opredeleniya Snegozapasov. Gidrometeoizdat: Leningrad. (Published 1963 as Snow Cover and Snow Reserves. [English Translation by Israel Program for Scientific Translation, Jerusalem]. National Science Foundation: Washington, DC).

Lee, H., Sivapalan, M., and E. Zehe E. 2005. Representative Elementary Watershed (REW) approach, a new blueprint for distributed hydrologic modelling at the catchment scale: the development of closure relations. In: *Predicting Ungauged streamflow in the Mackenzie River Basin: Today's techniques and tomorrow's solutions*. Spence, C., Pomeroy, J.W, and A. Pietroniro (Eds). Canadian Water Resources Association (CWRA), Ottawa, Canada, 165–218.

Liston, G. E., 1995: Local advection of momentum, heat, and moisture during the melt of patchy snow covers. *J. Appl. Meteor.*, **34**, 1705-1715.

Liston, G. E., 1999. Interrelationships among snow distribution, snowmelt, and snow cover depletion: Implications for atmospheric, hydrologic, and ecologic modeling. *J. App. Meteor.*, **38**, 1474-1487.

Liston, G. E., McFadden, J. P., Sturm, M., and R. A. Pielke. 2002. Modelled changes in arctic tundra snow, energy and moisture fluxes due to increased shrubs. *Global Change Biology*, **8**, 17–32.

Liston, G. E. and K. Eldera. 2006. Distributed Snow-Evolution Modeling System (SnowModel). *J. Hydrometeor.*, **7**, 1259-1276.

Littlewood, I. G. 2003. Improved unit hydrograph identification for seven Welsh rivers: implications for estimating continuous streamflow at ungauged basins. *Hydrol. Sci. J.*, **48**, 743-762.

Lundberg, A. and S. Halldin. 2001. Snow interception evaporation—rates, processes and measurement techniques. In: *Land-surface/Atmosphere Exchange in High-latitudes Landscapes*. Grassl, H., Halldin, S., Gryning, S. E., and C. R. Lloyd CR (Eds). Theoretical and Applied Climatology 70, pp: 117–133.

Lundberg, A., Nakai, Y., Thunehed, H. and S. Hallin. 2004. Snow accumulation in forest from ground and remote-sensing data. *Hydrol. Process*., **18**, 1941-1955.

Luce, C. H., Tarboton, D. G., and K. R. Cooley. 1999. Subgrid parameterisation of snow distribution for and energy and mass balance snow cover model. *Hydrol. Process.*, **13**, 1921-1933.

Luce, C. H. and D. G. Tarboton. 2004. The application of depletion curves for parameterization of subgrid variability of snow. *Hydrol. Process.*, **18**, 1409-1422.

Madsen, H., 2000. Automatic Calibration of a conceptual rainfall-runoff model using multiple objectives. *J. Hydrol.*, **235**, 276-288.

Madsen, H., 2003. Parameter estimation in distributed hydrological catchment modelling using automatic calibration with multiple objectives. *Adv. Water Resour*., **26**, 205-216.

Male, D. H. 1980. The seasonal snowcover. In: *Dynamics of Snow and Ice Masses*. Colbeck, S. H. (Ed.). Academic Press. pp: 305–395.

Marks, D., T. Link, A. Winstral, and D. Garen. 2001. Simulating snowmelt processes during rain-on-snow over a semi-arid mountain basin. *A. Glaciol.*, **32**,195-202.

Marks, D., A. Winstral, and M. Seyfried. 2002. Investigation of terrain and forest shelter effects on patterns of snow deposition, snowmelt and runoff over a semi-arid mountain catchment using simulated snow redistribution fields. *Hydrol. Process.*,**16**, 3605-3626.

Marsh P. and M. K. Woo. 1984a. Wetting front advance and freezing of meltwater within a snow cover 1. Observations in the Canadian Arctic. *Water Resour. Res*., **20**, 1853-1864.

Marsh, P. and M. K. Woo. 1984b. Wetting front advance and freezing of meltwater within a snow cover. 2. A simulation model. *Water Resour. Res.*, **20**, 1865-1874.

Marsh, P. and J. W. Pomeroy. 1996. Meltwater fluxes at an arctic forest–tundra site. *Hydrol. Process.*, **10**, 1383–1400.

Marsh, P., Pomeroy, J. W., and N. Neumann. 1997. Sensible heat flux and local advection over a heterogeneous landscape at an Arctic tundra site during snowmelt. *A. Glaciol.*, **25**, 132-136.

Martinec, J. 1985. Snowmelt runoff models for operational forecasts. *Nordic Hydrol.*, **16**, 129-136.

Martinec, J. and A. Rango. 1986. Parameter values for snowmelt runoff modelling. *J. Hydrol.*, **84**, 197–219

McCartney, S. E., Carey, S. K., and J. W. Pomeroy. 2006. Intra-basin variability of snowmelt water balance calculations in a subarctic catchment. *Hydrol. Process.*, **20**, 1001–1016.

McNamara, J. P., Kane, D. L., and L. D. Hinzman. 1998. An analysis of streamflow hydrology in the Kuparuk River basin, arctic Alaska: a nested watershed approach. *J. Hydrol.*, **206**, 39–57.

Merz, R and G. Blöschl, 2004. Regionalisation of catchment model parameters. *J. Hydrol.*, **287**, 95-123.

Morris, E. M. 1989. Turbulent transfer over snow and ice. *J. Hydrol.*, **105**, 205-24.

Neumann, N and P. Marsh. 1998. Local advection of sensible heat in the snowmelt landscape of arctic tundra. *Hydrol. Process.*, 1**2**, 1547-1560.

Parajka, J., Blöschl, G., and R. Merz. 2007. Regional calibration of catchment models: potential for ungauged catchments. *Water Resour. Res.*, **43**, 6406, doi: 10.1029/2006WR005271.

Pietroniro, A. and E.D. Soulis. 2003. A hydrology modeling framework for the Mackenzie GEWEX programme. *Hydrol. Process.*, **17**, 673-676.

Pohl, S., Marsh, P., and A. Pietroniro. 2005a. Spatial-temporal variability in solar radiation during spring snowmelt. *Nord Hydrol.*, **37**, 1-19.

Pohl, S., Davison, B., Marsh, P., Pietroniro, P., 2005b. Modelling spatially distributed snowmelt and meltwater runoff in a small arctic catchment with a hydrology – land surface scheme (WATCLASS). *Atmos. Ocean*, **43**, 193-211.

Pohl, S., Marsh, P., 2006. Modelling the spatial-temporal variability of spring snowmelt in an arctic catchment. *Hydrol. Process.*, **20**, 1773-1792.

Pohl, S., Marsh, P., and G. Liston. 2006. Spatial-temporal variability in turbulent fluxes during spring snowmelt. *Arct. Antarct. Alp. Res.*, **38**, 116-146.

Pomeroy, J. W., Gray, D. M., and P. G. Landline. 1993. The Prairie Blowing Snow Model: Characteristics, validation, operation. *J. Hydrol.*, **144**, 165–192.

Pomeroy J. W. and D. M. Gray. 1995. Snowcover accumulation, relocation and management. National Hydrology Research Institute, Science Report No. 7, Saskatoon, Environment Canada, pp: 144.

Pomeroy, J. W., Marsh, P., and D. M. Gray. 1997. Application of a distributed blowing snow model to the arctic. *Hydrol. Process.*, **11**, 1451-1464.

Pomeroy J. W., Parviainen, J., Hedstrom, N., and D. M. Gray. 1998a. Coupled modelling of forest snow interception and sublimation. *Hydrol. Process.*, **12**, 2317-2337.

Pomeroy J. W., Gray, D. M., Shook, K. R., Toth, B., Essery, R. L. H., Pietroniro, A., and H. Hedstrom. 1998b. An evaluation of snow accumulation and ablation processes for land surface modelling. *Hydrol. Process.*, **13**, 2339–2367.

Pomeroy, J. W., Hedstrom, N., and J. Parviainen. 1999. The snow mass balance of Wolf Creek, Yukon: effects of snow sublimation and redistribution. In: *Wolf Creek Research Basin: Hydrology, Ecology, Environment*. Pomeroy, J. W. and R. J. Granger (Eds). Environment Canada, Saskatoon, pp: 15–30.

Pomeroy, J. W. and L. Li. 2000. Prairie and Arctic areal snow cover mass balance using a blowing snow model. *J. Geophys. Res.*, **105**, 26619–26634.

Pomeroy, J. W., Gray, D. M., Hedstrom, N. R., and J. R. Janowicz. 2002. Prediction of seasonal snow accumulation in cold climate forests. *Hydrol. Process.*, **16**, 3543-3558.

Pomeroy, J. W., Toth, B., Granger, R. J., Hedstrom, N. R., and R. L. H. Essery. 2003: Variation in surface energetics during snowmelt in a subarctic mountain catchment. *J. Hydrometeor.*, **4**, 702–719.

Pomeroy, J., R. Essery, and B. Toth. 2004. Implications of spatial distributions of snow mass and melt rate for snow-cover depletion: observations in a subarctic mountain catchment. *A. Glaciol.*, **38**, 195-201.

Pomeroy, J. W., Granger, R. J., Hedstrom, N. R., Gray, D. M., Elliot, J., Pietroniro, A., and J. R. Janowicz. 2005. The process hydrology approach to improving prediction of ungauged basins in Canada. In: *Predictions in Ungauged Basins: Approaches for*

Canada's Cold Regions. Spence, C., Pomeroy, J.W, and A. Pietroniro (Eds). Canadian Water Resources Association, City, Canada, pp: 67-99.

Pomeroy, J. W., Bewley, D. S., Essery, R. L. H., Hedstrom, N. R., Link, T., Granger, R. J., Sicart, J. E., Ellis, C. R., and J. R. Janowicz. 2006. Shrub tundra snowmelt. *Hydrol. Process.*, **20**, 923-942.

Quick, M.C. and A. Pipes. 1977. UBC watershed model. *Hydrol. Sci. Bull.*, **221**, 153–161.

Quinton, W. L. and P. Marsh. 1998. The influence of mineral earth hummocks on subsurface drainage in the continuous permafrost zone. *Permafrost and Periglacial Process.*, **9**, 213–228.

Quinton, W. L. and P. Marsh. 1999. A conceptual framework for runoff generation in a permafrost environment. *Hydrol. Process.*, **13**, 2563–2581.

Quinton, W. L., Gray, D. M., and P. Marsh. 2000. Subsurface drainage from hummock-covered hillslopes in the arctic tundra. *J. Hydrol.*,**237**, 113–125.

Quinton, W. L., Shirazi, T., Carey, S. K., and J. W. Pomeroy. 2005. Soil water storage and active-layer development in a sub-alpine tundra hillslope, southern Yukon Territory, Canada. *Permafrost and Periglacial Process.*, **16**, 369-382.

Refsgaard, J. C. and B. Storm. 1996. Construction, calibration and validation of hydrological models. In: *Distributed Hydrological Modelling*, Abbott, M. B. and Refsgaard, J.C. (Eds.). Kluwer Academic Press, The Netherlands, pp. 41-54

Refsgaard, J. C. 1997. Parameterisation, calibration and validation of distributed hydrological models. *J. Hydrol.*, **198**, 69-97.

Reggiani, P. and J. Schellekens. 2003. Modelling of hydrological responses: the representative elementary watershed approach as an alternative blueprint for watershed modelling. *Hydrol. Process.*, **17**, 3785-3789.

Sicart, J. E., Pomeroy, J. W., Essery, R. L. H., and D. Dewley. 2006. Incoming longwave radiation to melting snow: observations, sensitivity and estimation in northern environments. *Hydrol. Process.*, **20**, 3697-3708.

Sivapalan, M., Takeuchi, K., Franks, S. W., Gupta, V. K., Karambiri, H., Lakshmi, V., Liang, X., McDonnell, J. J., Mendiondo, E. M., O'Connell, P. E., Oki, T., Pomeroy, J. W., Schertzer, D., Uhlenbrook, S., and E. Zehe. 2003a. IAHS Decade on Predictions in Ungauged Basins (PUB), 2003-2012: Shaping an exciting future for the hydrological sciences. *Hydrol. Sci. J.*, **48**, 857-880.

Sivapalan, M., Blöschl, G., Zhang, L., and R. Vertessy. 2003b. Downward approach to hydrological prediction. *Hydrol. Process.*, **17**, 2101-2111.

Shook, K. R. 1995. Simulation of the ablation of prairies snowcovers. Ph. D. Thesis, University of Saskatchewan, pp:

Shook, K. and D. M. Gray. 1997. The role of advection in melting shallow snowcovers. *Hydrol. Process.*, **11**, 1725-1736.

Singh, V.P. 1995. *Computer models of watershed hydrology*. Water resources publications

Singh P. and V. P. Singh. 2001. Snow and glacier hydrology. WaterScience and technology Library Vol. 37. Kluwer Academic Publishers. pp: 742.

Slater G., Schlosser C. A., Desborough C. E., Pitman A. J., Henderson- Sellers, A., and 31 others. 2001. The Representation of Snow in Land-surface Schemes; results from PILPS 2(d). *J. Hydrometeor.*, **2**, 7-25.

Sorooshian, S, and V. K. Gupta. 1995. Model calibration. In: Singh VP, editor. Computer Models of Watershed Hydrology. Colorado. Water Resources Publications, pp.23-68.

Sturm, M., McFadden, J. P., Liston, G. E., Chapin, F. S., Racine, C. H., and J. Holmgren. 2001. Snow–shrub interactions in arctic tundra: a hypothesis with climatic implications. *J. Climate*, **14**, 336–344.

Verseghy, D. L. 1991. CLASS -A Canadian land surface scheme for GCMs. I. Soil model. Int. *J. Climatol.*, **11**, 111–133.

Verseghy, D. L., McFarlane, N. A., and M. Lazare. 1993. CLASS -A Canadian land surface scheme for GCMs. II. Vegetation model and coupled runs. *Int. J. Climatol.*, **13**, 347–370.

Verseghy, D. L. 2000. The Canadian Land Surface Scheme (CLASS): Its History and Future. *Atoms.-Ocean*, 38, 1-13.

Young, P. C. and A. J. Jarvis. 2002. Data-based mechanistic modelling and state dependent parameter models. CRES Report No. TR/177, Department of Environmental Science, Lancaster University, UK.

Woo, M. K., Stone, J. M. R., Rouse, W. R., and R. E. Stewart. 2005. Overview of the Mackenzie GEWEX study. In: Final report of the Mackenzie GEWEX study (MAGS): Proc. of the Final (11^{th}) Annual Scientific Meeting. di Censo P. (Ed.). 22-25 Ottawa, ON.

Woo, M. K. and P. Marsh. 1978. Analysis of error in the determination of snow storage for small high arctic basins. *J. Hydromet.*, **17**, 1537-1541.

Wood, E. F., Sivaplan, M., Beven, K., and L. Band. 1988. Effects of spatial variability and scale with implications to hydrologic modeling. *J. Hydrol*., **102**, 29-47.

Woods, R., Sivapalan, M., and M. Dunccan. 1995. Investigating the Representative Elementary Area concept: An approach based on field data. *Hydrol. Process.*, **9**, 291-312.

Yapo, P. O., Gupta, H. V., and S. Sorooshian. 1998. Multi-objective global optimization for hydrological models. *J. Hydrol.*, **204**, 83-97.

Zhao, L. and D. M. Gray. 1999. Estimating snowmelt infiltration into frozen soils. *Hydrol. Process.*, **13**, 1827-1842.

3.0 Cold Regions Hydrological Model Description and Tests in Wolf Creek

This section describes the CRHM, its components, how it was assembled for Wolf Creek and how it was parameterized and run for Wolf Creek using test datasets previously prepared. No calibration was performed which permitted a completely honest assessment of the model capability using estimated and measured parameters for ungauged basins.

3.1 Preparing the Cold Regions Hydrological Model for Wolf Creek

The version of the Cold Region Hydrological Model (CRHM) suited for Wolf Creek includes several modules, which have been applied to the generic framework described by Pomeroy *et al.* (2007). CRHM has previously been applied to Wolf Creek by Janowicz et al., (2004) and Dornes et al., (2008).

Described in detail by Pomeroy et al. (2007), CRHM operates through interaction of its four main components: (1) observations, (2) parameters, (3) modules, and (4) variables and states. The description of each component below focuses on the requirements of CRHM for forest, shrub and alpine environments characteristic of Wolf Creek:

1. Observations: CRHM requires the following meteorological forcing data for each simulation timestep, t (nomenclature shown in *italics*, and units in []):
   a. air temperature , T_a [°C];
   b. humidity, either as vapour pressure, e_a [kPa] or relative humidity, rh [%];
   c. precipitation, P [kg m^{-2} t^{-1}];
   d. wind speed, observed either above, or within the canopy, u [m s^{-1}];
   e. shortwave irradiance, $K\downarrow$ [W m^{-2}];
   f. longwave irradiance, $L\downarrow$ [W m^{-2}] (in the absence of observations, $L\downarrow$ may be estimated from T_a and e_a).

2. Parameters: provides a physical description of the site, including latitude, slope and aspect, forest cover density, height, species, and soil properties. In CRHM, forest cover need only be described by an effective leaf area index (LAI) and forest height (h); the forest sky view factor (v) may be specified explicitly or estimated from LAI. The heights at which meteorological forcing data observations are collected are also specified here.
3. Modules: algorithms implementing the particular hydrological processes are selected here by the user.
4. Initial states and variables: specified within the appropriate module.

Modules

The following provides an outline of the main modules and associated algorithms in CRHM.

Observation module

To allow for the distribution of meteorological observations away from the point of collection, appropriate corrections are applied to observations within the *observation* module. These include correction of air temperature, humidity, and the amount and

phase of precipitation for elevation, as well as correction of shortwave and longwave irradiance for topography.

Snow mass-balance module

In CRHM, snow is conserved within a defined single spatial unit, with changes in mass occurring only through a divergence of incoming and outgoing fluxes. In clearing environments, snow water equivalent (SWE) at the ground may be expressed by the following mass-balance equation of vertical and horizontal snow gains and losses

$$[1] \qquad \mathrm{SWE} = \mathrm{SWE_o} + P_s + P_r + H_{in} - H_{out} - S - M$$

where $\mathrm{SWE_o}$ is the antecedent snow water equivalent [kg m^{-2}], P_s and P_r are the respective snowfall and rainfall rates, H_{in} is the incoming horizontal snow transport, H_{out} is the outgoing horizontal snow transport, S is the sublimation loss, and M is the melt loss [all units kg m^{-2} t^{-1}]. In forest environments Eq. 1 is modified to

$$[2] \qquad \mathrm{SWE} = \mathrm{SWE_o} + P_s - (I_s - U_l) + P_r - (I_r - R_d) - M$$

in which I_s is amount of canopy intercepted snow, U_l is the addition of sub-canopy snow from canopy unloading, I_r is the amount of intercepted rain, and R_d is the addition of sub-canopy rainfall from canopy drip [all units kg m^{-2} t^{-1}].

The amount of snowfall intercepted by the canopy is dependent on various physical factors, including tree species, forest density, and the antecedent intercepted snowload. In CRHM, a dynamic canopy snow-balance is calculated, in which the amount of snow interception is determined by

$$[3] \qquad I_s = I^*_s \left(1 - e^{-C_l P_s / I^*_s}\right)$$

where C_l is the 'canopy-leaf contact area per unit ground' [] and I^*_s is the species-specific maximum intercepted snowload [kg m^{-2}], which is determined as a function of the maximum snowload per unit area of branch, $\overline{S}$ [kg m^{-2}], the density of falling snow, ρ_s [kg m^{-3}], and $LAI`$ by

$$[4] \qquad I^*_s = \overline{S}\left(0.27 + \frac{0.46}{\rho_s}\right) LAI` \; .$$

Sublimation of intercepted snow is estimated following Pomeroy et al.'s (1998) multi-scale model, in which the sublimation rate of intercepted snow, V_i [s^{-1}], is multiplied by the intercepted snowload to give the canopy sublimation flux, q_e [kg m^{-2} s^{-1}], i.e.

$$[5] \qquad q_e = V_i \, I_s \; .$$

Here, V_i is determined by adjusting the sublimation flux for a 500 μm radius ice-sphere, V_s [s^{-1}], by the intercepted snow exposure coefficient, C_e [], i.e.

$$V_i = V_s \, C_e \quad [6]$$

In which C_e was defined by Pomeroy and Schmidt (1993) as

$$C_e = k \left(\frac{I_s}{I_s *} \right)^{-F} \quad [7]$$

where k is a dimensionless coefficient indexing the shape of intercepted snow (i.e. age and structure) and F is the fractal dimension of intercepted snow [~0.4]. Ventilation wind speed of intercepted snow may be set as the measured within-canopy wind speed, or approximated from above-canopy wind speed by

$$u_\xi = u_h \, e^{-\psi \xi} \quad [8]$$

where u_ξ [m s^{-1}] is the estimated within-canopy wind speed at a vertical depth of ξ []from the canopy top, u_h [m s^{-1}] is the observed wind speed above the canopy, and ψ is the canopy wind speed extinction coefficient [], determined as a linear function of *LAI`* for various needleleaf species (Eagleson, 2002). Unloading of intercepted snow to the sub-canopy snowpack is calculated as an exponential function of time following Hedstrom and Pomeroy (1998). Additional unloading resulting from melting intercepted snow is estimated by specifying a threshold ice-bulb temperature (T_b) in which all intercepted snow is unloaded when exceeded for three hours.

Blowing snow transport and sublimation module

PBSM calculates two-dimensional blowing snow transport and sublimation rates for steady-state conditions over a landscape element using mass and energy balances. Figure 1 shows the main PBSM fluxes and stores, represented as a control volume. PBSM was initially developed for application over the Canadian Prairies, characterized by relatively flat terrain and homogeneous crop cover (e.g. Pomeroy, 1989; Pomeroy et al., 1993). Versions have been applied to variable vegetation height (Pomeroy et al., 1991), over alpine tundra (Pomeroy, 1991), arctic tundra (Pomeroy and Li, 2000) and mountainous subarctic terrain (MacDonald et al., 2009). Only key equations are presented here. Refer to Pomeroy and Gray (1990), Pomeroy and Male (1992), Pomeroy et al. (1993) and Pomeroy and Li (2000) for further details.

The snow mass balance over a uniform element of a landscape (e.g. a HRU) is a result of snowfall accumulation and the distribution and divergence of blowing snow fluxes both within and surrounding the element given by:

$$\frac{dS}{dt}(x) = P - p\left[\nabla F(x) + \frac{\int E_B(x) dx}{x} \right] - E - M \quad [9]$$

where dS/dt is the surface snow accumulation (kg m^{-2} s^{-1}), P is snowfall (kg m^{-2} s^{-1}), p is the probability of blowing snow occurrence within the landscape element, F is the blowing snow transport out of the element (kg m^{-2} s^{-1}) which is the sum of snow transport in the saltation and suspension layers, F_{salt} and F_{susp}, $\int E_B(x)dx$ is the vertically integrated blowing snow sublimation rate (kg m^{-1} s^{-1}) over fetch distance x (m), E is the snowpack sublimation (kg m^{-2} s^{-1}) and M is snowmelt (kg m^{-2} s^{-1}).

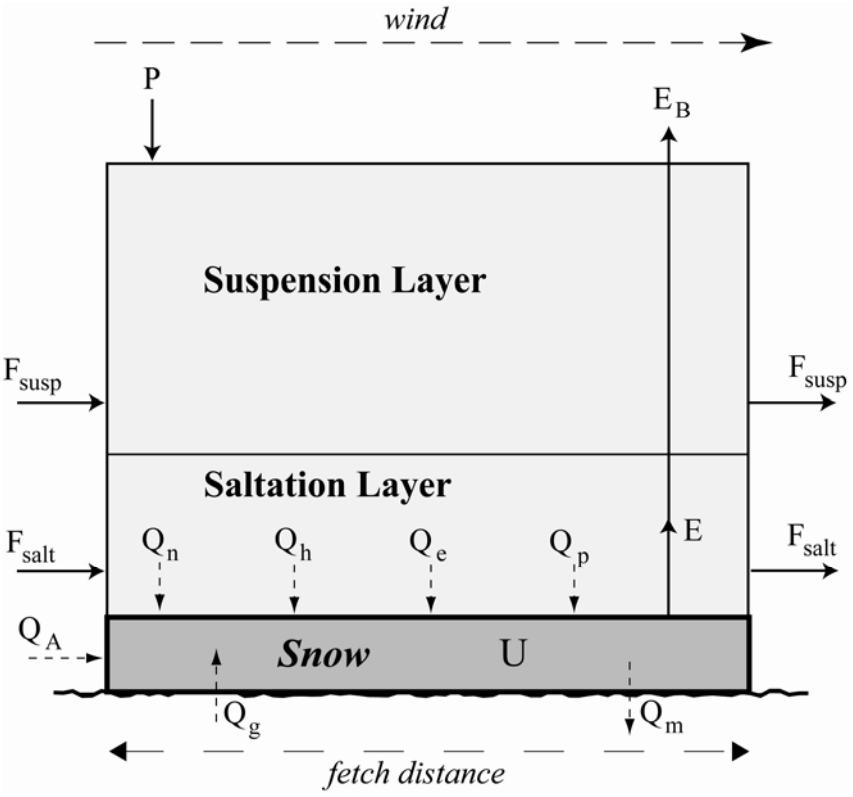

Figure 1. Control volume for blowing snow describing PBSM snow fluxes and mass balance calculation for snow accumulation.

Since PBSM is for fully-developed blowing snow conditions, PBSM is restricted to minimum fetch distances of 300 m following measurements by Takeuchi (1980). Blowing snow transport fluxes are the sum of snow transport in the saltation and suspension layers, F_{salt} and F_{susp} (kg m^{-1} s^{-1}), respectively. Saltation of snow must be initiated before snow transport can occur in the suspension layer and blowing snow sublimation can occur.

F_{salt} is calculated by partitioning the atmospheric shear stress into that required to free particles from the snow surface, to that applied to nonerodible roughness elements and to that applied to transport snow particles (Pomeroy and Gray, 1990),

$$F_{salt} = \frac{c_1 e \rho u^*_t}{g}\left(u^{*2} - u^{*2}_n - u^{*2}_t\right) \quad [10]$$

where c_1 is the dimensionless ratio of saltation velocity to friction velocity ($up/u^* = 2.8$), e is the dimensionless efficiency of saltation ($1/4.2u^*$), ρ is atmospheric density (kg m^{-3}), g is acceleration due to gravity (m s^{-2}), u^* is the atmospheric friction velocity (m s^{-1}), and u^*_n and u^*_t refer to the portions of the u^* applied to nonerodible roughness elements such as vegetation (nonerodible friction velocity) and the open snow surface itself (threshold friction velocity), respectively. Mechanical turbulence controls atmospheric exchange during blowing snow, thus u^* is calculated using the Prandtl logarithm wind profile as:

$$[11] \qquad u^* = \frac{u_z k}{\ln\left[\frac{z}{z_o}\right]}$$

where k is the von Karman constant (0.41), u_z is the wind speed (m s^{-1}) at height z (m) above the snow surface and z_0 is the aerodynamic roughness length (m). z_0 is controlled by the saltation height and is given by,

$$[12] \qquad z_0 = \frac{c_2 c_3 u^{*2}}{2g} + c_4 \lambda$$

where c_2 is the square root of the ratio of the initial vertical saltating particle velocity to u^*, c_3 is ratio of z_0 to saltation height (0.07519; Pomeroy and Gray, 1990), c_4 is a drag coefficient (0.5; Lettau, 1969) and λ is the dimensionless roughness element density.

u^*_n is calculated using an algorithm developed by Raupach et al. (1993) for wind erosion of soil calculations that relates the partitioning of the shear stress to the geometry and density roughness elements given by:

$$[13] \qquad \frac{u^*_n}{u^*} = \frac{(m\beta\lambda)^{0.5}}{(1 + m\beta\lambda)^{0.5}}$$

where β is the ratio of element to surface drag and λ is the dimensionless roughness element density. Raupach et al. (1993) found $\beta \approx 170$ which is used for shortgrass and crop stalks. m is an empirical coefficient to account for the difference in average and maximum surface shear stress to initiate erosion. The default value for m in PBSM is 1.0 for grass and cereal grain stalks. Wyatt and Nickling (1997) determined a mean $\beta = 202$ and mean $m = 0.16$ for desert creosote shrubs (*Larrea tridentata*) in a Nevada desert. Wyatt and Nickling's β and m are presumed to be more suitable for shrubs found in northern and western Canada than the grass and cereal grain default values in PBSM. λ is calculated as per Pomeroy and Li's (2000) modification of an original equation by Lettau (1969),

$$[14] \qquad \lambda = N d_v \left(h_v - \frac{S}{\rho_s} \right)$$

where N is the vegetation number density (number m^{-2}), d_v is the vegetation stalk diameter (m), h_v is the height of vegetation and the snow depth is snow accumulation, S, divided by snow density (kg m^{-3}).

u^*_t is calculated from the meteorological history of the snowpack using an algorithm developed by Li and Pomeroy (1997a) from observations at low vegetation sites in the Canadian prairies.

F_{susp} is calculated as a vertical integration from a reference height near the top of the saltation layer, h^*, to the top of blowing snow boundary layer (z_b), given by Pomeroy and Male (1992)

$$F_{susp} = \frac{u^*}{k}\int_{h^*}^{z_b} \eta(z) \ln\left(\frac{z}{z_0}\right) dz \quad [15]$$

where k is von Kármán's constant (0.41), η is the mass concentration of blowing snow at height z (m) and z_0 is the aerodynamic roughness height. z_b is governed by the time available for the vertical diffusion of snow particles from h^*, calculated using turbulent diffusion theory and the logarithmic wind profile. h^* increases with friction velocity and is estimated as given by Pomeroy and Male (1992),

$$h^* = 0.08436 u^{*1.27} \quad [16]$$

For fully-developed flow it is constrained at z_b = 5 m. At z_b shear stress is constant ($d\tau/dt$ = 0) and suspension occurs under steady-state conditions ($d\eta/dt$ = 0). Note that as suspension diffuses from the saltation layer, saltation must be active for suspension to proceed.

E_B is calculated as a vertical integration of the sublimation rate of a single ice particle with the mean particle mass being described by a two-parameter gamma distribution of particle size that varies with height. The vertically integrated sublimation rate is given by:

$$E_B = \int_0^{z_b} \frac{1}{m(z)} \frac{dm}{dt}(z) \eta(z) dz \quad [17]$$

where m is the mean mass of a single ice particle at height z. The rate that water vapour can be removed from the ice particle's surface layer, dm/dt, is calculated assuming particles to be in thermodynamic equilibrium. dm/dt is controlled by radiative energy exchange convective heat transfer to the particle, turbulent transfer of water vapour from the particle to the atmosphere and latent heat associated by sublimation, and is given by (Schmidt, 1972). E_B calculations are highly sensitive to ambient relative humidity, temperature and wind speed (Pomeroy et al., 1993; Pomeroy and Li, 2000).

Field observations show that blowing snow is a phenomenon that is unsteady over both space and time. The time steps most frequently used in PBM studies (i.e. 15, 30 or 60 minutes) do not match the highly variable and intermittent nature of blowing snow. In addition, small scale spatial variability in snowcover properties produce sub-element (e.g. grid cell or HRU) variability in snow

transport. Li and Pomeroy (1997b) developed an algorithm to upscale blowing snow fluxes from point to area. The probability of blowing snow occurrence, p, is approximated by a cumulative normal distribution as a function of mean wind speed (location parameter), the standard deviation of wind speed (scale parameter). Empirical equations for the location and scale parameter were developed from six years of data collected at 15 locations in the Canadian Prairies and are calculated from the number of hours since the last snowfall and the ambient atmospheric temperature.

Rainfall interception and evaporation module

Although the overall focus of this manuscript is snow-forest interactions, winter rainfall may represent substantial of water and energy inputs to snow. The fraction of rainfall to sub-canopy snow received as direct throughfall is assumed to be inversely proportional to the fractional horizontal canopy coverage, C_c. All other rainfall is intercepted by the canopy, which may be lost by evaporation or dripped to the sub-canopy upon exceeding the maximum canopy storage depth (I^*_r) [kg m^{-2}]. Rain interception (I_r) in CRHM is estimated using a simplified Rutter model approach in which a single storage is determined and is scaled for sparse canopies by C_c (Valente et al., 1997). Upon reaching the maximum canopy storage depth (S_{max}) [mm], additional water storage in the canopy is routed to the sub-canopy. Evaporation from a fully wetted canopy (E_p) [kg m^{-2}] is calculated using the Penman-Monteith combination equation (Monteith, 1965) for the case of no stomatal resistance, i.e.

$$E = C_c E_p \qquad \text{for } C = S_{max} \text{.} \tag{18a}$$

For partially-wetted canopies is reduced in proportion to the canopy storage depth, i.e.

$$E = C_c E_p C/S_{max} \qquad \text{for } C < S_{max} \text{.} \tag{18b}$$

Rainfall to the sub-canopy is added to the water equivalent of the snowpack. For the case of rain on melting snow (i.e. T_s = 0°C) for which no refreezing occurs daily Q_p [MJ m^{-2}] is given by

$$Q_p = 4.2(P_r - I_r)T_r \tag{19}$$

Snow energy-balance module

Energy to snow (Q^*) is resolved in CRHM as the sum of radiative, turbulent, advective and conductive energy fluxes to snow, i.e.

$$K^* + L^* + Q_h + Q_e + Q_g + Q_p = \frac{dU}{dt} + Q_m = Q^* \tag{20}$$

where Q_m is the energy for melt, dU/dt is the change in internal (stored) energy of snow ; K^* and L^* are net shortwave and longwave radiations, respectively; Q_h and Q_e are the net sensible and latent heat turbulent fluxes, respectively; and Q_g is the net ground heat flux

[all units W m^{-2}]. In Eq. 20, positive magnitudes are considered as energy gains to snow and negative magnitudes as energy losses. Daily melt depth, M [kg m^{-2}], is calculated from Q_m by

$$M = 0.0864 \frac{Q_m}{\rho_w B \lambda_f} \quad [21]$$

where B is the fraction of ice in wet snow [0.95 – 0.97].

Before snowmelt can be estimated the *Global* module accomplishes the partitioning of the incoming solar radiation according to slope and aspect and cloudiness effects. Direct short wave radiation (K_{dir}), diffuse short wave radiation (K_{dif}), and a cloudiness index (c) are calculated using expressions proposed by Garnier & Ohmura (1970). The cloudiness index (c) is determined from the comparison between the observed incoming short wave radiation (K) and the theoretical clear sky direct-beam component of solar radiation (K_{theo}) over flat areas, and then is used to calculate K_{dir} on slopes having some aspect. The contribution of diffusive sky radiation, K_{dif}, is first estimated for flat areas (List, 1968) using the extra-terrestrial solar irradiation on a horizontal surface at the outer limit of the atmosphere K_{ext}, and then corrected by slope and aspect following Garnier & Ohmura (1970) as

$$K_{dir} = I \cdot p^m \left[(\sin\theta \cos H)(-\cos A \sin Z) - \sin H (\sin A \cos Z) \right. \quad [22]$$
$$\left. + (\cos\theta \cos H) \cos Z \right] \cos\delta + \left[\cos\theta (\cos A \sin Z) + (\sin\theta \cos Z) \right] \sin\delta \text{ `}$$

$$K_{dif} = 0.5\left((1 - aw - ac) K_{ext} - K_{dir} \right) \quad [23]$$

where I is the intensity of extraterrestrial radiation, p is the mean zenith path transmissivity of the atmosphere, m is the optical air mass (calculated from Kasten and Young, 1989), δ is declination of the sun, θ is the latitude, H is the hour angle measured from solar noon positively towards west, A is the slope azimuth measured from the north through east, Z is the slope angle, aw is the radiation absorbed by water vapour (7%), and he radiation absorbed by ozone (2%).

The *Slope_Qsi* module calculates incident solar radiation on slopes based on the ratio of measured incident shortwave radiation on a level and the calculated clear sky direct an diffuse shortwave radiation on a level plane (from *Global*).

Net radiation and ground heat flux are calculated in the *Netall* module using the algorithm presented by Satterland (1979) for estimating daily net long-wave and presuming that ground heat flux is proportional to net radiation. Net radiation calculated in the *Netall* module is not used for snowmelt calculations but for evapotranspiration.

Snow-cover albedo is estimated in the *Albedo* module which assumes that the albedo depletion of a shallow snow cover, not subject to frequent snowfall events, can be approximated by three line segments of different slope describing the periods premelt,

melt, and postmelt (the period immediately following disappearance of the snow cover) (Gray & Landine, 1987).

Snow-cover ablation is estimated using the Energy-Budget Snowmelt Model (*EBSM* module) (Gray & Landine, 1988). The model uses the snowmelt energy equation as its physical framework, and physically based procedures for evaluating radiative, convective, advective, and internal-energy terms from standard climatological measurements. Daily estimates of net radiation, maximum and minimum air temperature, a threshold air temperature for melt initiation, and snow-cover and snowfall depths to establish the 'start' of the melt and albedo depletion rate are used to drive EBSM. The net radiation is calculated for premelt as follows:

$$Q_N = -0.04 + 0.76 \cdot \left\{ \underbrace{Q_0 \cdot \left[0.052 + 0.052 \cdot \frac{n}{N} \right] \cdot (1 - A) + 0.097 \cdot \sigma \cdot T_a^4}_{net\ short\ wave\ term} \cdot \underbrace{\left[\left(-0.39 + 0.093 \cdot e_a^{0.5} \right) \cdot \left(0.26 + 0.81 \cdot \frac{n}{N} \right) \right]}_{net\ long\ wave\ term} \right\}$$

[24]

and for the melt period

$$Q_N = -0.53 + 0.47 \cdot Q_0 \cdot \left[0.52 + 0.52 \cdot \frac{n}{N} \right] \cdot (1 - A)$$

[25]

where Q_0 is the daily clear-sky short wave radiation incident to the surface ($MJ \cdot m^{-2} \cdot day^{-1}$), n is the number of hours of bright sunshine in the day, N is the maximum possible number of hours of bright sunshine in the day, A is the mean surface albedo, σ is the Stefan-Boltzmann constant (4.9×10^{-9} $MJ \cdot m^{-2} \cdot K^{-4} \cdot day^{-1}$), Ta is the mean daily air temperature (K), and e_a is the mean daily vapour pressure of the air (mbar). The ratio n/N can be estimated from c, the cloudiness index, using shortwave radiation measurements if sunshine hours are unavailable (as in this application).

The change in internal energy (dU/dt) of the snowpack is estimated using an algorithm that assumes a minimum state of internal energy determined by the minimum daily temperature, a maximum state equal to zero, a maximum liquid-water-holding content of the snow-cover equal to 5 percent by weight, a snow-cover density of 250 $kg \cdot m^{-3}$, and no melt unless indicated by the model.

Adjustment of energy fluxes to snow for needleleaf forest cover

Needleleaf or coniferous forests require modifications to the energy fluxes to snow to account for canopy effects.

Shortwave radiation to forest snow

In CRHM, net shortwave radiation to forest snow (K^*_f) is equal to the above-canopy irradiance ($K\downarrow$) transmitted through the canopy less the amount reflected from snow, given here by

$$K^*_f = K\downarrow \tau(1-\alpha_s) \quad [26]$$

in which α_s is the snow surface albedo [], and τ is the transmittance of forest cover to shortwave irradiance [] which is estimated using the following variation of Pomeroy and Dion's (1996) formulation (Pomeroy et al., 2009),

$$\tau = e^{-\frac{1.081\cos(\theta)LAI`}{\sin(\theta)}} \quad [27]$$

where θ is the solar angle above the horizon [radians]. In Eq. 15, the decay of α_s from an initial albedo value representing fresh snow conditions is approximated as a function of time [days].

Longwave radiation to forest snow (L_f)

As discussed previously, longwave irradiance to forest snow ($L\downarrow_f$) may be enhanced relative to that in the open as a result of additional thermal emissions from forest cover. Simulation of $L\downarrow_f$ to snow is resolved as the sum of sky and forest longwave emissions, weighted by the sky view factor (v), i.e.

$$L\downarrow_f = vL\downarrow + (1-v)\varepsilon_f \sigma T_f^{\,4} \quad [28]$$

.

Here, ε_f is the emissivity of the forest [], σ is the Stefan-Boltzmann constant [W m^{-2} K^{-4}], and T_f is the forest temperature [K]. Longwave exitance from snow ($L\uparrow$) is determined by

$$L\uparrow = \varepsilon_s \sigma T_s^{\,4} \quad [29]$$

where ε_s is the emissivity of snow [0.98], and T_s is the snow surface temperature [K] which is resolved following the longwave psychrometric approach developed by Pomeroy (in preparation)

$$T_s = T_a + \frac{\varepsilon\left(L\downarrow - \sigma T_a^4\right) + \lambda_v (e_a - e_s)\rho_a / r_a}{\varepsilon\sigma T_a^3 + (c_p + \lambda_v \Delta)\rho_a / r_a} \quad [30]$$

where ε is the emissivity of the atmosphere [ ], e_a and e_s are the respective observed and saturation vapour pressures [kPa], c_p is the specific heat capacity of air [KJ kg^{-1} K^{-1}], λ_v is the latent heat of vapourization [2501 kJ kg^{-1} at 0˚C], r_a is the aerodynamic resistance, and Δ is the slope of the saturation vapour pressure curve [kPa K^{-1}].

Sensible (Q_h) *and latent* (Q_e) *heat fluxes*

Determination of Q_h and Q_e in the open and forest sites are made using the semi-empirical formulations developed by Gray and Landine (1988)

[31] $$Q_h = -0.92 + 0.076u_{mean} + 0.19T_{max}$$

[32] $$Q_e = 0.08(0.18 + 0.098u_{mean})\ (6.11 - 10ea_{mean})$$

Where u_{mean} is the mean daily wind speed [m s^{-1}], T_{max} is the maximum daily air temperature [°C], and ea_{mean} is the mean daily vapour pressure [kPa] in the open and forest environments, respectively. The various snow and water mass and energy balance routines for both forest and clearing environments within CRHM are summarized in Figure 2.

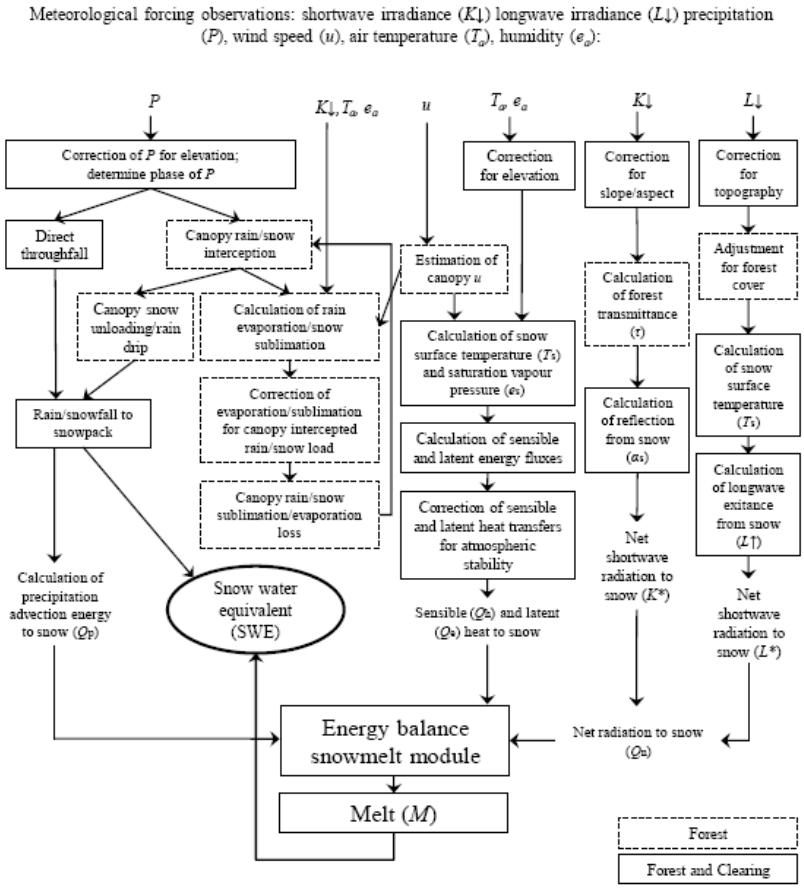

Figure 2 Flow diagram describing the algorithms for mass and energy calculations used in CRHM for forest and open shrub environments. In open alpine environments, the Prairie Blowing Snow Model (Fig. 1) is also used.

Infiltration to frozen soils

During the spring snowmelt, infiltration into frozen soils is estimated in the *Frozen* module using the approach proposed by Zhao & Gray (1999) and Gray *et al*. (2001). This module divides the soil into restricted, limited, and unlimited classes according to its infiltration characteristics. When limited, infiltration is governed primarily by the snow-cover water equivalent (SWE) and the frozen water content of the top 40 cm of soil. The frozen infiltration routine is disabled when the SWE of the snowpack is less than 5 mm. The cumulative snowmelt infiltration (mm) into frozen soils is computed as:

$$INF = C \cdot S_0^{2.92} \cdot (1 - S_I)^{1.64} \cdot \left(\frac{273.15 - T_I}{273.15} \right)^{-0.45} \cdot t_0^{\,0.44} \quad [33]$$

where C is a coefficient, S_0 is the surface saturation ($mm^3 \cdot mm^3$), S_I is the average soil saturation (water + ice) of 0-40 cm soil at the start of infiltration ($mm^3 \cdot mm^3$), T_I is the average temperature of 0-40 soil layer at start of infiltration (K), and t_0 is the infiltration opportunity time (h).

Infiltration opportunity time is estimated as the time required to melt a snow-cover assuming continuous melting and small storages and evaporation. Thus, t_0 is calculated by cumulating the hours when there is snowmelt according to the EBSM module.

Actual evapotranspiration is estimated in the *Evap* module using the algorithm proposed by Granger & Gray (1989) and Granger & Pomeroy (1997). This algorithm is an extension of the Penman equation for unsaturated conditions. The ability to supply water for evaporation is indexed using only the atmosphere aridity, so no knowledge of soil moisture status is required for this module. To ensure continuity however, evaporation is taken first from any intercepted rainfall store, then from the upper soil layer and then from the lower soil layer and restricted by water supply in the following module (see Pomeroy *et al*., 2007).

Runoff and soil moisture balance

Variations in the soil moisture balance are conceptually represented as a two layer soil profile in the *Soil* module. The upper layer or recharge layer, represents the top soil and is where infiltration and evaporation occurs. Depressional storage and wetland storage are also permitted and flow can be routed as fill and spill or as an output proportional to storage. Transpiration is withdrawn surface water and then sequentially from the entire soil profile. Snowmelt infiltration computed using the *Frozen* module occurs when soil moisture capacity is available in the soil profile, otherwise *snowmelt runoff* is generated. Excess water from both soil layers constitutes runoff. Runoff is generated when rainfall events exceed the soil moisture capacity and when the groundwater recharge has been satisfied or as infiltration excess. Snowmelt runoff and runoff, are added together in the term that represents the *overland flow*. Furthermore, a horizontal soil leakage, *subsurface runoff*, continuously diminishes the amount of water in the soil and follows an exponential or linear reservoir decay:

$$K_{ssr} = \frac{R_i}{R_{\max}} \quad [34]$$

where K_{ssr} is horizontal soil leakage (T^{-1}), and R_i (mm) and $R_{\max}$ (mm) are the actual and maximum soil moisture capacity in the recharge or top layer respectively. A diagram showing the *Soil* module and its inputs and outputs follows as Figure 3.

Routing

Outflow from an HRU, constituted by runoff and subsurface runoff flows, and eventually inflow from another HRU, are independently routed in the *Netroute* module using a hydraulic routing approach. Each flow is calculated by lagging its inflow by the travel time through the HRU, then routing it through an amount of linear storage defined by the storage constant, *K*. For a given HRU, the upstream inflow is conceptualised as the outflow from the upstream HRU, whereas runoff accounts for overland flow and soil storage effects are considered in the subsurface runoff component.

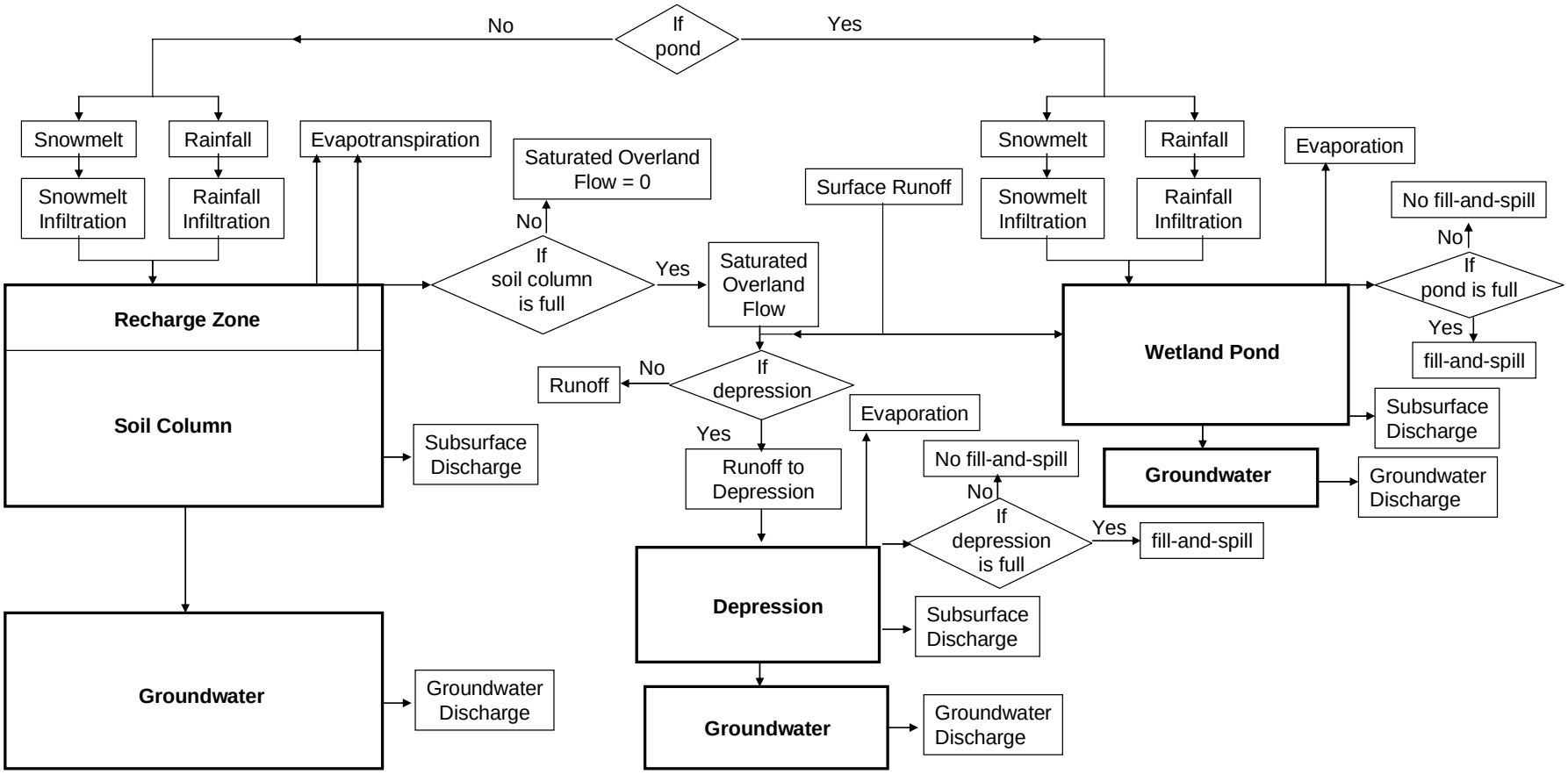

Figure 3. Flowchart of Soil, soil moisture balance calculation with wetland or depression storage and fill-and-spill.

3.2 Initial Tests of CRHM in Wolf Creek

CRHM was tested in Wolf Creek at a detailed scale for the tundra dominated Granger basin where parameters are relatively well known and at the whole basin scale (including forests) where there is more parameter uncertainty. The two scale evaluation provides a reference for the needed developments in CRHM to provide uncalibrated discharge calculations in the Yukon.

3.2.1 Granger Basin CRHM Test

The objective of this component of the study was to set up and test the performance of CRHM for Granger Basin (GB), a small basin located in the Wolf Creek Research Basin. The focus on the GB is to use available datasets and a well studied site to set up CRHM and evaluate the performance of the snow accumulation, snowmelt and surface snowmelt runoff routines. A further purpose for setting up and testing model at the GB is to gain experience in developing the appropriate model structure and parameterisation strategy so that this can be extended over all of Wolf Creek Research Basin.

3.2.1.1 CRHM structural setup

HRU setup

Five hydrological response units (HRUs): upper basin (UB), plateau (PLT), north facing slope (NF), south-facing slope (SF), and valley bottom (VB) were set up for the GB shown in Figure 4. These HRUs are landscape based units and are well adapted for snow hydrology calculations (Dornes et al., 2008; MacDonald et al., 2009).

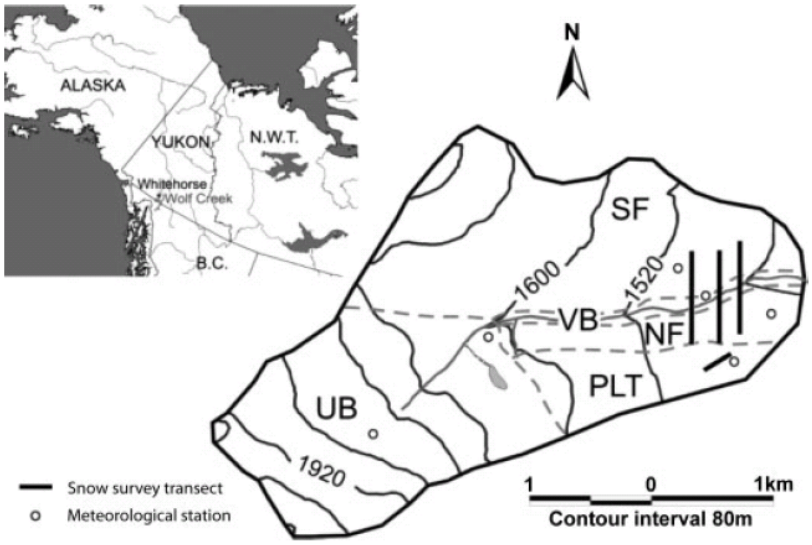

Figure 4. Granger Basin HRUs setup. Gray dashed lines denote the boundary for HRUs: upper basin (UB), plateau (PLT), north facing slope (NF), south-facing slope (SF), and valley bottom (VB) (from MacDonald et al., 2009).

Modules setup

As discussed in the previous section, CRHM is a hydrological model assembly platform that has a modular basis (Pomeroy et al., 2007). The modules in CRHM represent physiographic descriptions for the basin, observations, and physically-based algorithms for hydrological processes. A set of modules was linked in a sequential fashion to simulate the hydrological processes for the Granger Basin. Module selection was intended to be as physically based as possible given the available data and hydrological complexity of the basin. Figure 5 shows the schematic of these modules, which include:

1. observation module: reads the meteorological data (temperature, wind speed, relative humidity, vapour pressure, precipitation, and radiation), providing these inputs to other modules;
2. Garnier and Ohmura's radiation module (Garnier and Ohmura, 1970): calculates the theoretical global radiation, direct and diffuse solar radiation, as well as maximum sunshine hours based on latitude, elevation, ground slope, and azimuth, providing radiation inputs to sunshine hour module, energy-budget snowmelt module, net all-wave radiation module;
3. sunshine hour module: estimates sunshine hours from incoming short-wave radiation and maximum sunshine hours, generating inputs to energy-budget snowmelt module, net all-wave radiation module;
4. module for incoming short-wave radiation adjustment for slope;

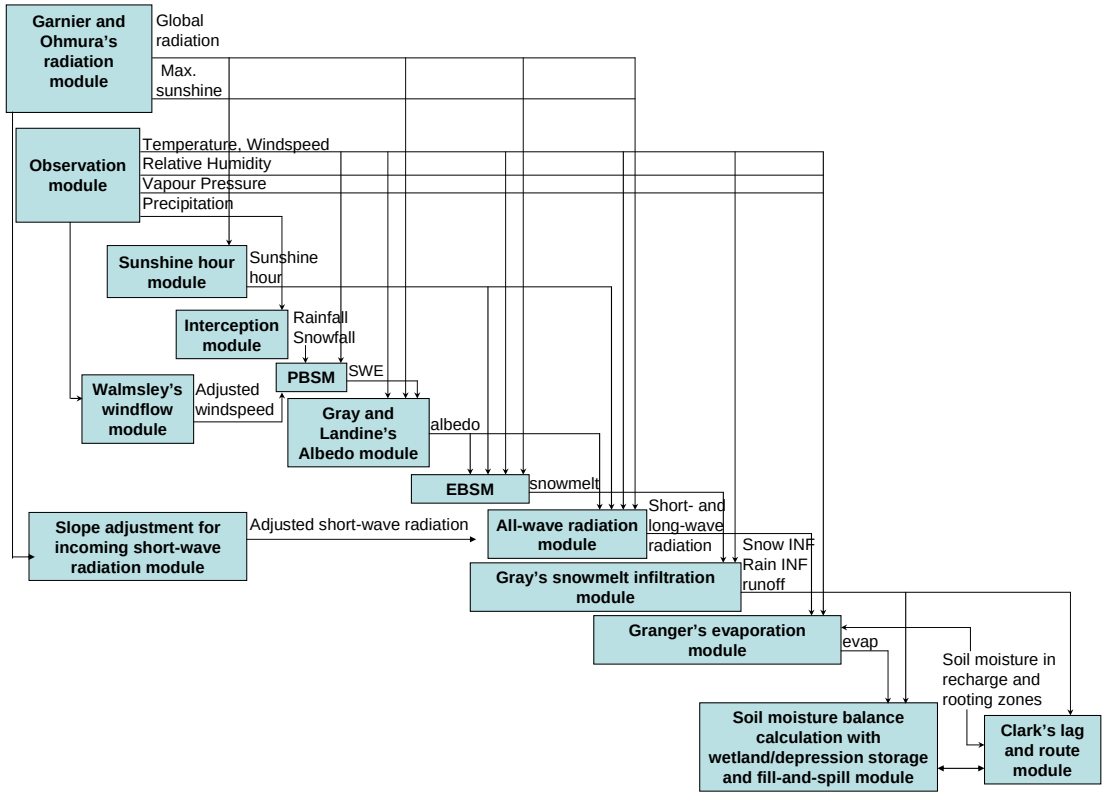

Figure 5. Flowchart of hydrological modules for Granger Basin CRHM test.

5. Gray and Landine's albedo module (Gray and Landine, 1987): estimates snow albedo throughout the winter and into the melt period and also indicates the beginning of melt for the energy-budget snowmelt module;
6. PBSM module or Prairie Blowing Snow Model (Pomeroy and Li, 2000): simulates the wind redistribution of snow and estimates snow accumulation throughout the winter period;
7. Walmsley's windflow module (Walmsley et al., 1989): adjusts the wind speed change due to local topographic features and provides the feedback of adjusted wind speed to the PBSM module;
8. EBSM module or Energy-Budget Snowmelt Model (Gray and Landine, 1988): estimates snowmelt by calculating the energy balance of radiation, sensible heat, latent heat, ground heat, advection from rainfall, and change in internal energy;
9. all-wave radiation module: calculates net all-wave radiation from the short-wave radiation and provides inputs to the evaporation module;
10. infiltration module: Gray's snowmelt infiltration (Gray et al., 2001) estimates snowmelt infiltration into frozen soils and updates moisture content in the soil column for soil moisture balance module;
11. evaporation module: Granger's evaporation expression (Granger and Gray, 1989) estimates actual evaporation from unsaturated surfaces, update moisture content in the soil column for soil moisture balance module;
12. soil moisture balance calculation with wetland/depression storage and fill-and-spill module: this is a newly developed module for basins with prominent wetland storage and drainage attributes. This new wetland module was developed by modifying a soil moisture balance model, which calculates soil moisture balance and drainage (Dornes et al., 2008). This model was modified from an original soil moisture balance routine developed by Leavesley et al. (1983);
13. lag and route runoff module: this is a Clark's lag and route timing estimation procedure for runoff routing (Clark, 1945).

Observations

The model simulation for Granger Basin was carried out from 1 October 1998 to 30 June 1999. Meteorological forcing data during this period were obtained from the stations within Granger Basin, including station GB2, 3, 4, 5 and Plateau. The forcing data for the model consisted of air temperature (t, ˚C), relative humidity (rh, %), wind speed (u, m s^{-1}), precipitation (p, mm), and incoming short-wave radiation (Q_{si}, W m^{-2}) at hourly intervals. The precipitation includes both snowfall and rainfall and was corrected to account for the elevation effects for different stations; snowfall was corrected for the wind undercatch. Each HRU used its respective station data, and Table 1 shows the corresponding stations for different HRUs.

In addition, 11 observations of snow accumulation were conducted on the snow transect across the Granger Creek valley from south-facing slope to north-facing slope during January-May 1999. The observations provided the pre-melt snow accumulation and snowmelt information for both south-facing and north-facing slopes as well as the valley bottom. Also, salt dilution experiments were carried out in the spring of 1999 to generate accurate channel discharge information for Granger Creek.

Table 1. Granger Basin meteorological stations.

HRU Name	Station
UB	GB5
PLT	PLT
NF	GB4
SF	GB3
VB	GB2

3.2.1.2 CRHM parameterisation for Granger Basin

Basin area
Intense surveys were conducted to determine the size of the basin as well as ways to delineate HRU within Granger Basin (McCartney et al., 2006). The area values for five HRUs were summarized by MacDonald et al. (2009) and were used for this modelling project.

Aspect, slope and elevation
An analysis using ArcGIS was carried out to estimate the aspect, slope, and elevation values. The respective average values of aspect, slope, and elevation were generated and used for each HRU.

Fetch distance
A computer program "FetchR" (Lapen and Martz, 1993) was used to estimate the fetch distance and the resulted values were reported in the literature (MacDonald et al., 2009).

Vegetation information
Vegetation heights determined by surveys were used for the model simulations. These are widely reported values (Quinton et al., 2005; McCartney et al., 2006; Dornes et al., 2008; MacDonald et al., 2009). In addition, reported values of vegetation density and vegetation stalk density by MacDonald et al. (2009) were used.

Blowing snow redistribution factor
Scheme 2 for snow redistribution allocation by MacDonald et al. (2009) was used to sect the redistribution factor for the blowing snow simulation.

Frozen infiltration parameters
Initial soil saturation prior to the snowmelt infiltration was estimated from both pre-melt soil moisture content and soil porosity. The pre-melt soil moisture was determined from water content reflectometer measurements at each station. Soil type (organic and mineral soils) and their porosity values were reported in literatures (Carey and Woo, 2005; Quinton et al., 2005) and are used for estimation of initial soil saturation. Furthermore, initial soil temperature was determined by soil thermocouple measurements prior to the major snowmelt. The environment coefficient and surface saturation were set up based on

the recommended values from Gray et al. (2001). Infiltration opportunity time was calculated by model simulation.

Soil and routing parameters
Previous studies on soil properties in the Wolf Creek (Carey and Quinton, 2004; Carey and Woo, 2005; Quinton et al., 2005) found that the active soil layer was composed of top organic soil layer with underneath mineral soil layer. The depth and porosity values for both organic and mineral soil layers were used to approximate the capacity of the soil column layer. The initial value available water in the soil column layer was assumed to be 50% of the soil column capacity. Soil recharge zone, a top layer of soil column, was assumed to be shallow and saturated. Moreover, capacity of surface depressional storage was assumed to be small for the initial model simulation, and GIS analysis will be undertaken in the future to derive the storage information for the depressions. In addition, a simple linear sequence routing order was used: 'PLT' HRU goes to 'NF' HRU, and 'UB', 'NF', and 'SF' HRUs routed to 'VB' HRU, which is the outlet of Granger Basin.

3.2.1.3 Preliminary results for Granger Basin

The model simulations of snow accumulation for Granger Basin and spring channel discharge for the Granger Creek were conducted from 1 October 1998 to 30 June 1999. The preliminary results of winter snow accumulation and spring runoff discharge are shown in Figure 6 and 7, respectively.

Comparisons between the observed simulated snow accumulations during pre-melt and melt periods as well as observed and simulated spring discharge were taken. The results of comparison for snow accumulation and discharge are shown in Figure 8 and 9, respectively. The pre-melt snow accumulation during January-March was well simulated for south-facing, north-facing, and valley bottom as well as the Granger Basin compared to the observations. The spatial difference of pre-melt snow accumulation is reasonably simulated; that is, more snow is accumulated in north-facing slope and valley bottom when compared to south-facing slope. The difference between the observation and simulation of snow accumulation in the melt period (April-May) is large for the south-facing slope and valley bottom, while the difference for north-facing slope and the whole Granger Basin is smaller (Figure 8). Figure 9 illustrates that the discharge of Granger Creek is quite small in the spring 1999 and some discrepancy exits between the observed and simulated values. With calibration this discrepancy could be compensated for, but mimicking the hydrograph is not the point of this exercise and for a no calibration run it shows promise.

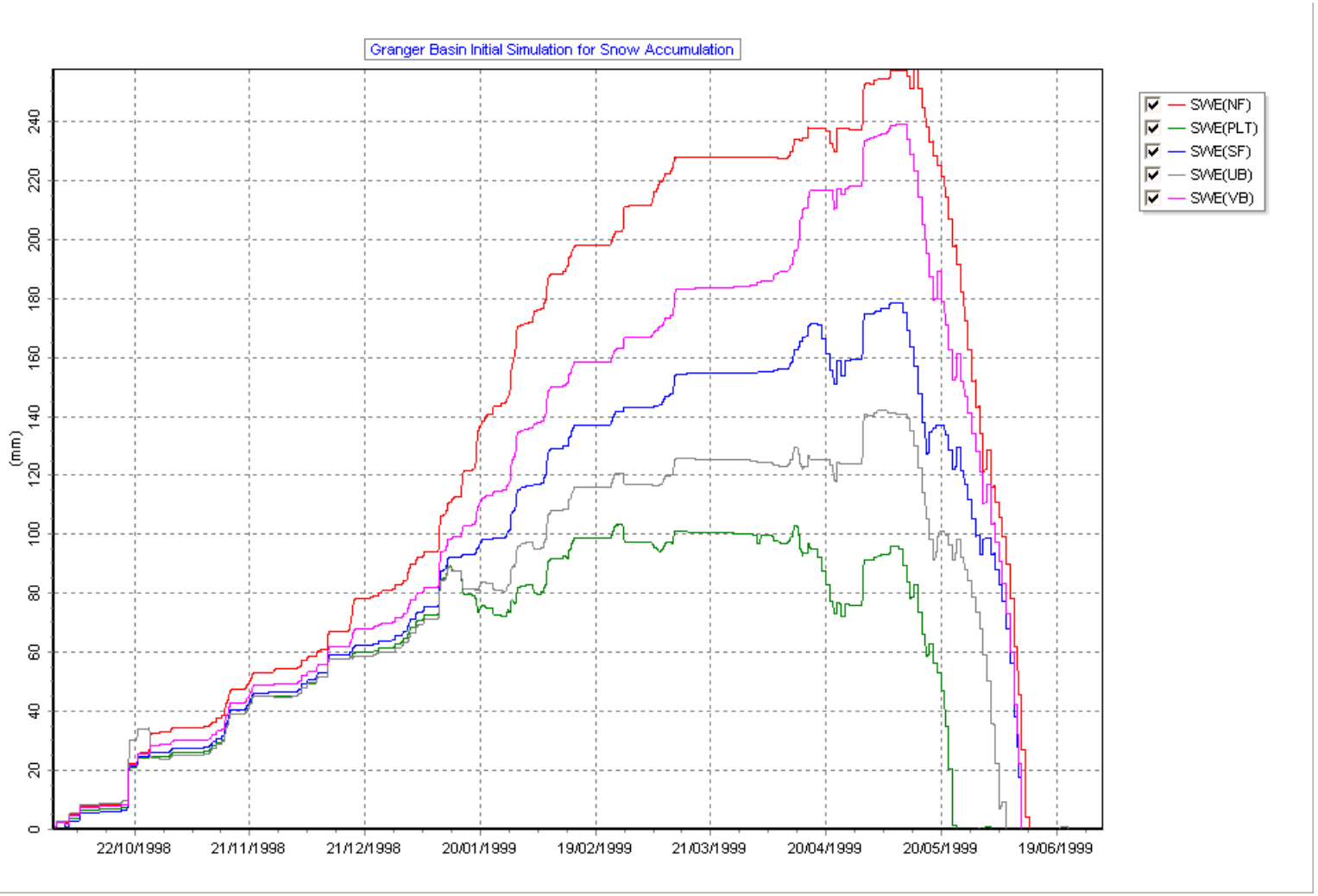

Figure 6. CRHM initial simulation for snow accumulation in the Granger Basin during 1 October 1998-30 June 1999 for HRUs: north-facing (NF), plateau (PLT), south-facing (SF), upper basin (UB), and valley bottom (VB).

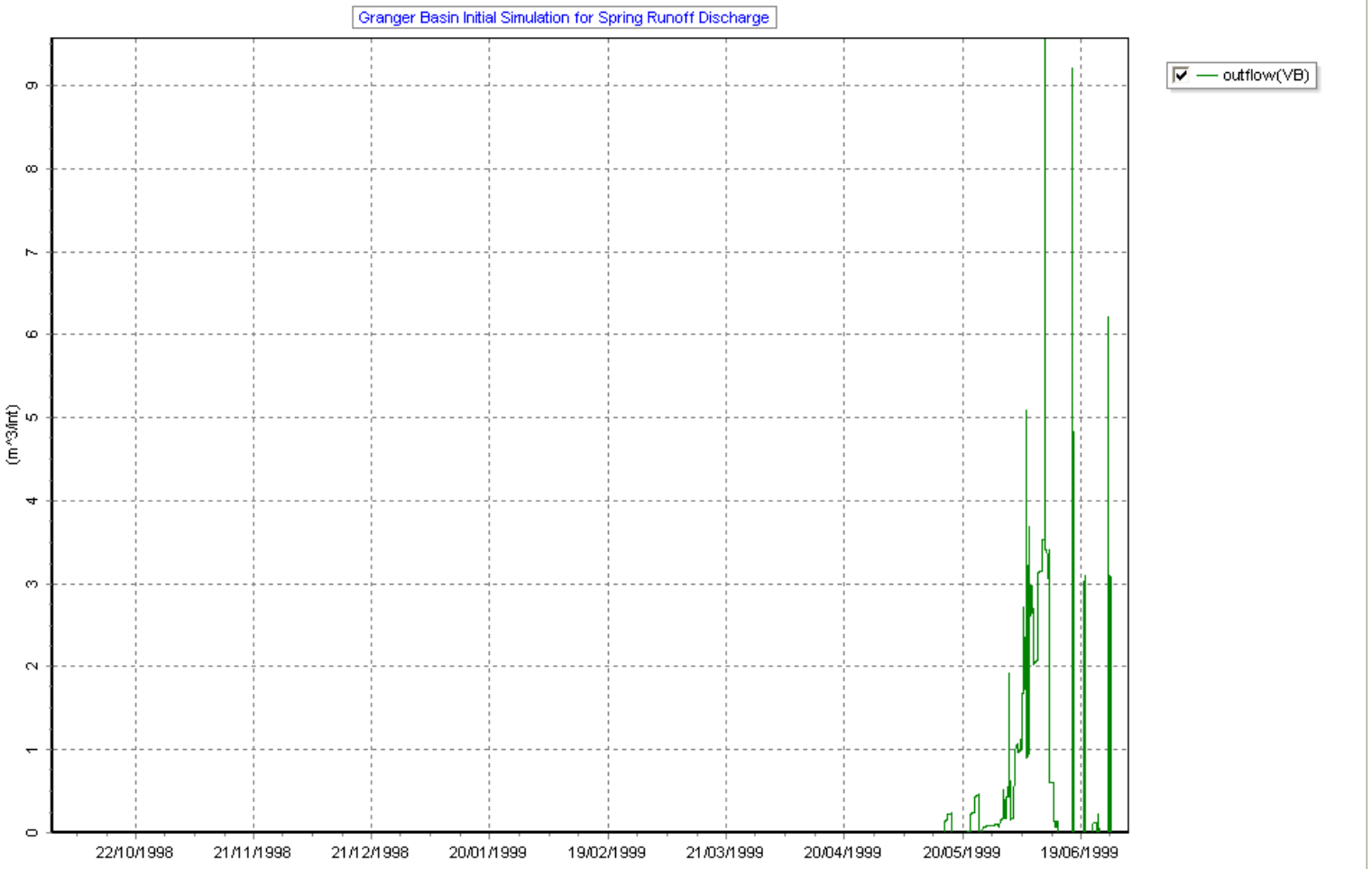

Figure 7. CRHM initial simulation for runoff discharge of Granger Creek in spring 1999.

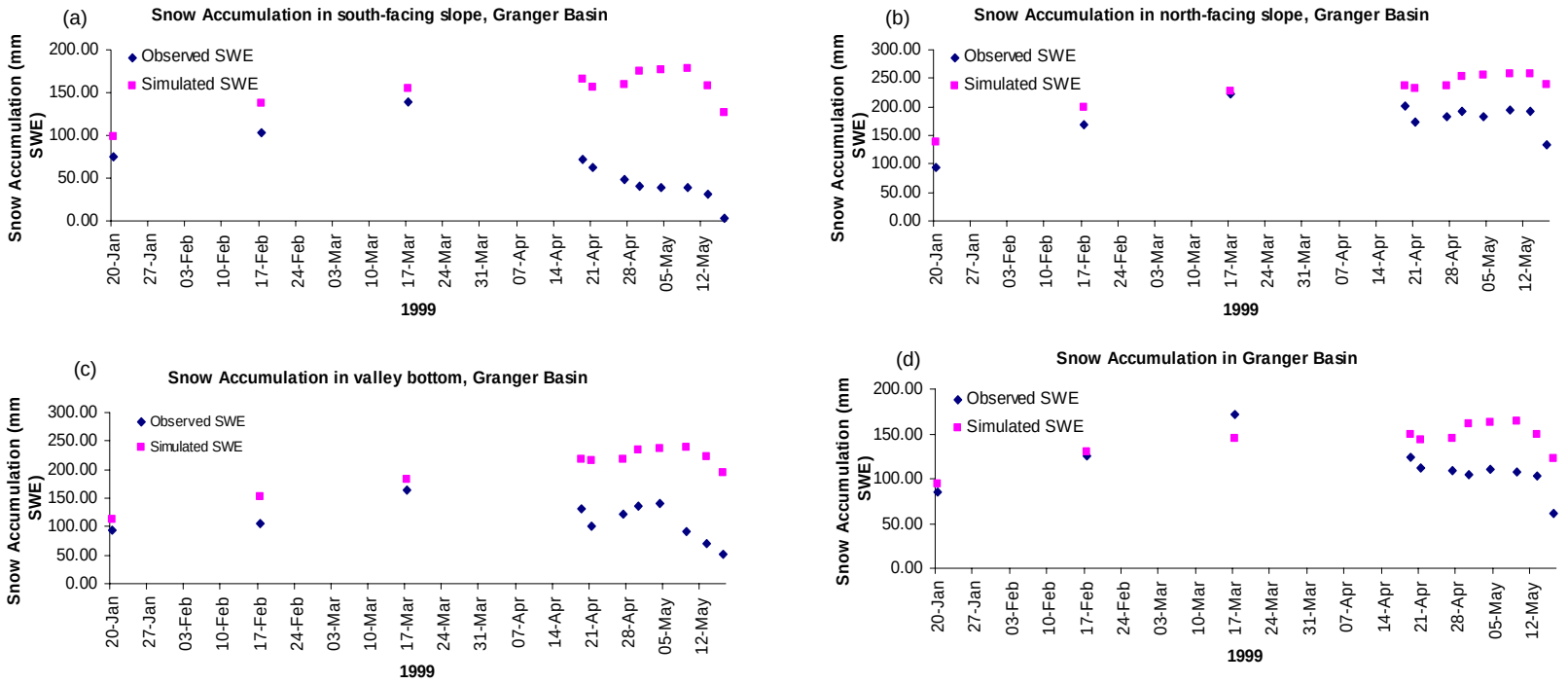

Figure 8. Comparisons of observed and simulated snow accumulation during January-May 1999 for (a) south-facing slope, (b) north-facing slope, (c) valley bottom, and (d) Granger Basin.

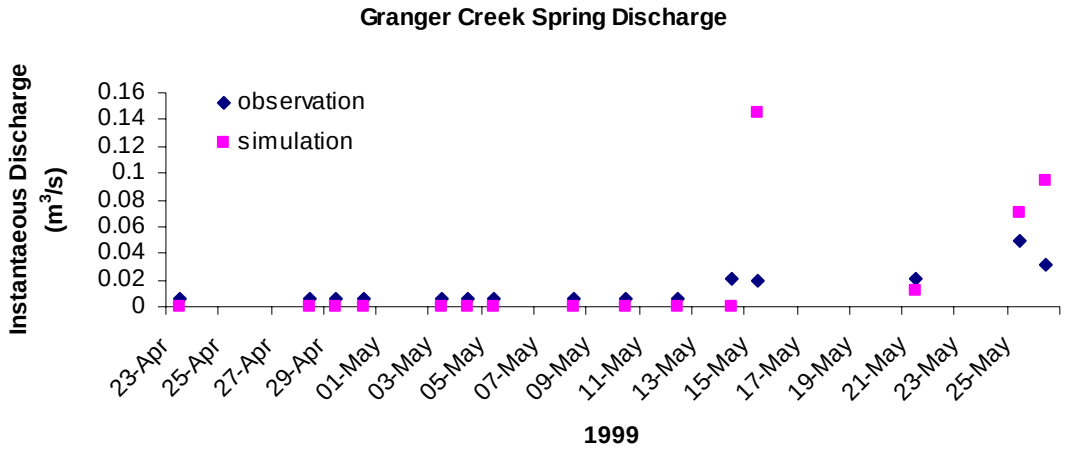

Figure 9. Comparison of observed and simulated instantaneous discharge of Granger Creek in spring 1999.

To evaluate the model performance for these initial simulations, root mean square difference (RMSD) is computed (Table 2). The RMSD is quite large for south-facing and valley bottom SWE, 31.3 and 31.1 mm, respectively, and with a smaller value of RMSD for north-facing slope. The RMSD for the area-weighted snow accumulation of Granger Basin and the instantaneous spring discharge of Granger Creek is 12.5 mm SWE and 0.013 $m^3 s^{-1}$, respectively. It should be noted that values of RMSD for snow accumulation are strongly affected by the relatively poorer simulations in the melt period – the accumulation periods are well simulated. The initial simulations at the moment are conducted with no calibration; better simulations can be achieved with calibrations as discussed by Dornes et al. (2008).

Table 2. Evaluation of initial simulations of snow accumulation and spring discharge with root mean square difference (RMSD) (n = 11).

	Snow Accumulation (mm)	Spring Discharge ($m^3 s^{-1}$)
South-facing slope	31.3	N/A
North-facing slope	17.8	N/A
Valley Bottom	31.1	N/A
Granger Basin	12.5	0.013

3.2.2 Wolf Creek Basin Test

With the modelling strategy and parameterisation experience gained from the initial simulations from the Granger Basin, a new CRHM project was set up for the entire Wolf Creek Research Basin (WCRB). The WCRB is a large basin (~195 km^2) and consists of three principle ecosystems, boreal forest, subalpine taiga (shrub-tundra) and alpine tundra. Thus, in addition to the physically process modules used for the Granger Basin, a newly developed 'Canopy' module was incorporated into the model to simulate hydrological processes in the boreal forest environment.

3.2.2.1 CRHM structural setup

HRU setup

Three hydrological response units (HRUs): alpine tundra, subalpine taiga (buckbrush taiga), and forest were set up for the WCRB shown in Figure 10. These HRUs are essentially ecozone units (Janowicz, 1999).

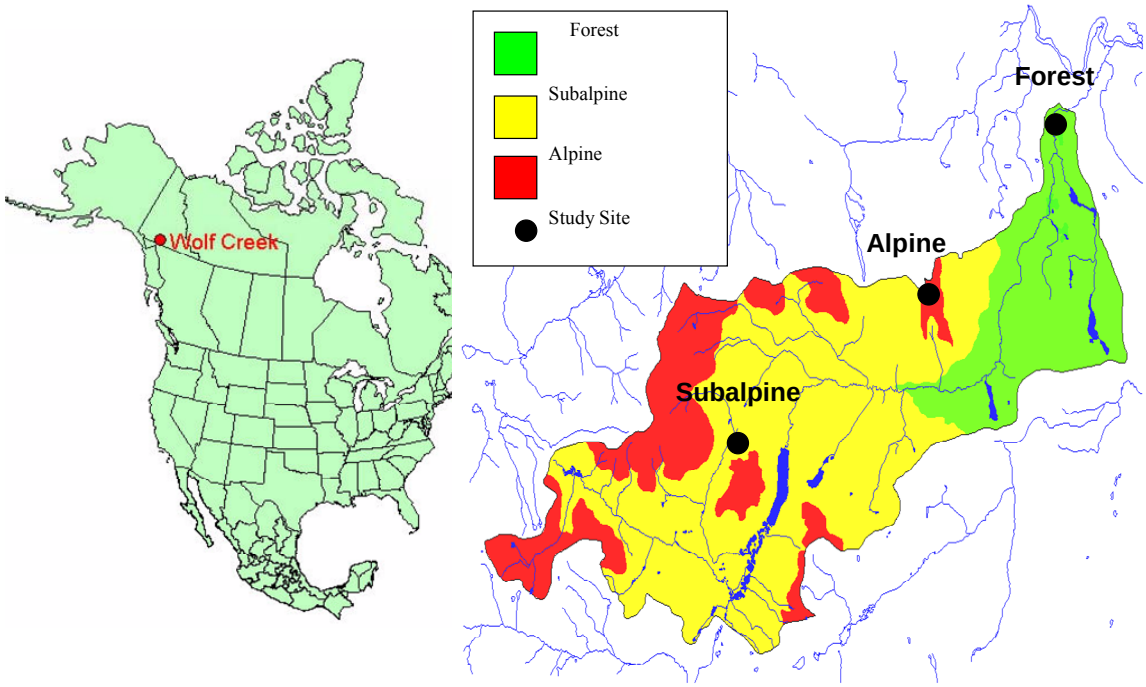

Figure 10. HRUs setup for the Wolf Creek Research Basin, Yukon. Black dots denote the location of study site and meteorology station for each HRU.

Module setup

A set of physically process based modules was linked in a sequential fashion to simulate the hydrological processes for the Wolf Creek Research Basin. Figure 11 shows the schematic of these modules, and these modules include:

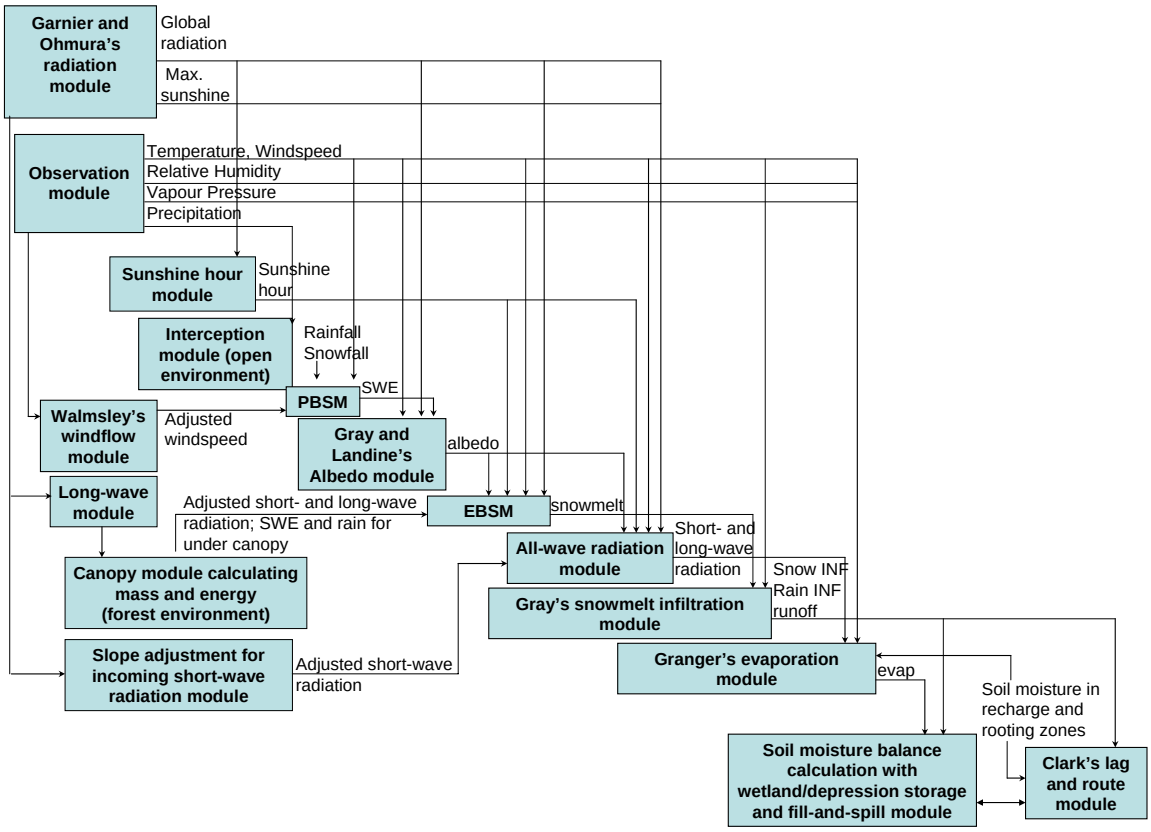

Figure 11. Flowchart of physically based hydrological modules for Wolf Creek Basin.

1. observation module: reads the meteorological data (temperature, wind speed, relative humidity, vapour pressure, precipitation, and radiation), providing these inputs to other modules;
2. Garnier and Ohmura's radiation module (Garnier and Ohmura, 1970): calculates the theoretical global radiation, direct and diffuse solar radiation, as well as maximum sunshine hours based on latitude, elevation, ground slope, and azimuth, providing radiation inputs to sunshine hour module, energy-budget snowmelt module, net all-wave radiation module;
3. sunshine hour module: estimates sunshine hours from incoming short-wave radiation and maximum sunshine hours, generating inputs to energy-budget snowmelt module, net all-wave radiation module;
4. module for incoming short-wave radiation adjustment for slope;
5. Gray and Landine's albedo module (Gray and Landine, 1987): estimates snow albedo throughout the winter and into the melt period and also indicates the beginning of melt for the energy-budget snowmelt module;
6. PBSM module or Prairie Blowing Snow Model (Pomeroy and Li, 2000): simulates the wind redistribution of snow and estimates snow accumulation throughout the winter

period, and this is module is used for open environments such as alpine tundra and subalpine taiga;
7. Walmsley's windflow module (Walmsley et al., 1989): adjusts the wind speed change due to local topographic features and provides the feedback of adjusted wind speed to the PBSM module;
8. canopy module (Ellis et al., 2010): this is newly developed in CRHM, and the module has snow-mass balance, rainfall interception and evaporation, and snow energy-balance components and is used for forest environment;
9. EBSM module or Energy-Budget Snowmelt Model (Gray and Landine, 1988): estimates snowmelt by calculating the energy balance of radiation, sensible heat, latent heat, ground heat, advection from rainfall, and change in internal energy;
10. all-wave radiation module: calculates net all-wave radiation from the short-wave radiation and provides inputs to the evaporation module;
11. infiltration module: Gray's snowmelt infiltration (Gray et al., 2001) estimates snowmelt infiltration into frozen soils and updates moisture content in the soil column for soil moisture balance module;
12. evaporation module: Granger's evaporation expression (Granger and Gray, 1989) estimates actual evaporation from unsaturated surfaces, update moisture content in the soil column for soil moisture balance module;
13. soil moisture balance calculation with wetland/depression storage and fill-and-spill module: this is a newly developed module for basins with prominent wetland storage and drainage attributes. This new wetland module was developed by modifying a soil moisture balance model, which calculates soil moisture balance and drainage (Dornes et al., 2008). This model was modified from an original soil moisture balance routine developed by Leavesley et al. (1983);
14. lag and route runoff module: this is a Clark's lag and route timing estimation procedure for runoff routing (Clark, 1945).

3.2.2.2 Observations

The model simulation for was carried out from 1 October 1998 to 11 July 1999. Meteorological forcing data during this period were obtained from hydrometeorological stations within Wolf Creek Research Basin, including the alpine tundra, buckbrush taiga, and white spruce forest stations. The forcing data for the model consisted of air temperature (t, $^{\circ}$C), relative humidity (rh, %), wind speed (u, m s^{-1}), precipitation (p, mm), and incoming short-wave radiation (Q_{si}, W m^{-2}) at hourly intervals. For the 'alpine tundra' HRU, no record of snowfall and rainfall exists and the wind undercatch corrected precipitation from the nearby upper Granger basin was used. For the 'subalpine taiga' HRU, the precipitation record at the buckbrush standpipe was used and corrected for the wind undercatch. For the 'forest' HRU, there is no precipitation record and the wind undercatch corrected precipitation from the Whitehorse airport (~15 km^2 to the north) was used.

Additionally, observations of snow accumulation were conducted on snow survey transects at the alpine tundra, buckbrush taiga, and white spruce forest sites during 1998-99. The observations provided the pre-melt snow accumulation and snowmelt

information for alpine, subalpine, and forest environments. A hydrometric station located at the outlet of the Wolf Creek basin provided measured basin discharge data.

3.2.2.3 Model parameterisation

Basin area
The total basin of 195 km^2 was used, and HRU area was set as 39, 113, and 43 km^2 for alpine, subalpine, and forest HRUs, respectively. These were decided from reported values (Janowicz, 1999).

Aspect, slope and elevation
An analysis using ArcGIS was carried out to estimate the aspect, slope, and elevation values. The respective average values of aspect, slope, and elevation were generated and used for each HRU.

Fetch distance
Long fetch distancea (i.e. 1000 m) were used for the open environments (e.g. alpine and subalpine shrub tundra HRUs). Short fetch distances (i.e. 300 m) were used for the forest environment.

Vegetation information
Vegetation heights determined by field surveys were used for the model simulations.

Blowing snow redistribution factor
Values of blowing snow redistribution factor were 2 and 5 for the alpine and subalpine HRUs, respectively. The setup of redistribution factor allows snow to redistribute from the short alpine tundra HRU to the subalpine shrub tundra HRU. Blowing snow is inhibited for the forest HRU.

Frozen infiltration parameters
Initial soil saturation prior to the snowmelt infiltration was estimated from both pre-melt soil moisture content and soil porosity. The pre-melt soil moisture was determined from water content reflectometer measurements at each station. Soil type (organic and mineral soils) and their porosity values were reported in the literature (Carey and Woo, 2005; Quinton et al., 2005) and were used for estimation of initial soil saturation. Furthermore, initial soil temperature was determined by soil thermocouple measurements prior to the major snowmelt. The environment coefficient and surface saturation were set up based on the recommended values from Gray et al. (2001). Infiltration opportunity time was calculated by model simulation.

Soil and routing parameters
Previous studies on soil properties in the Wolf Creek (Carey and Quinton, 2004; Carey and Woo, 2005; Quinton et al., 2005) found that the active soil layer was composed of top organic soil layer with underneath mineral soil layer. The depth and porosity values for both organic and mineral soil layers were used to approximate the capacity of the soil

column layer. The initial value available water in the soil column layer was assumed to be 50% of the soil column capacity. The soil recharge zone, a top layer of soil column, was assumed to be shallow and saturated. Moreover, capacity of surface depressional storage was assumed for the initial model simulation, and GIS analysis will be undertaken in the future to derive the storage information for the depressions. Based on the observed evidence of good subsurface drainage in the Wolf Creek (Quinton et al., 2005), a subsurface drainage factor 20 mm d^{-1} was used for the initial simulations.

In addition, a simple linear sequence routing order was adapted: the 'alpine' HRU is routed to 'subalpine' HRU, which in turn is routed to 'forest' HRU that is set as the outlet of Wolf Creek basin. In the routing module, a lag time was used to delay the routing from each HRU to the basin outlet based on the concept of how long the runoff would be delayed in each ecozone HRU. For the initial simulations, 48 hours were assigned to the alpine tundra and subalpine shrub tundra HRUs, and 96 hours were set for the forest HRU. For the future simulations, a more sophisticated Muskingum routing will be used to calculate the routing time for different HRU. The usage of the Muskingum routing requires parameters of channel length, slope, shape, etc.; detailed analysis using GIS will be needed to estimate these parameters.

3.2.2.4 Preliminary results for Wolf Creek Research Basin

Initial simulations of snow accumulation were conducted for three ecozone HRUs: alpine tundra, subalpine shrub tundra, and conifer forest during 1 October 1998-10 July 1999 (Figure 12). The solid lines in the Figure 12 are the simulated evolution of snowpacks in each HRU during winter and spring periods; the dots shown in the Figure 12 represent the observed values of snow accumulation on the field transects in each HRU. The figure demonstrates the comparisons between simulated SWE for each ecozone HRU and observed SWE based on point observations in the corresponding HRU. The model generally simulated the sequence of snow accumulation well; subalpine shrub tundra (i.e. taller vegetated area) had more snow accumulation than the alpine tundra (i.e. shorter vegetated area) or the forest which had interception losses. During the snowmelt period (i.e. April and May), the model had better simulations for the alpine HRU than for the subalpine HRU. For the forest HRU, the newly developed forest canopy module was used to estimate the snow mass and energy balance in the forest environment, and blowing snow was inhibited. The simulated SWE during both pre-melt (i.e. February and March) and melt (i.e. April and May) had a fairly close agreement with the observed SWE. This test is quite encouraging for the further application of this forest module in CRHM.

In addition, model simulations of spring discharge were carried out for the Wolf Creek basin in spring 1999 (Figure 13). The comparison between the simulated and observed

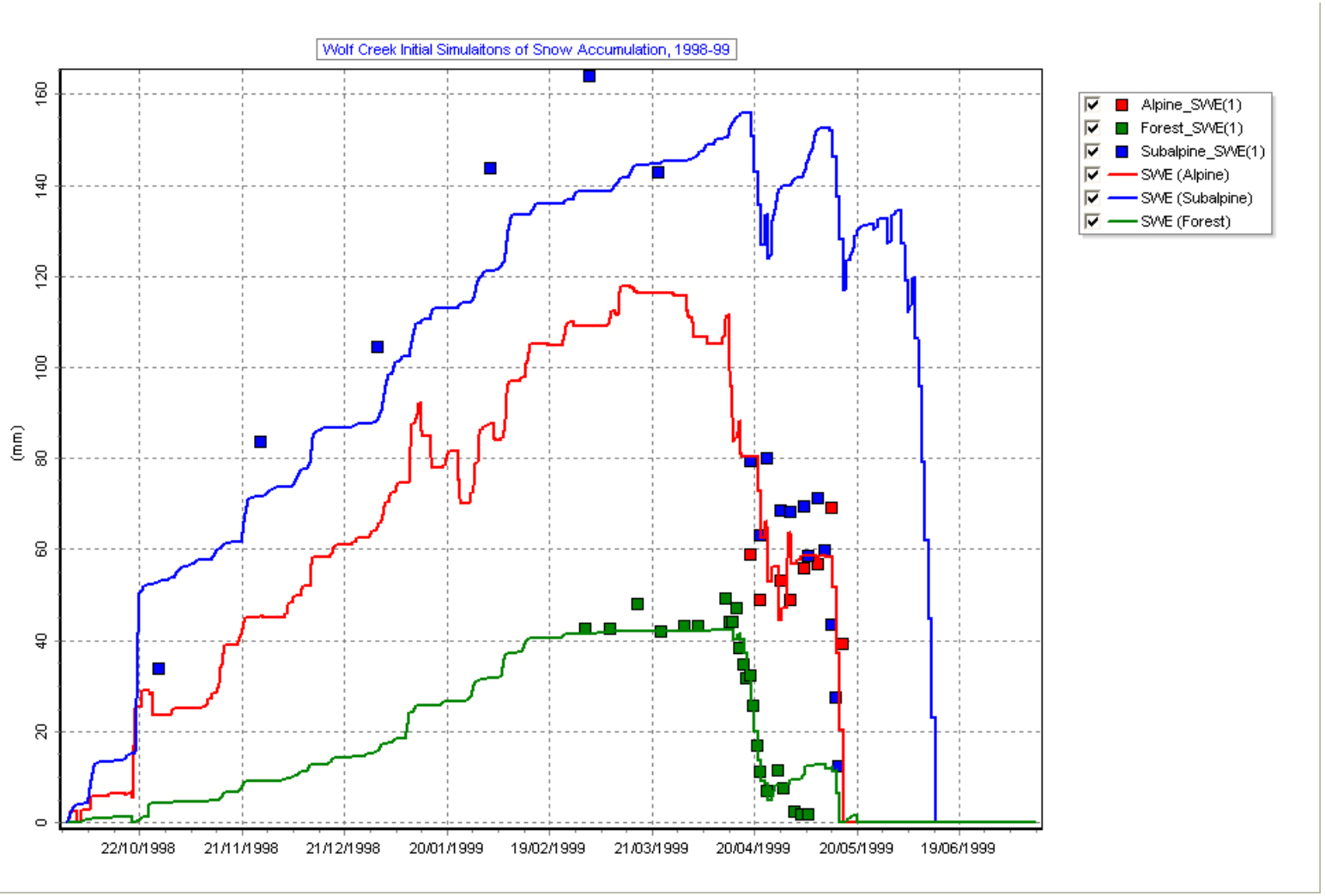

Figure 12. CRHM initial simulation for snow accumulation in the Wolf Creek Research Basin during 1 October 1998-11 July 1999 for HRUs: alpine, subalpine, and forest. The solid lines are the time-series of simulated SWE (mm); the dots are the observed SWE from the transects in each HRU.

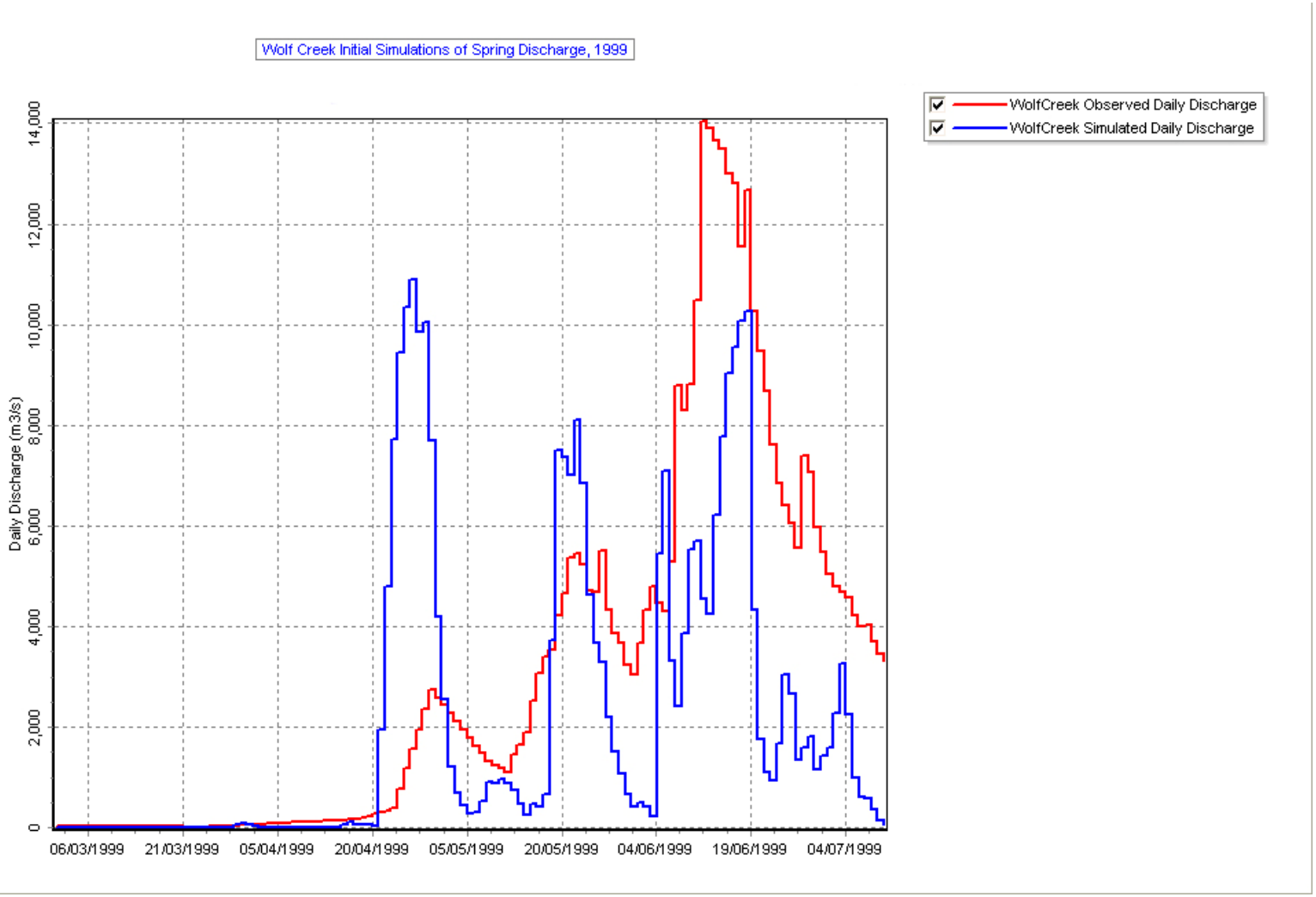

Figure 13. CRHM initial simulation for daily runoff discharge of Wolf Creek basin in spring 1999. The solid lines in red and blue are for observation and simulation, respectively.

basin daily discharge in the Figure 13 illustrates that there are differences between the model simulation of basin discharge and the discharge observed at the basin outlet. That is, both peak discharge and total volume of the discharge are not comparable between the simulation and observation. There are reasons for these initial simulated results. The first one is only three ecozone HRUs were set up for the Wolf Creek Research Basin and this preliminary setup might be insufficient for the complex environment, and other criteria (e.g. aspect, landscape) will need to be incorporated into HRU setup for the future model simulations. Another reason is that the preliminary model run was created with simple routing module that does not consider the physiographic characteristics of stream channels; a more physically based routing module – Muskingum routing will be used for the future model runs. Finally, no calibration whatsoever was used and with parameter calibration the hydrograph could be fitted better. However, the point of this exercise was not to mimic the hydrograph but to demonstrate the model physics against two objective parameters and this is a satisfactory first test.

3.3 Conclusions for CRHM Tests

CRHM was set up to comprehensively calculate the cold regions hydrological cycle in Granger Creek Sub-basin and Wolf Creek Basin. The model included components dealing with blowing snow, intercepted snow, sublimation, energetics of snowmelt, forest effects on meltrate, infiltration to frozen soils, soil moisture balance, fill and spill runoff generation and basic basin routing. This if the first time to the Authors' knowledge that such a comprehensive year-found calculation has been performed for a Yukon basin. The tests were satisfactory in that all the modules represented the processes and produced features of snow redistribution, forest interception effects and variable melt rates that are consistent with the physics of hydrology in the region. The simple tests were not calibrated and so there was no attempt to match snow accumulation regimes or streamflow hydrographs, but the similarity of some model runs to observations suggests that with minimal calibration the model could produce reasonable simulations of streamflow for the Wolf Creek main basin and its sub-basins.

3.4 CRHM Modelling References

Carey, S.K. and Quinton, W.L. 2004. Evaluating snowmelt runoff generation in a discontinuous permafrost catchment using stable isotope, hydrochemical and hydrometric data. Nordic Hydrology **35**: 309-324.

Carey, S.K. and Woo, M.K. 2005. Freezing of subarctic hillslopes, Wolf Creek Basin, Yukon, Canada. Arctic, Antarctic, and Alpine Research **37**: 1-10.

Clark, C.O. 1945. Storage and the unit hydrograph. Proceedings of the American Society of Civil Engineering **69**: 1419-1447.

Dornes, P.F., Pomeroy, J.W., Pietroniro, A. and Verseghy, D.L. 2008. Effects of spatial aggregation of initial conditions and forcing data on modeling snowmelt using a land surface scheme. Journal of Hydrometeorology **9**: 789–803.

Ellis, C.R., Pomeroy, J.W., Brown, T. and MacDonald, J. 2010. Simulation of snow accumulation and melt in needleleaf forest environments. Hydrology Earth System Sciences Discussions **7**: 1033-1072.

Garnier, B.J. and Ohmura, A. 1970. The evaluation of surface variations in solar radiation income. Solar Energy **13**: 21-34.

Granger, R.J. and Gray, D.M. 1989. Evaporation from natural non-saturated surfaces. Journal of Hydrology **111**: 21–29.

Gray, D.M. and Landine, P.G. 1987. Albedo model for shallow prairie snow covers. Canadian Journal of Earth Sciences **24**: 1760-1768.

Gray, D.M. and Landine, P.G. 1988. An energy-budget snowmelt model for the Canadian Prairies. Canadian Journal of Earth Sciences **25**: 1292-1303.

Gray, D.M., Toth, B., Zhao, L., Pomeroy, J.W. and Granger, R.J. 2001. Estimating areal snowmelt infiltration into frozen soils. Hydrological Processes **15**: 3095-3111.

Janowicz, J.R. 1999. Wolf Creek Research Basin – overview. In Pomeroy, J.W. and Granger, R.J. (Eds), Wolf Creek Research Basin: Hydrology, Ecology, Environment. Saskatoon: Environment Canada, pp. 121-130.

Lapen, D.R. and Martz, L.W. 1993. The measurement of two simple topographic indices of wind sheltering exposure from raster digital elevation models. Computer & Geosciences **19**: 769-779.

Leavesley, G.H., Lichty, R.W., Troutman, B.M. and Saindon, L.G. 1983. Precipitation-runoff modelling system: user's manual. US Geological Survey Water Resources Investigations Report 83-4238. 207 pp.

MacDonald, M.K., Pomeroy, J.W. and Pietroniro, A. 2009. Parameterizing redistribution and sublimation of blowing snow for hydrological models: tests in a mountainous subarctic catchment. Hydrological Processes **23**: 2570-2583.

McCartney, S.E., Carey, S.K. and Pomeroy, J.W. 2006. Intra-basin variability of snowmelt water balanced calculations in a subarctic catchment. Hydrological Processes **20**: 1001–1016.

Pomeroy, J.W. and Li, L. 2000. Prairie and Arctic areal snow cover mass balance using a blowing snow model. Journal of Geophysical Research **105**: 26619-26634.

Pomeroy, J.W., Gray, D.M., Brown, T., Hedstrom, N.R., Quinton, W., Granger, R.J. and Carey, S. 2007. The Cold Regions Hydrological Model, a platform for basing process representation and model structure on physical evidence. Hydrological Processes **21**: 2650–2667.

Quinton, W.L., Shirazi, T., Carey, S.K. and Pomeroy, J.W. 2005. Soil water storage and active-layer development in a subalpine tundra hillslope, southern Yukon Territory, Canada. Permafrost Periglacial Processes **16**: 369–382.

Walmsley, J.L., Taylor, P.A. and Salmon, J.R. 1989. Simple guidelines for estimating windspeed variations due to small-scale topographic features – an update, Climatological Bulletin **23**: 3-14.

4.0 Introduction to the Hydrograph Model

The objective of this section of the report is to demonstrate the application of the Hydrograph model, developed by Prof. Yuri Vinogradov and Dr. Olga Semenova, currently at the Russian State Hydrological Institute (SHI) in St. Petersburg, for the conditions of the watersheds in the Yukon, and, specifically the Wolf Creel experimental watershed. This model is developed with physically based parameters and has proven to be able to provide good simulations of runoff at spatial scales ranging from a few square km to watersheds of over 2.4 Million km^2 in watersheds in both European Russia and Siberia, in conditions quite similar to those found at the Wolf Creek watershed. Consequently, the model has the potential for operational forecasting use in both flash floods and main stem floods.

The results presented in this section should be considered to be preliminary, given the incompleteness of the data required to run the model with directly observable parameters. We will continue to refine the information to take advantage of the best characteristics of the Hydrograph model, namely its ability to use parameters that are obtained directly from field observations.

4.1 Model Description

4.1.1 Basic model structure

In this section a concept of the basic model elements is presented. These will be described in more detail below.

In the horizontal dimensions, the model divides the watershed into a number of Representative Points (RP). Although the area represented by each point could be arbitrary, we have chosen each area to be a regular hexagon (see Fig. 1). Also in the horizontal dimensions, the watershed is divided into the runoff formation complexes, or RFCs which are assumed to be homogeneous for soils, vegetation, topography, hydrology, etc. and which may cover from a fraction of an RP to several RPs. An RFC is analogous to the hydrological response unit discussed for CRHM.

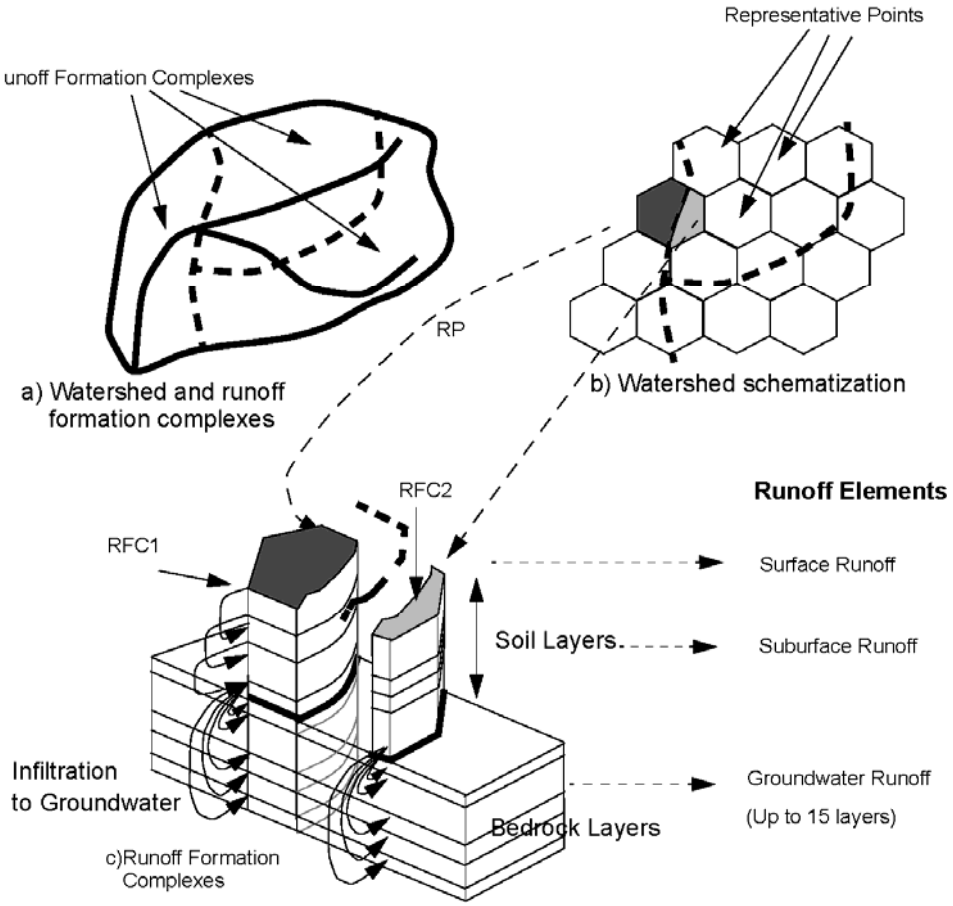

Figure 1. Basin schematization in the Hydrograph model

In the vertical direction, the model represents the soil column with at least 3 strata (usually, up to 10-15), for which energy and water balances are computed, and whose physical properties (model parameters) are arranged by RFCs. In addition, the model considers 15 layers for the deeper ground water flows, for which only the water balance is computed (See the section on runoff elements below).

The model algorithm includes the following computational routines:
i) precipitation and its interception,
ii) snow accumulation and melting,
iii) evaporation from snow,
iv) soil and vegetation cover,
v) surface flow and infiltration,

vi) soil water dynamics and flow,
vii) heat dynamics and phase change in soil strata,
viii) ground flow formation,
ix) slope and channel flow transformation, and
x) flow discharge (see Fig. 2).
For a detailed description of approaches used in the model see Vinogradov & Vinogradova (2010), Vinogradov (2003a, b, c, d).

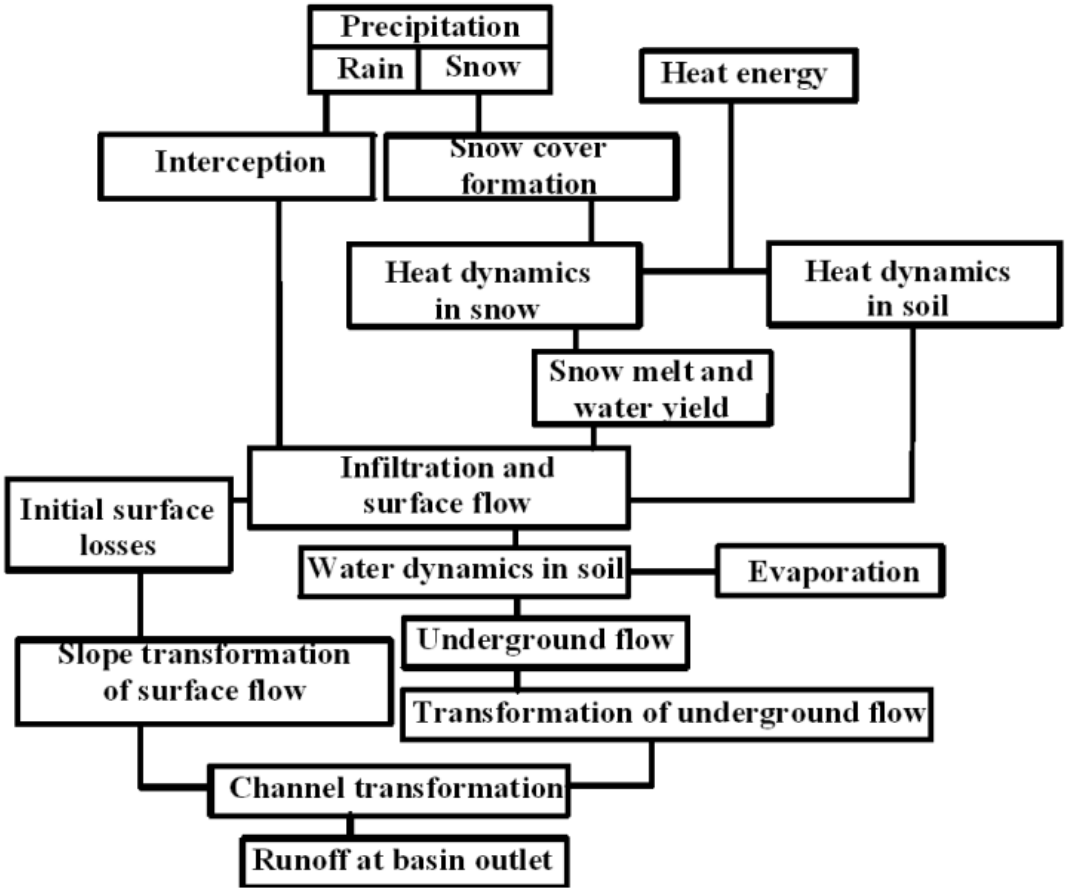

Figure 2. Block diagram of the Hydrograph model modules

The model input consists of standard meteorological information such as values of air temperature and relative humidity, precipitation.

As the model describes the complete land hydrological cycle it has various output results. First of all, there are the continuous runoff hydrographs at the outlet, from any part of the basin, from a specified landscape or any set of representative points. In addition, the model also presents the distributed state variables, reflecting water and heat dynamics in soil strata and snow cover. The model can be run at time intervals of one day or less, although it only has been tested with daily data. Results from the model, including spatial and temporal distribution of water balance elements including precipitation; evaporation from snow, soil and vegetation cover; surface, soil and underground runoff can be obtained at any averaging time interval.

4.1.2 Methodology of water movement in the basin

In this section we discuss three main processes which are at the heart of the Hydrograph model. They are:

i) infiltration, water movement in the soil layer, formation of classical surface and subsurface flow;
ii) slope (surface, subsurface and underground) inflow to channel network;
iii) flow routing.
We focus on these three problems because our approaches are particularly different from those used in conventional physically based models.

4.1.2.1 Formation of surface flow and infiltration

An initial and at the same time an important stage of mathematical model construction is getting a clear idea about the modelling objective formulated in the language of hydrology. The specific aspect here is the following: it is not suitable to apply the principles and approaches which are successfully used for description of phenomena of completely different character to the specification of other processes that have only formal resemblance (Myshkis, 1994). The one example of a contradiction of this rule seems to be the idea that sets the parallel between the "diffusion of water in soil" and heat conductivity, which is unfounded from our point of view: by this we mean the Richard's equation which is widely used in hydrology. Leaving without consideration the whole set of minor incongruities we mention just the context which shakes the base of this theory. For example, the coefficients of water hydraulic conductivity and diffusion are not constant, in contrast to the coefficients of heat conductivity. Moreover, they both depend on soil moisture content which is the main variable of the hydraulic conductivity equation in which they stay as coefficients. Within the range of natural soil moisture variation, the diffusion coefficient may change by 10^4 times and the hydraulic conductivity coefficient by 10^6–10^7 times (Gardner, 1960).

The problem is worsened by the inability of the analogy to describe soil water behaviour. The essence of the heat conductivity equation is connected with the idea of temperature distribution in a given volume. The behaviour of water in soil has a completely different character. Water contained in an upper layer of the soil does not drain down to the next layer, even if a strong gradient in soil moisture exists between both layers, until the maximum water holding capacity of the upper layer is satisfied. Another example is that the moisture rises up from a drier soil layer through a wet one to the evaporation surface, so called Haillare's effect (Haillare, 1960, 1962).

Let's consider the following simple approach. We imagine such a picture: during rainfall, drops are falling down on an elementary plot occasionally and independently of each other. The quantity and volume of drops per unit of area and time is determined by the rainfall intensity. It means that the rainfall intensity serves as an argument which together with the maximum possible infiltration rate (that is infiltration coefficient f_0) determines the relative size of infiltration area. We assume that the increment of the infiltration area corresponding to an increment of rainfall intensity i decreases proportionally to this area. Then it follows that the intensity of surface flow q is determined by Equation (1):

$$q = i - f = i - f_0\left[1 - \exp(-i / f_0)\right]. \qquad (1)$$

This allows us to draw attention at the inaccuracy of the statement (Horton's overland flow law) that rainfall results in soil surface impoundment if and only if the rainfall intensity exceeds the hydraulic conductivity of the saturated soil. In fact, surface runoff can form even in a case when the rainfall intensity is lower then infiltration coefficient (hydraulic conductivity of saturated soil).

Equation (1) allows us to calculate the surface flow formation by a given pluviogram. It is useful to get the equation for computation of surface flow for the whole period of rainfall apart from the initial losses. With this purpose let's turn to the possibility of transforming the stochastic process of rainfall intensity $i\{t\}$ to that of the rate of surface flow generation $q\{t\}$.

A stochastic function (or process) is such a function in which the variable is random regardless of any argument (in this instance time, t) value. For convenience we consider some random process

$$\mathrm{i}^*\{t\} = i\{t\}/I \tag{2}$$

where

$$I = (1/T)\int_0^T i\{t\}dt \tag{3}$$

is the mean rainfall intensity for the period of rainfall T. The fact is that the random process $\mathrm{i}^*\{\mathrm{t}\}$ has acquired the so named ergodic property, when each of its realizations is a valid element of a single stationary process whose statistical average is equal to 1. It is known that the distribution law of $i\{t\}$ can be suitably represented by an exponential distribution (see, for example, Eagleson 1978):

$$\varphi(\mathrm{i}) = (1/I)\exp(-i/I) \tag{4}$$

$$\varphi(i^*) = \exp(-i^*) \tag{5}$$

Herein, the asterisk notation (*) along with any argument indicates that the last is divided by I.

Accounting for the physical equation (1) the probabilistic average of random process such as the difference between the rainfall intensity and infiltration is calculated as

$$\mathrm{M}(\mathrm{q}^*) = \int_0^\infty \{i^* - f_0^*[1 - \exp(-i^*/f_0^*)]\}\varphi(i^*)di^* = 1/(f_0^* + 1) \tag{6}$$

Finally,

$$\mathrm{M}(\mathrm{q}) = I^2/(I + f_0) \tag{7}$$

Then the value of surface flow formation $\mathrm{H_q}$ during the period T is the following:

$$\mathrm{H_q} = H^2/(H + f_0 T) \tag{8}$$

where H is the precipitation depth, and equals I T.

The use of a constant infiltration rate is a key assumption of the Hydrograph model, and it is the main difference between our approach and the traditional Richard's equation-based approaches, VIC (Liang at al. 1994), tRib (Ivanov et al. 2004) etc., or even most conceptual models such as

the Stanford Watershed model (Crawford and Linsley, 1966), the Sacramento model (Burnash and Ferral, 1974), PRMS (Leavesley et al. 1983), to cite just a few. The variable infiltration rate can be observed under pressure head, which only occurs under ponding (if the underneath soil is dry), or on a dry floodplain, or under exceptionally heavy precipitation intensities. Then the traditional models assume a uniform wetting front across each grid cell. In our approach we are assuming that the infiltration rate is limited by the saturated conductivity, because, once the top layer of the soil becomes saturated (and it happens quickly even under moderate precipitation), that limits the amount of water that can be supplied to the lower layers. To allow for cracks, preferential infiltration paths, worm holes, etc. and those features that do occur in nature, it may be necessary to calibrate the infiltration coefficient.

After the filling of any discrete soil stratum to its maximum water holding capacity, water starts to flow to the next underlying layer. Water leaving the last discrete soil stratum is redistributed between different aquifers. This distribution is controlled by means of coefficients that require manual calibration.

4.1.2.2 Concept of runoff elements

The concept of runoff elements, briefly stated here, offers the possibility of a unified methodological approach to modelling the surface, subsurface and underground runoff of different layers. The solution of the multiple-scale problem by means of directly including the basin area into the algorithms of conversion of runoff elements parameters into coefficients of main calculating equations is presented below.

Water flowing before it reaches the river network is dispersed over the runoff elements. These are the natural formations originating as a result of the interaction between water on one hand, and soil cover and the upper layer of the lithosphere on the other hand. The runoff elements can be surface, subsurface (soil) and underground. Their linear dimensions change over an extremely wide range: from several centimetres (at the surface of eroded slopes) to many (tens, hundreds, thousands) kilometres (in the underground lithosphere structures).

The theory of runoff elements is very simple. The basis is the usual water balance relation

$$dW / dt = S - R \qquad (9)$$

where W is the water volume that is accumulated by runoff element (m^3), S and R – inflow and outflow to/from it (m^3 sec^{-1}). There is the nonlinear relation between W and outflow discharge R described in the model by an empirical equation:

$$R = b[\exp(aW) - 1] \qquad (10)$$

From Equation (10) it is possible to derive the corresponding equation of the outflow hydrograph from runoff elements of a given layer, although the derivation is too elaborate to be included here:

$$R = (S + b) / \{1 + [(S - R_0) / (R_0 + b)] \exp[-a\Delta t(S + b)]\} - b \qquad (11)$$

Here R_0 is the initial value of runoff R and S is the input rate (m^3 s^{-1}); Δt is the computational time interval (sec) during which S is constant; where a, b - hydraulic coefficients (which determine the conditions of outflow) with dimension m^{-3} and m^3 s^{-1} In the general case, we can assume that the number of runoff elements is proportional to the basin area F (m^2) or a fraction

of it ΔF, as we'll see below and then a=a*×F-1 and b=b*×F. The coefficients a* and b* are the subject of our further intent attention.

It is useful to attach to the coefficient a* the status of a conditional constant systematized by types of flow and the coefficient b* to put into the list of main parameters of runoff model. The units are the following: a* – m^{-1}, b* – m sec^{-1}, F – m2. The product $ab = a*b* = \tau*$ can be named as the specific time of discharging of a runoff element. In addition, the specific values of outflow q and water storage J have sense. They are also determined by the values of the conditional constant a*, parameter b* and are connected by the relation

$$J = \ln\left(q / b^* + 1\right) / a^* \qquad (12).$$

Next, we offer a probable idealization – hierarchical sequence of layers of runoff elements arrangement which take part in river inflow. It does not contradict known processes, phenomena and laws.

All specific values of runoff elements are determined by the conditional constant a* and the median value of parameter b*=10^{-6} m sec^{-1}. The "constant" itself is sequentially determined by expression a*=10^{i}, where i=3 for surface flow, i=2 for subsurface flow, and further for different layers of underground flow from i=1 to i=–6 with step Δ= 0,5. Let's accept some logical and expected assumption: the infiltration capacity of water-holding rocks naturally decrease with increase of deepness. At the same time two empirical facts should be taken into account – the decrease of outflow rate and the simultaneous increase of water storage with depth in groundwater aquifers. So we postulate the following hierarchical system of layers located each under another layer of runoff elements, feeding the river and corresponding types of underground flow (Table 1). Therefore, the model assumes that the groundwater runoff is modelled by having different constituents of the groundwater flow, and the contributions to each from the bottom layer of the soil is controlled by parameters that need calibration. Notice that, likely, historical underground runoff (i.e. layers 13 – 15) can be referred to as "hydrological illusions" but their inclusion gives some completeness to the proposed schematization.

Table 1 The system of runoff elements

№	Type of runoff	a*, m^{-1}	Time (τ)	Outflow intensity, $dm^3\ sec^{-1}\ km^2$	Water storage, mm
–	Surface	1000	17 minutes	10^5	4.6
–	Subsurface	100	2.8 hours	10^4	24
1		10	1.2 days	10^3	69.3
2	Rapid ground	3.162	3.7 days	464	121
3		1	11.6 days	215	195
4		0.3162	1.2 months	100	301
5	Ground	0.1	3.8 months	46.4	454
6		0.03162	1 year	21.5	674
7	Upper underground	10^{-2}	3.2 years	10	995
8		$3.162*10^{-3}$	10 years	4.64	1464
9		10^{-3}	32 years	2.15	2152
10	Deep underground	$3.162*10^{-4}$	100 years	1	3161
11		10^{-4}	320 years	0.464	4640
12		$3.162*10^{-5}$	1000 years	0.215	6812
13	Historical underground	10^{-5}	3200 years	0.1	10000
14		$3.162*10^{-6}$	10000 years	0.0464	14678
15		10^{-6}	32000 years	0.0215	21450
$\sum_{(1-15)}$					67166

It is interesting to compare the total sum of specific stores of water in the system of underground runoff elements of different layers which amounted 67166 mm (without 15th layer 45716 mm) with the data of different sources: from 45000 to 70800 mm. Those are typical values for each layer, computed from the a* and b* parameters.

4.1.2.3 Channel flow and lag time

Now let's discuss the task of routing water from the place of its appearance in the system of river network to the basin outlet. The concept we use is very easy. It consists of two assumptions:

- The lag time of water channel run to the basin outlet is assumed to be a constant for each point chosen in the basin.
- We use the data of directly measured mean flow velocities for cross-sections of river channel. Such data was being published in Russia at hydrological year-books.

Table 2 illustrates the presented approach and presents the velocity values for the four large rivers of Eastern Siberia. These velocities are computed by averaging the velocities corresponding to the top 10 % of flow values for each of the rivers.

We have drawn a conclusion that a great many factors affecting the acceleration or conversely slowing down of flow velocity surprisingly lead to general order, steadiness and relative constancy as a result of some "self-regularity". The values on Table 2 indicate that the departures of flow velocities from their average value are insignificant, and not too dependent on basin size and spatial variability. In such a way the averaged minimum value of lag time (corresponding to maximum velocities) is taken as the calculating value. It is due to the fact that short time lags correspond to peak limb of flow hydrograph. At the same time we assume that the underestimated shift of hydrograph shape during the period of low flow does not affect the resulting runoff significantly.

Table 2 Characteristics of average flow speed (m s^{-1}) observed at the hydrometric stations in main rivers of Eastern Siberia

Range of basin scales (km^2)	Lena River		Yana River		Indigirka River		Kolyma River	
	V	C_V	V	C_V	V	C_V	V	C_V
<100	0.94	0.42	1.28	0.22	1.4	0.16	1.60	0.14
100 – 1 thousand	1.31	0.34	1.31	0.32	1.52	0.18	1.62	0.15
1 – 10 thousands	1.10	0.42	1.60	0.32	1.77	0.21	1.90	0.11
10 – 100 thousands	1.55	0.20	–	–	2.15	0.19	2.14	0.23
> 100 thousands	1.72	0.19	–	–	–	–	–	–
Average	1.40	0.30	1.39	0.28	1.52	0.25	1.65	0.21
The number of observational stations	228		50		46		117	

C_V – absolute variation coefficient of averaged velocities

4.1.3 Basin schematization

This section explains in more detail the concepts of representative points and runoff formation complexes that were introduced earlier in the brief model description section. In addition, we also describe how the model treats the problem of heterogeneity of snow cover.

4.1.3.1 System of Representative Points

If we are able to mathematically and algorithmically describe the runoff formation processes at the local point (or better to say at some elementary unit) within the river basin area, then there is the need to formulate the principle that some multitude of these points can completely represent

this river basin. In other words, a regular system of points within the watershed is required. There are not as many of variants of that system. For our purposes, a hexagonal grid seems to be appropriate because it possesses such a property that each centre point of each grid cell is equally distanced from the six neighbouring points at a distance ΔL. We call the points which evenly cover the basin area and are located from each other, the representative point (RP). Each RP has under its "control" the hexagonal area. We call it RP-area:

$$\Delta F = 0.866\Delta L^2 \qquad (13)$$

The basin area *F*, the number of points *n* and the distance between neighbouring points (the size of hexagonal grid) are related between each other by the following ratio:

$$n = 1.1547F / \Delta L^2 \qquad (14)$$

The representative point is characterized by geographical coordinates, altitude above sea level, aspect and surface inclination. The forcing data of meteorological stations is interpolated into RP. The interpolation methods generally are those required for the modelling procedure while preparing the information. In such a way, the RP-areas are the equal equivalent elements of a river basin (apart from those which are crossed by a water divide).

It is difficult to recommend a number of RPs for each given basin. But it is obvious that it should be nonlinearly related to the basin area. As a rule of thumb, the number of RPs can be estimated according to the following equation:

$$\mathrm{n} = \mathrm{kF}^{0.3}(1+\Delta\mathrm{H}), \qquad (15)$$

where F is a basin area (km^2), $\Delta\mathrm{H}$ is the difference of altitude in the basin (km). The value k can vary from 0.5 to 1.5 depending on the task, object complexity, landscape heterogeneity, availability of information (especially meteorological).

4.1.3.2 System of Runoff Formation Complexes

The basin map with the ordered set of RP is combined with the scheme of runoff formation complexes (RFC) to which the information about most of model parameters is related. The RFC is the part of river basin which is relatively homogenous regarding topography, soil and vegetation. We assume the process of runoff formation to be uniform within the range of one RFC and its quantative characteristics can be averaged. In essence, the RFC is similar to concepts such as the Hydrologic Response Units of PRMS (Leavesley et al., 1983) or CRHM, or the approach taken by the SLURP model (Kite and Kouwen, 1992). The system of RFCs in the basin is the subject for generalization depending on scales of mapping and modelling. It is supposed that all parameters of the model defining the RFC in whole are fixed within its range and change step-wise at RFC borders.

The model parameters

Any model can be characterized by the set of its parameters. Their list testifies to the extent of the factors governing the runoff formation process which are taken into account. And of course, it almost completely determines the necessary information which should be prepared for any other realization of the model at a given river basin.

The list of the model main parameters and the way of their estimation is presented in Table 3. They are divided into groups according to the four elements of a river basin which are defined in conformity with their functional role in the system of surface hydrological cycle.

All parameters from the first and second group and related to three upper underground layers from the third group are individual for each RFC. Other parameters from the third group are determined by more large-scale geological and hydrogeological structures.

Table 3 List of the model parameters (general recommendations about parameters estimation can be found in Vinogradov (2003b, c, d)

#	Parameters	Way of estimation
I. Vegetation and surface:		
1–4	Four phenological dates	Characterize the phases of vegetation growth; may be obtained in the literature. Trapezoidal "phenological" approximation is applied in the model.
5–6	Maximum and minimum values of seasonal shadow fraction by vegetation cover	Characterize the changes of parameters within the phases of vegetation growth; may be obtained in literature
7–8	Maximum and minimum interception water capacities	
9–10	Maximum and minimum landscape albedo	
11–12	Maximum and minimum coefficients of potential evaporation	$k = E_0 \cos\alpha / d\Delta t$, where E_0 – potential evaporation, d – effective air humidity deficiency, Δt – time period, α is slope inclination. It fluctuates usually in the range of $(0.3 \div 0.6)10^{-8}$ m (mbar s) depending on the type of evaporating surface. For snow cover, water, bare soil, rock-talus complex value can be considered to be constant. For vegetation it can have an annual course in concordance with the parameters 1 – 4.
13	Coefficient of evaporation from the interception storage during the maximum development of vegetation cover	The same as previous but for conditions of maximum development of vegetation
14–15	Maximum and minimum values of the snow redistribution coefficient	Values may be obtained by analyzing the data of snow surveys
16	Spatial variation coefficient of SWE in snow cover	
17	Spatial variation of infiltration capacity of upper soil layer	May be obtained from the literature for small experimental watersheds
18	Maximum ponding fraction	May be obtained from the literature, visual and aerial photo observations of the basin
19	Maximum surface depression storage	Obtained from the literature; or calibrated (preferably, for small watersheds)
20	Hydraulic parameter of surface runoff elements	$= 10^{-6}$; may need calibration
21	Orographic shadow fraction	Obtained from DEM
II. Discrete soil strata (unsaturated zone)		
22	Density	Typical values for soil types may be obtained from literature, soil surveys; usually do not require any further calibration
23	Porosity	
24	Maximum water holding capacity	

25	Infiltration coefficient	Values can be obtained from literature; may be calibrated against runoff at small watersheds
26	Specific heat capacity	Typical values may be obtained from literature, soil surveys or estimated by soil texture; do not require any calibration
27	Specific heat conductivity	
28	Index of ice content influence at infiltration	4 – sand, 5 – loam sand, 6 – loam, 7 - clay
29	Contribution ratio to evaporation	The contribution ratio of the first soil stratum K_1 changes from 0.1 (deep penetration of vegetation roots) to 0.5 (for sand soils with lack of vegetation). For other soil stratum K_i is calculated as the following $K_i = K_1(1-K_1)^{i-1}$
30	Hydraulic parameter of soil runoff elements	= 10^{-6}; may need calibration
31	Infiltration coefficient from soil stratum to groundwater	Values can be obtained from the literature; geological information about mother rock is important; may need calibration
32–36	Five parameters (average, two phases and two amplitudes) describing temperature at maximum available depth (usually 3.2 m in Russia)	Available in climate reference books or soil surveys; or could be estimated from soil temperature observations
III. Saturated zone (in case of shallow groundwater)		
37 – 39	Thickness, porosity and specific water yield coefficient in the groundwater flow area	Can be obtained in literature; or calibrated at small watersheds (this module of the model is being refined)
40 – 41	Height of capillary raise and index of nonlinearity in the equation of capillary moisture capacity	
IV. The system of underground runoff elements (specific for each 15 layers of underground water – up to 15)		
42	Hydraulic parameter	= 10^{-6}; may need calibration
43	Values of redistribution of water volume among modelling groundwater layers	Need calibration against observed runoff; usually may be easily transferred to the basins in the same conditions without changes; can be systematized for different hydrogeological conditions
V. Other parameters		
44	Lag time from each RP to the basin outlet	See Section Channel flow and lag time; if there are no observations, initial velocity can be estimated as 1.5 ms^{-1} and then adjusted.

4.1.4 Model implementation

The following data and information initially available for this study included a GIS database of watershed characteristics, forcing meteorological data and control runoff data.

4.1.4.1 Time series information

Meteorological information was provided for three micrometeorological stations (Alpine Tundra – AP, Buckbrush Taiga – BT, and White Spruce Forest – WSF) for the period 1993–2007 and included weather and soil data in 30 min time interval. Daily discharge was provided for the same period for the hydrometric station located at the Wolf Creek basin outlet nearby the Alaska Highway. In addition there was a dataset for sloped surfaces in a sub-basin of the Wolf Creek basin – Granger Basin.

As the runoff data had daily time step interval there was no reason for us to use the finer time step interval for the simulations. Therefore we have aggregated 30 min observations to daily time series for all sites and variables. For the model setup we took three years: 1999–2001.

In general, the data is raw, characterized by various gaps and discrepancies and needs much care and analysis to be used in the modelling procedure. Meteorological data was available from 1993 to 2001, but precipitation was only available from 1998 – 2001. The data was not continuous at all stations, and missed the precipitation data for the winter months at two of the stations.

Winter precipitation

The main problem turned out to be winter precipitation which is measured only at BT. For the other two sites, available data includes snow depth, snow density and SWE. While snow depth is observed every time step, the snow density is measured much rarely. From those two values SWE is calculated. Figure 3 shows one of many examples of the disagreement between those data (here BT, 2000): at the end of January the decrease of SWE is observed from 155 to 85 mm (about 40 %) while the snow depth is decreasing by 5 cm, from 70 cm to 65 cm. A 40% decrease in SWE in about 3 or 4 days while snow depth only decreases 5 cm does not seem likely. Also the snow density looks rather unrealistic here.

Pomeroy *et al.* (1998) analysed the snow mass balance for the Wolf Creek watershed. From their findings we could estimate the ratio of winter precipitation for the AT and WSF in comparison to BT. They amounted to 0.90 and 0.60 accordingly. Using those coefficients we recovered winter precipitation for AT and WSF from the data of BT site. According to Pomeroy *et al.* (1998) we introduced wind correction coefficients to winter precipitation as the following: 1.15 for AT and BT; 1.1 for WSF. The summer precipitation correction factors were set as 1.1 for all stations.

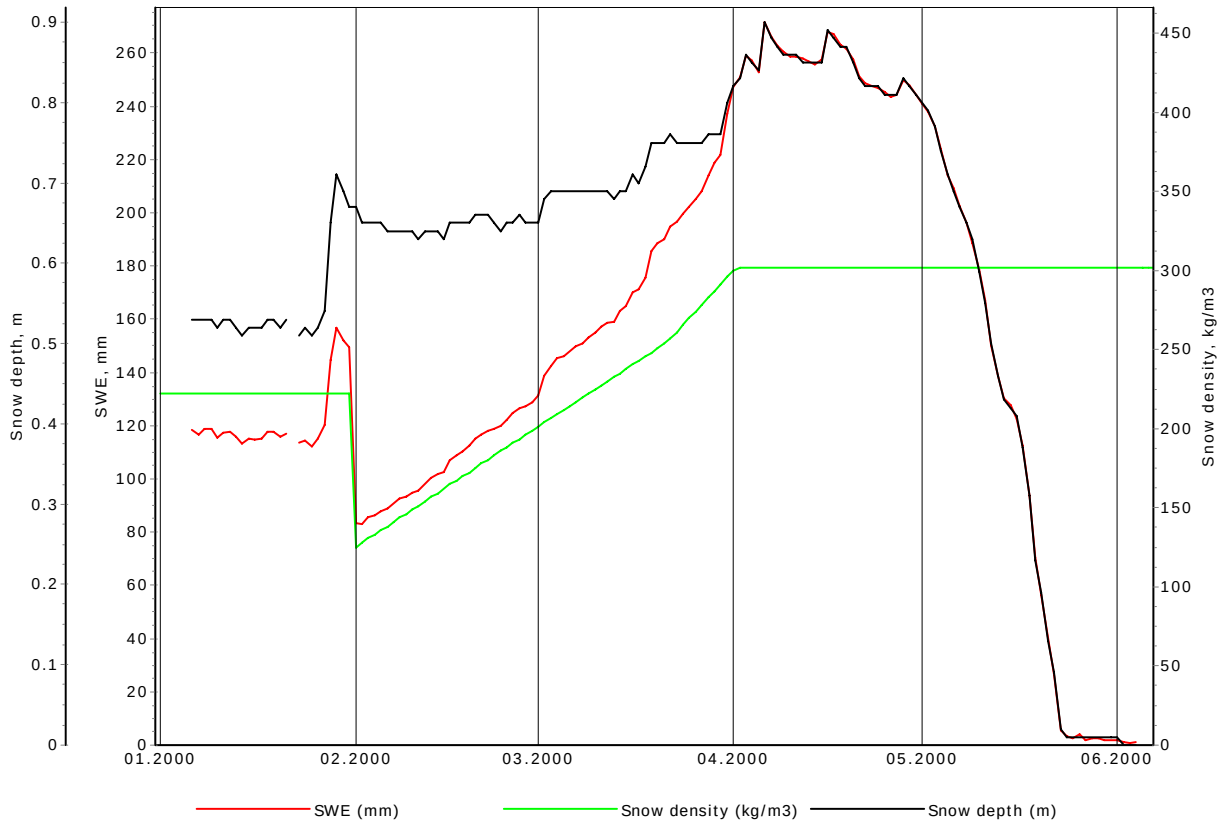

Figure 3. Example of snow data unconformity (Buckbrush Taiga Site, 2000)

Solar radiation

Altitude and exposure variation play key role in the calculation of heat balance in mountainous areas since the slope properties determine the net of direct solar radiation that comes into the earth surface. We use the approach of enhancing meteorological data input in terms of their effectiveness. It suggests air temperature and moisture deficit should be corrected to account for the flux of direct solar radiation. The following expression for effective temperature (T_{EF}) is used (a similar equation is used for effective moisture deficit):

$$T_{EF} = T + \varepsilon S_{corr} \qquad (20)$$

Here T is air temperature; S_{corr} is the direct incoming solar radiation (S), corrected for albedo, relief, cloudiness and vegetation cover; ε is the model parameter that can be estimated while comparing calculated and observed variables. The value S is calculated in the model for every day depending on latitude and altitude, aspect and inclination angle of a given slope.

In the database, the values of incoming solar radiation already corrected for cloudiness were presented for three observational sites. However, the values of cloudiness, necessary for our calculations, were not available. As the relief of the watershed is complex and dominated by rather steep slopes of opposite orientation the use of the data of the meteorological sites would be not proper as the radiation is measured over a horizontal surface.

To overcome this problem we calculated the direct solar radiation for sites with observations. Then for every day we estimated the coefficient of decay of solar radiation as the ratio between the calculated (with 0 cloudiness) and really observed (see Figure 4). Then we used that daily

coefficient (assuming it to present the conditions of cloudiness and be uniform for the whole watershed) to correct the calculated solar radiation for the other slopes of the basin.

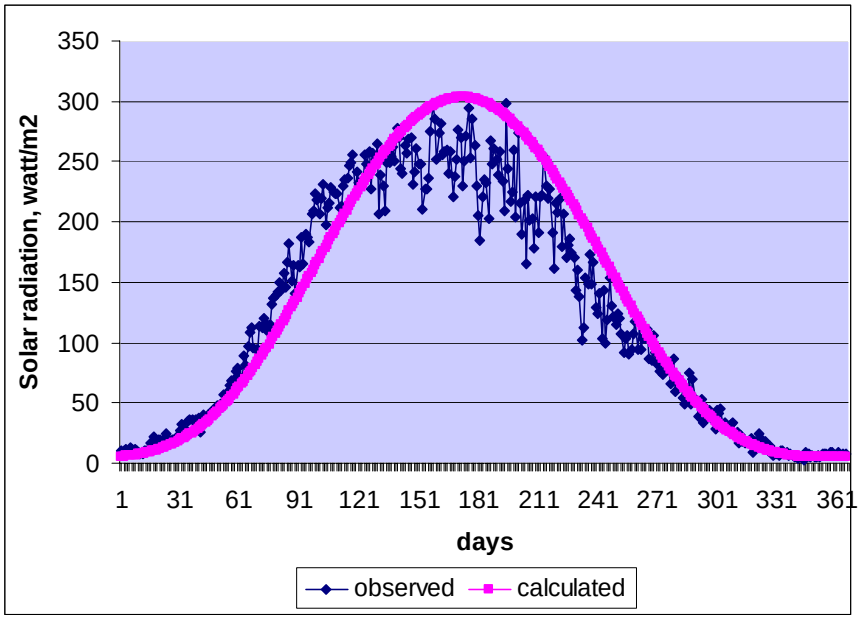

Figure 4. Observed and calculated values of direct solar radiation (AT site, 2000)

Winter temperature inversion

The analysis of the air temperature data showed that winter temperature inversions are typical for the studied basin. We calculated the average monthly gradient of air temperature (degree C/ 100 m) using the data of AT and WSF sites with an elevation span 865 m. The gradient value varies in the range from 0.7 (Jan, Dec) to -0.7 (May, June) degree C/100m. We used the biharmonic approximation to fit the observed values (see Figure 5). Afterwards we used this gradient while interpolating the air temperature from the observational sites to the representative points.

Soil moisture and temperature

Because of the unavailability of soil data at this point, it was not meaningful to proceed with a verification of the soil moisture and temperature.

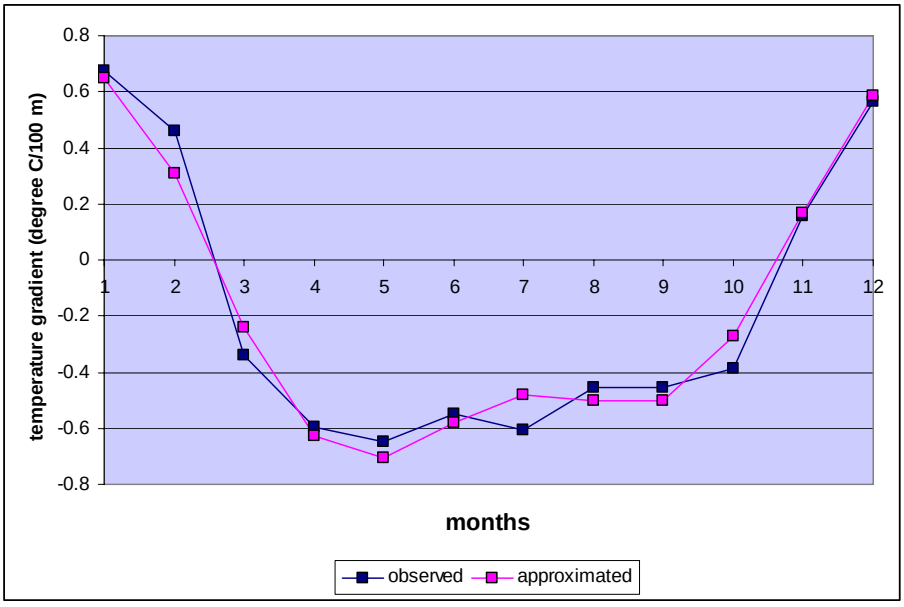

Figure 5. Observed and calculated values of air temperature gradient (degree C/100m)

4.1.4.2 Use of GIS information

The GIS information supplied by the University of Saskatchewan consisted of the digital elevation model, different aspects of relief features distribution (slope exposure, elevation), the watershed borders, the river network, the distribution of vegetation types, and the location of meteorological and runoff gauges.

We have set up a regular hexagonal grid over the basin consisting of 108 Representative Points (RPs). For each RP the following characteristics were obtained from the GIS information: elevation, slope orientation and angle, distance to the basin outlet. It is important to draw attention that those characteristics are not averaged within the RP area but taken as the RP is the representative slope for its corresponding area. The scheme of Wolf Creek watershed with location of RPs, meteorological and runoff stations is shown at Fig. 6. The forcing data was interpolated into each RP from the meteorological stations according to the elevation.

The basin map with the ordered set of RP is combined with the scheme of runoff formation complexes (RFC) to which the information about most of model parameters is related. The RFC is the part of river basin which is relatively homogenous regarding topography, soil and vegetation.

Here we followed a scheme of vegetation distribution which divides the watershed into three zones: alpine, sub-alpine and boreal forest (Fig. 6). Those zones were set as three RFCs. Within each RP area we estimate the ratio of each RFC and the simulations are conducted separately for each RFC within the RPs.

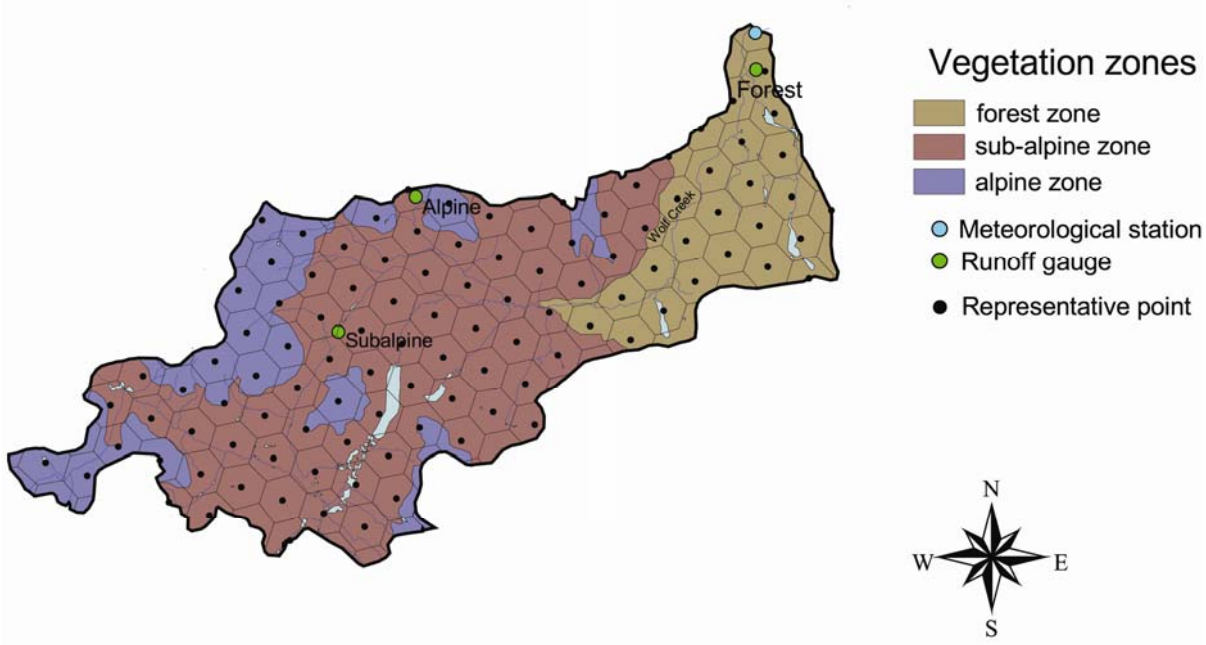

Figure 6. Discretization of the watershed into computational elements

4.1.4.3 Assessment of model parameters

Vegetation

According to the Francis *et al.* (1998) GIS dataset we assigned the dominant vegetation type for each RFC:

1) forest – white spruce-feathermoss forest;
2) subalpine – willow-dwarf birch shrubland;
3) alpine – tundra vegetation (grass-forb-lichen).

For those vegetation types the parameters were estimated; they are presented in Table 4.

The parameters 1–4 were estimated from the simple analysis of air temperature distribution within the year. They are needed for the approximation of temporal stages of vegetation development within the year and appropriate characteristics (parameters 5–14). The parameters 5 – 10 can be obtained from the literature; 5 – 9 are used to correct the direct solar radiation. The parameters 11 – 13 can be estimated in the way described in Table 3; but usually it is easier to manually calibrate them. Here the data on evaporation from different vegetation zones obtained in Granger (1998) was used for that procedure. The parameter 14 is the normalized heat transfer coefficient for the type of underlying surface; it changes from 2 to 5 depending on the vegetation type.

Table 4 Estimated parameters of vegetation cover

		RFC 1	RFC 2	RFC 3
1	Phenological date 1 (dd.mm)	10.05	25.05	10.06
2	Phenological date 2 (dd.mm)	10.06	20.06	01.07
3	Phenological date 3 (dd.mm)	15.08	10.08	31.07
4	Phenological date 4 (dd.mm)	30.09	15.09	31.08
5	Maximum value of seasonal shadow fraction by vegetation cover	0.95	0.5	0.1
6	Minimum value of seasonal shadow fraction by vegetation cover	0.75	0.1	0.0
7	Maximum landscape albedo	0.15	0.17	0.20
8	Minimum landscape albedo	0.10	0.12	0.15
9	Maximum interception water capacities (mm)	5	2.5	0.1
10	Minimum interception water capacities (mm)	4	0.5	0
11	Maximum coefficient of potential evaporation, 10^{-8} m/(mbar s)	0.95	0.72	0.55
12	Minimum coefficient of potential evaporation, 10^{-8} m/(mbar s)	0.35	0.15	0.08
13	Coefficient of evaporation from the interception storage during the maximum development of vegetation cover, 10^{-8} m/(mbar s)	1.1	0.80	0.60
14	Parameter of soil heat supply, Wt/m^2 degree C	5	4	2

Soils

The acquisition of the soil profile properties became a real problem for the model implementation in the Wolf Creek watershed. Although much research was conducted to determine the differences of heat and water balances for different slopes, the information about the soil types and their distribution was not available. For our model, the physical properties of the soils, such as porosity and hydraulic conductivity governing the water infiltration in the soils, are important; soil composition and bulk densities are needed to estimate the soil thermal properties, the distribution of soil temperature within the profile which is needed to set up the permafrost presence and parameters and set up the initial conditions.

Papers by Carey and Woo (2001) and Seguin et al. (1998) provide some information about the physical and hydraulic properties of the soils but, in some cases, that information was questionable. Carey and Woo (2001) described the soil properties of four experimental slopes located within the subalpine area (RFC 2). The differences in the properties were related with different slope orientation which governs the corresponding heat balance types and the presence of the permafrost or only seasonal frost. According to Carey and Woo (2001) the north facing slope is underlain by clayey soils with stone inclusions and capped by an organic layer (0.05–0.3 m thick) consisting of peat, lichens, mosses, sedges and grasses. It is underlain by permafrost at depths from 0.6 to 2 m. The soil of south facing slope consists of thin leaf litter overlying homogeneous silt to a depth of >2 m. No permafrost is found under this slope. An east-facing slope is underlain by sandy soils with large stone inclusions, capped by an organic layer (0.05–

0.25 m thick) consisting of peat, lichens, mosses, sedges and grasses. This slope retains a saturated zone at or near the surface for most of the thawed season. Only seasonal frost is found down to a maximum depth of approximately 1 m. The east facing slope is located at the base of a large alpine upland contributing area that supplies water to the study site throughout most of the summer. A west-facing slope is similar to that of the E-slope but the organic layer is much thicker (0.25–0.45 m) and consists of peat, lichens and mosses with few sedges and grasses. This slope is underlain by permafrost at depths between 0.45 and 0.6 m.

The following information useful for the task of parameters estimation can be summarized from the findings of Carey and Woo (2001):

- three slopes out of four have a thick organic layer (up to 40 cm) characterizing by high porosity (up to 90 %) and hydraulic conductivity (orders of 10^{-3}–10^{-4} m/s);
- mineral soil underlining the organic layer has a porosity of about 50% and hydraulic conductivity of the order of 10^{-6}–10^{-9} with minimum values found in the north-facing permafrost site.

At first glance, the values of porosity appear to be very high. In some cases, they are not in consistence with provided values of bulk density: for the mineral soil of south facing slope the density of soil particles calculated from the values of porosity and bulk density exceeds the density of granite.

The results of soil properties estimation by Seguin *et al.* (1998) based on hydrogeological methods are different. The mean porosity of the mineral soil for different sites varies from 24 to 32 %. The values of hydraulic conductivity of topsoil range from 9 to 108 * 10^{-6} m/s but the most frequent are around 20*10^{-6} m/s, and the largest are found over discontinuous permafrost zone. Hydraulic conductivities in permafrost are very low, for instance 0.4 to 15 * 10^{-8} m/s.

In this study we assigned the values of soil properties proposed by Carey and Woo (2001) not accordingly to RFCs, as we do it usually, but by the slope orientation. So all north facing slopes got the same properties, etc. Some parameters were taken as observed, such as bulk density; porosity of mineral soil was slightly corrected towards lowering its value. Other parameters were estimated from literature sources, such as thermal capacity and conductivity accordingly to the soil composition and porosity/density ratio. Maximum water holding capacity, being unknown, was roughly estimated as 90 % of porosity. The wilting point values, also unknown, were estimated as 25-30 % of maximum water holding capacity. The ranges of published values of hydraulic conductivities are rather wide and this parameter needed manual calibration which results that, in the future, it should be verified by the soil moisture observations.

Since we are still hoping to obtain better soil information for the watershed, it is premature at this point to include a table with the soil parameters.

Slope surface

The main parameters of slope surface are those characterizing the process of snow redistribution within the basin. Snow Water Equivalent (SWE) for river basins of middle and high latitudes is one of the most important elements in the system of characteristics of hydrological cycle. It determines not only the possibility of water inflow to the watershed but also governs many quantitative relations of hydrometeorological processes in soil and snow. Snow drifts and blizzards redistribute snow across the territory by filling gullies, narrows, gorges and crevices. The resulting heterogeneity of SWE should be taken into account.

It is appropriate to assign several additional “calculating” points – cP characterized by its own value of snow water equivalent. The calculating points are attached to representative ones (RP)

and do not have exact locations. They refer to any point at the surface and exist only in a statistical way.

The general scheme is the following. For this report, we used the precipitation sum Y^* for a given RP-area. For accounting of spatial heterogeneity, the spatial distribution of snow is approximated by using typically five quantiles which correspond to the centres of equal intervals at the probability scale: 0,1; 0,3; 0,5; 0,7; 0,9 (the normal distribution law is assumed). If necessary a sixth calculating point is added to five "quantile" ones and it corresponds to the snow accumulation in a system of gullies. As a result we have:

$$Y_1^* = Y^* / \left[m_1 (m_2 - 1) + 1 \right] \tag{16}$$

at the territory which surrounds gullies after the drift of part of snow to the system of gullies,

$$Y_2^* = m_2 Y_1^* \tag{17}$$

in gullies. Here m_1 is a fraction of the RFC area covered with gullies and m_2 is the ratio of the snow depth at gullies and the surrounding territory.

Thus, the snow redistribution which takes place not actually during the snow fall but mainly afterwards is imitated simultaneously with the snow fall. The layer of solid precipitation at five quantile points is calculated by multiplying the module coefficients k_p with accepted variation coefficient Cv(Y*) by Y_1^*

$$Y_p^* = k_p Y_1^* . \tag{18}$$

The value of k_p depending on C_v(H*) is determined by equation

$$k_p = 1 + U_p C_v(Y^*) , \tag{19}$$

where U_p is the quantile of normalized normal distribution. The magnitudes of k_p for some values of C_v(Y*) are presented at Table 5. The variation coefficient C_v(Y*) is usually estimated by the data of snow surveys.

In this study we assigned five additional "quantile" points and a gully point for the alpine and subalpine RFCs. The snow distribution in the forest was assumed to be homogeneous. Maximum and minimum values of the snow redistribution coefficient were set as 10 and 1, while spatial variation coefficient of SWE in snow cover was estimated as 0.20 for forest zone and 0.35 for alpine/subalpine zones.

Table 5 Values of the coefficient k_p

Interval	The middle of the interval	U_p	Values of k_p for each C_v(Y*)				
			0.1	0.2	0.3	0.4	0.5
0.0 – 0.2	0.1	–1.282	0.872	0.744	0.615	0.487	0.359
0.2 – 0.4	0.3	–0.524	0.948	0.895	0.843	0.790	0.738

0.4 – 0.6	0.5	0	1.000	1.000	1.000	1.000	1.000
0.6 – 0.8	0.7	0.524	1.052	1.105	1.157	1.210	1.262
0.8 – 1.0	0.9	1.282	1.128	1.256	1.385	1.513	1.641

Groundwater

The treatment of the subsurface and groundwater processes remains very uncertain in hydrological modelling. Usually hydrological models have a detailed representation of the surface processes, while the subsurface processes tend to be either simplified (splitting flow between a fast and a slow component) or considerably complicated (physically-based approaches). The split-flow technique does not take into consideration the different levels of interaction between groundwater and surface flow that is a function of the basin scale and geographical conditions. The more complex methods have a different problem, namely that of the estimation of the parameters of the model for large basins. Here we present the conceptual approach but linking it to the general notion of hydrogeology. It is also simple from the point of view of parameter calibration.

The observed data has gaps in winter period. Analyzing the flow data for the period different from the one used in this study we have the feeling that winter flow can be relatively high and stable; that means that there are the storages supplying it. It is not clear for us what the nature of those storages is; they could be groundwater or lake reservoirs. In severe winter frosts the footpaths from such storages can be completely frozen and the contribution to runoff may decrease considerably. The analysis of recession curves of 2000–2001 shows considerable storage potential in summer time. Initially the water is stored and then distributed into flow stream with some delay. Intuitively the runoff hydrographs resemble those observed in the Eastern Siberia but for the large-scale rivers as Lena or Aldan which are characterized by large storage volumes and large lag times. Rather quick reaction to snowmelt and rainfall forcing is typical for small rivers of the Eastern Siberia which have similar conditions of runoff generation. Those facts have also indirect confirmation of the idea of the presence of some water storage supposed in previous paragraph. For full analysis of the process we would need the information about the Coal Lake and the flow observations for the gauges different from the final outlet.
Taking into consideration the above hypothesis we estimated the groundwater parameters as presented in Table 6.

Table 6 Estimated parameters of groundwater

Layer of runoff elements	1	2	3	4	5
Type of runoff	Rapid ground			Ground	
Outflow time	1.2 days	3.7 days	11.6 days	1.2 months	3.8 months
Values of redistribution of water volume among modelling groundwater layers	0.15	0.15	0.20	0.25	0.25

4.1.4.4 Initial conditions

Knowledge of the initial conditions is of high importance to correctly simulate the basin response; especially when it is applied for the case of short data available for the model calibration when a one year simulation warm up period is not affordable. In the Hydrograph model, the following initial conditions are necessary to start the modelling procedure: antecedent soil wetness conditions (amount of liquid water and ice in every discrete soil stratum);

temperature of each soil stratum; state of snow cover (SWE, density, temperature, and saturation index); amount of water in each of layers of groundwater runoff elements.

As a rule, we start the simulations at the snow-free period of the year, preferably in autumn, during the flow recession stage. That way, the snow cover state variables may be set to zero. The soil wetness is set to the value of maximum water holding capacity (or a half of it). Depending on the studied area and the depth of individual soil strata, the moisture can be set as liquid or solid (ice). Temperature of soil strata is estimated accordingly to known annual dynamics. Usually those initial conditions are set according to the process understanding; further we come back and refine them (for example, set up the soil completely frozen if the observed spring melt flow identified those conditions).

In this study the observational data of soil and snow variable states were used to set up the initial conditions. Special attention was paid to the differences in soil state variables distribution accordingly to soil properties and permafrost conditions.

When the parameter of redistribution of water volume among modelling groundwater layers (see Tables 4 and 7) were estimated for the basin, the initial volume of water storage in each layer was evaluated accordingly to the system of runoff elements. This initial condition has considerable impact on the results of flow simulations if the deeper layers are used as their recession time of stored water volumes may be large.

4.1.4.5 Calibration, validation and adjustment of the parameters

A split sample technique is the most common approach used for the calibration and verification of hydrological models. During the calibration stage, the model parameters are optimized based on the evaluation of the discrepancy between the simulated and observed hydrological characteristics. At the following validation stage, the modelling procedure is conducted with the use of calibrated parameters but for a period different from the calibration one.

In this study we had only three years of the data to calibrate the model parameters. The following parameters were manually adjusted from those initial values found in the literature:

- Evapotranspiration coefficients;
- Hydraulic conductivity;
- Coefficient of solar radiation influence on effective air temperature;
- Indexes of incoming water content distribution between modelled groundwater layers were defined for the watershed based on the observed hydrographs but in accordance with the theory of runoff elements which describes the hierarchical sequence of underground runoff elements layers participating runoff contribution assuming that rates of inflow decrease and water store increase with depth (Vinogradov & Vinogradova, 2010). In this way, the model is able to divide groundwater flow into components related to different underground water layers. Although they are still conceptual model-specific components and may not be directly related to specific flow aquifers and paths, but, rather, they reflect a hypothetical view of groundwater hydrology that does not contradict available observational information.

4.2 Results

The simulations were conducted for the period of 1999–2001 for Wolf Creek watershed (195 km^2) with its outlet near the Alaska Highway. The results of flow simulations were compared with the observed values (see Fig. 7–10). Table 7 illustrates the values of statistical characteristics for observed *vs* simulated daily flows for the periods of available observed data.

Table 7 Simulation statistics for Wolf Creek watershed

	01.01 – 21.10.1999	09.05 – 27.10.2000	29.05 – 21.10.2001	Avg.
Simulated flow (mm)	104	130	107	114
Observed flow (mm)	80	138	115	111
Precipitation (mm)	262	332	261	285
Evaporation (mm)	216	297	252	255
Relative absolute daily error	3.38	0.33	0.29	1.33
Nash-Sutcliffe	0.65	0.15	0.65	0.48
Correlation	0.94	0.80	0.78	0.84
RMSE	0.43	0.70	1.15	0.76

For the period of in which statistics were calculated, the water balance values were estimated as follows: total precipitation amounted to 285 mm (with maximum 332 mm in 2000), total evaporation from the surface of the studied basin ranged from 216–297 mm (with average 255 mm). Mean Nash-Sutcliffe efficiencies (NS) is 0.48, the average relative error in its absolute value is about 0.84, average correlation coefficient is 0.84, while RMSE is 0.76.

The observed data has gaps in during the winter period. Analyzing the flow data for a period different from the one used in this study we have the feeling that winter flow can be relatively high and stable; that means that there are the storages supplying it. It is not clear for us what the nature of those storages is; they could be groundwater or lake reservoirs. In severe winter frosts the footpaths from such storages can be completely frozen and the contribution to runoff may decrease considerably. The analysis of recession curves of 2000–2001 shows considerable storage potential in summer time. Initially, the water is stored and then distributed into flow stream with some delay.

Intuitively, the runoff hydrographs resemble those observed in the Eastern Siberia but for the large-scale rivers as Lena or Aldan which are characterized by large storage volumes and large lag times. Rather quick reaction to snowmelt and rainfall forcing is typical for small rivers of the Eastern Siberia which have similar conditions of runoff generation. Those facts have also indirect confirmation of the idea of the presence of some water storage supposed in previous paragraph. For a full analysis of the process we would need the information about the Coal Lake and the flow observations for the other gauges located at places different from the final outlet. The calculated and observed hydrographs have a timing mismatch, and large discrepancy in terms of runoff volume. The calculated flows do not capture small peaks which are previous to the principal snowmelt runoff. At the same time the main peaks of snowmelt are overestimated. The reason can be the improper accounting for precipitation and the snow redistribution, and different timing of snow melt. In summer period the flows are generally underestimated (2000, 2001). The recession curve has a more smooth shape which is not considerably disturbed by smaller peaks as at the observed hydrographs. Those observed small peaks show that there is some saturated zone or storage which can react fast in spite of generally drying soils. Can it be

lakes surfaces? In addition to flows, Figure 11 shows the comparison of simulated and observed values of snow depth at the Backrush Taiga Site. In general, the obtained results can be considered satisfactory for such a fast study. Although the question of the right reasons of getting those results is not closed.

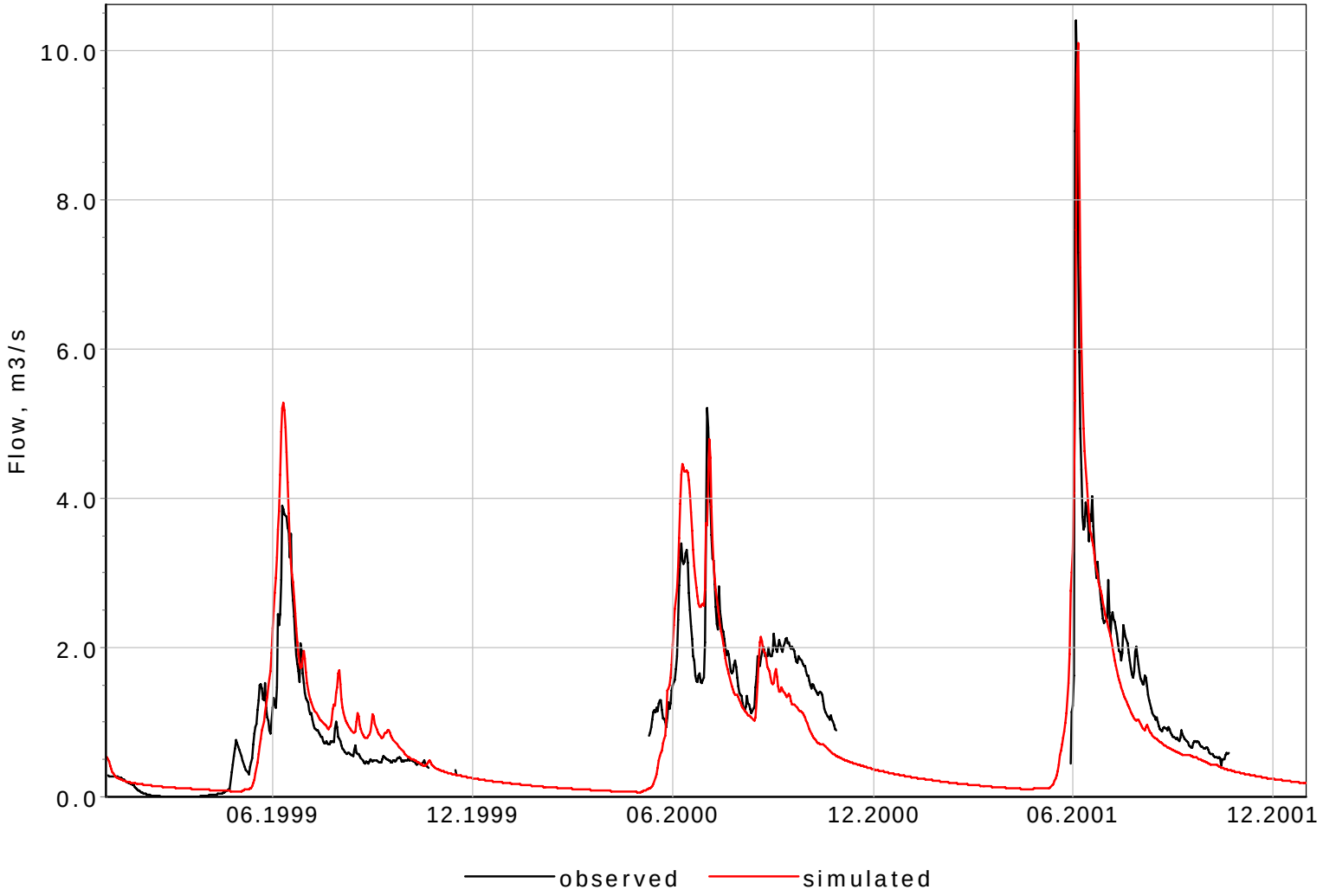

Figure 7. Observed and simulated flow at Wolf Creek watershed, 1999 – 2001.

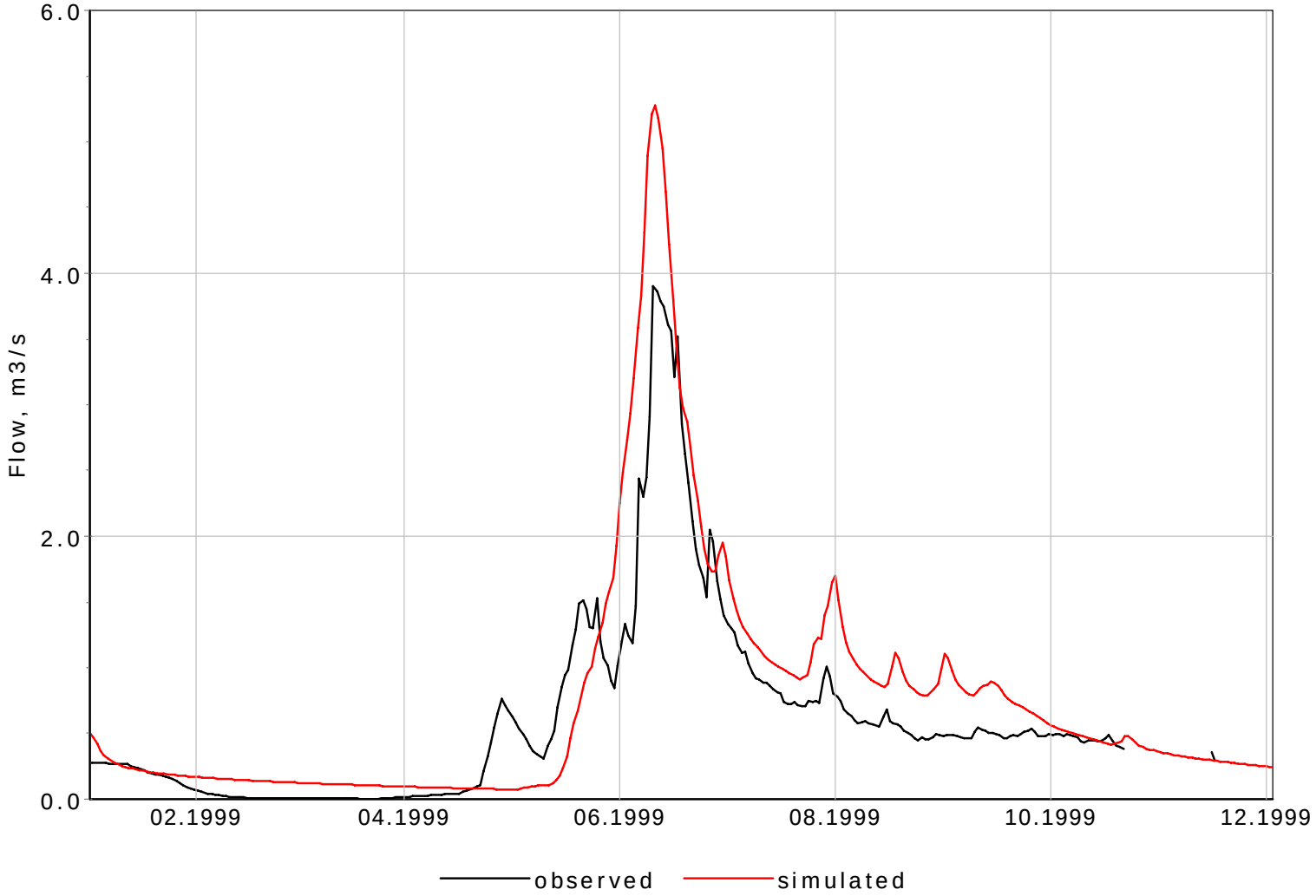

Figure 8. Observed and simulated flow at Wolf Creek watershed, 1999.

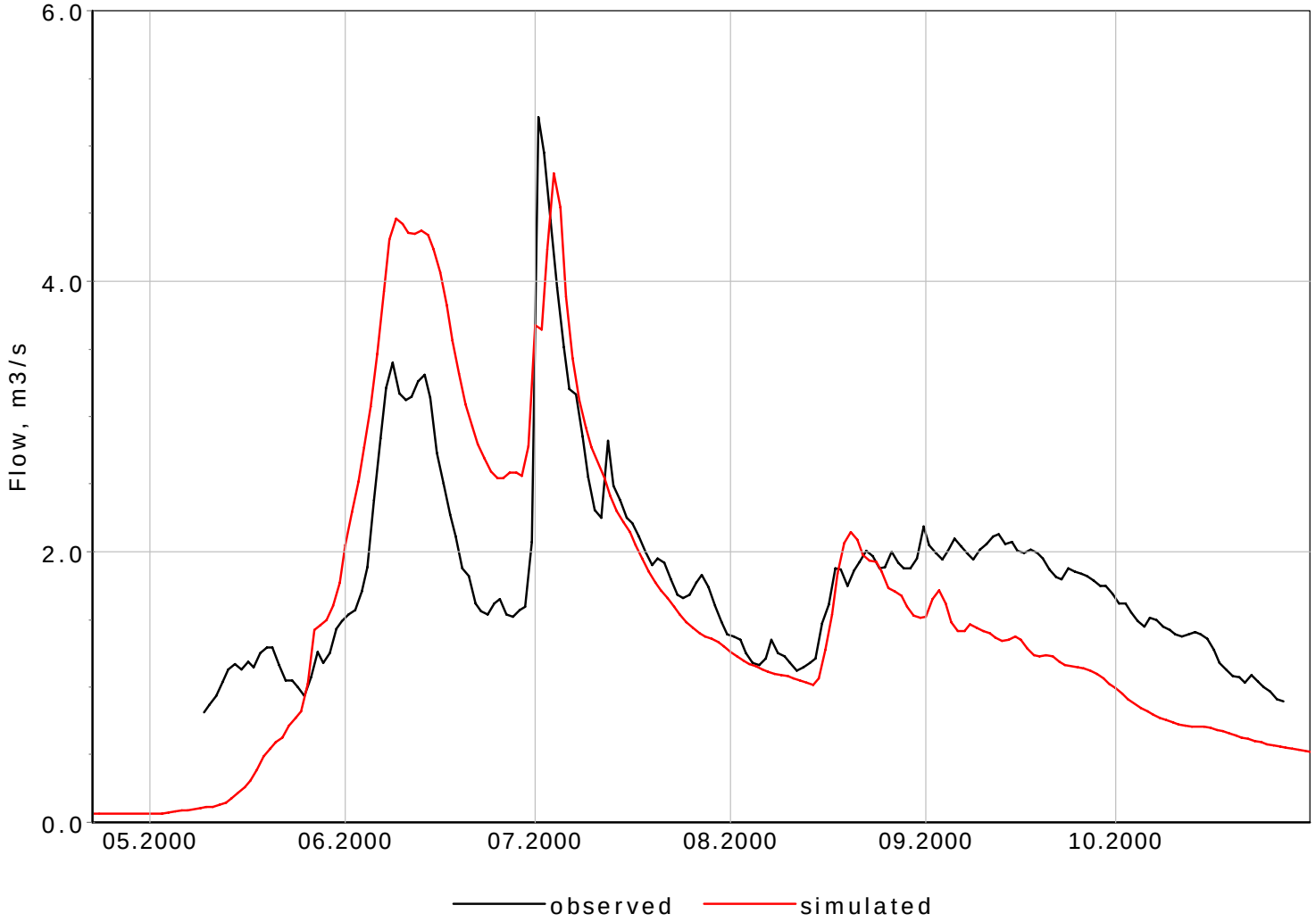

Figure 9. Observed and simulated flow at Wolf Creek watershed, 2000.

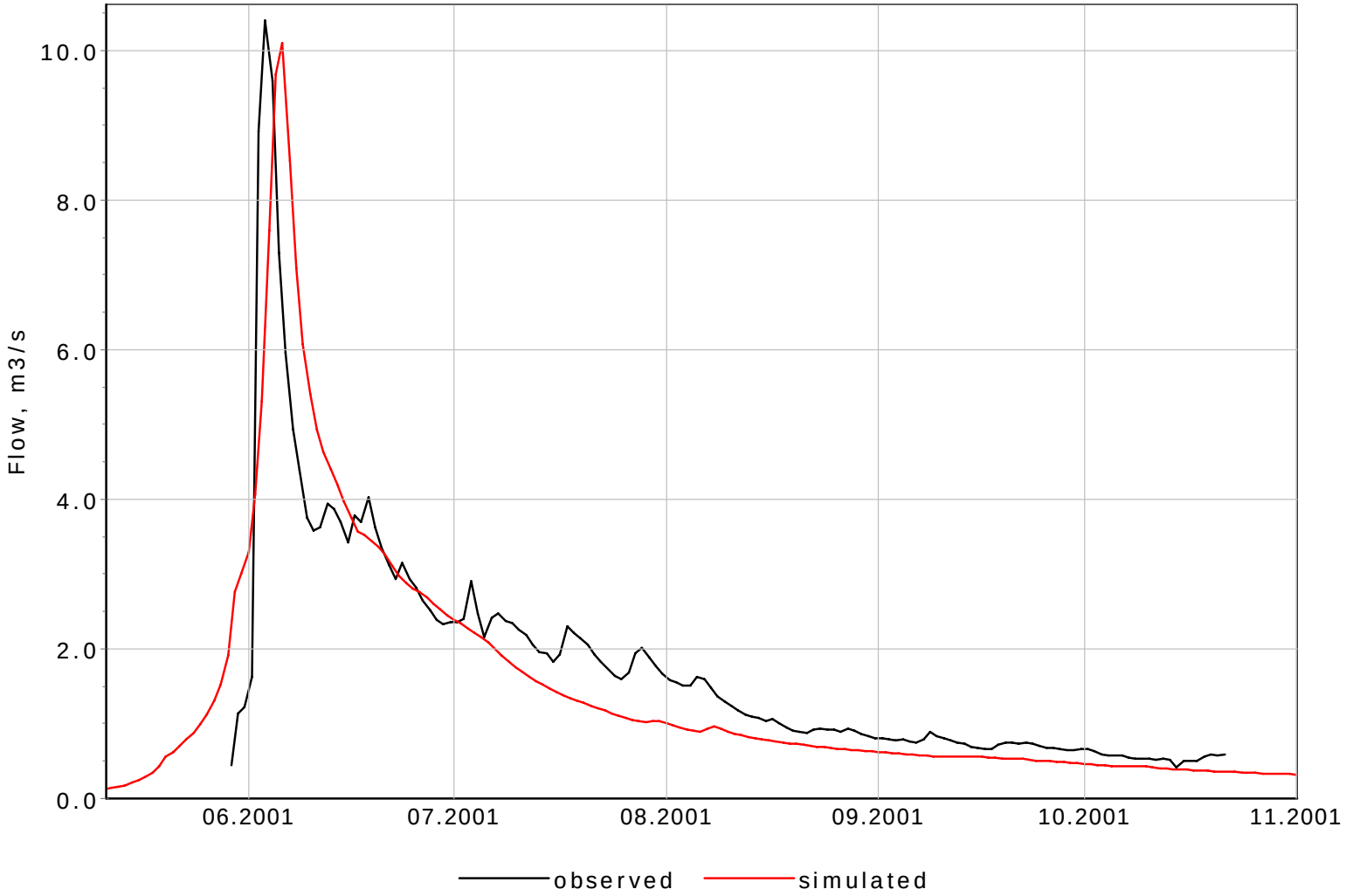

Figure 10. Observed and simulated flow at Wolf Creek watershed, 2001.

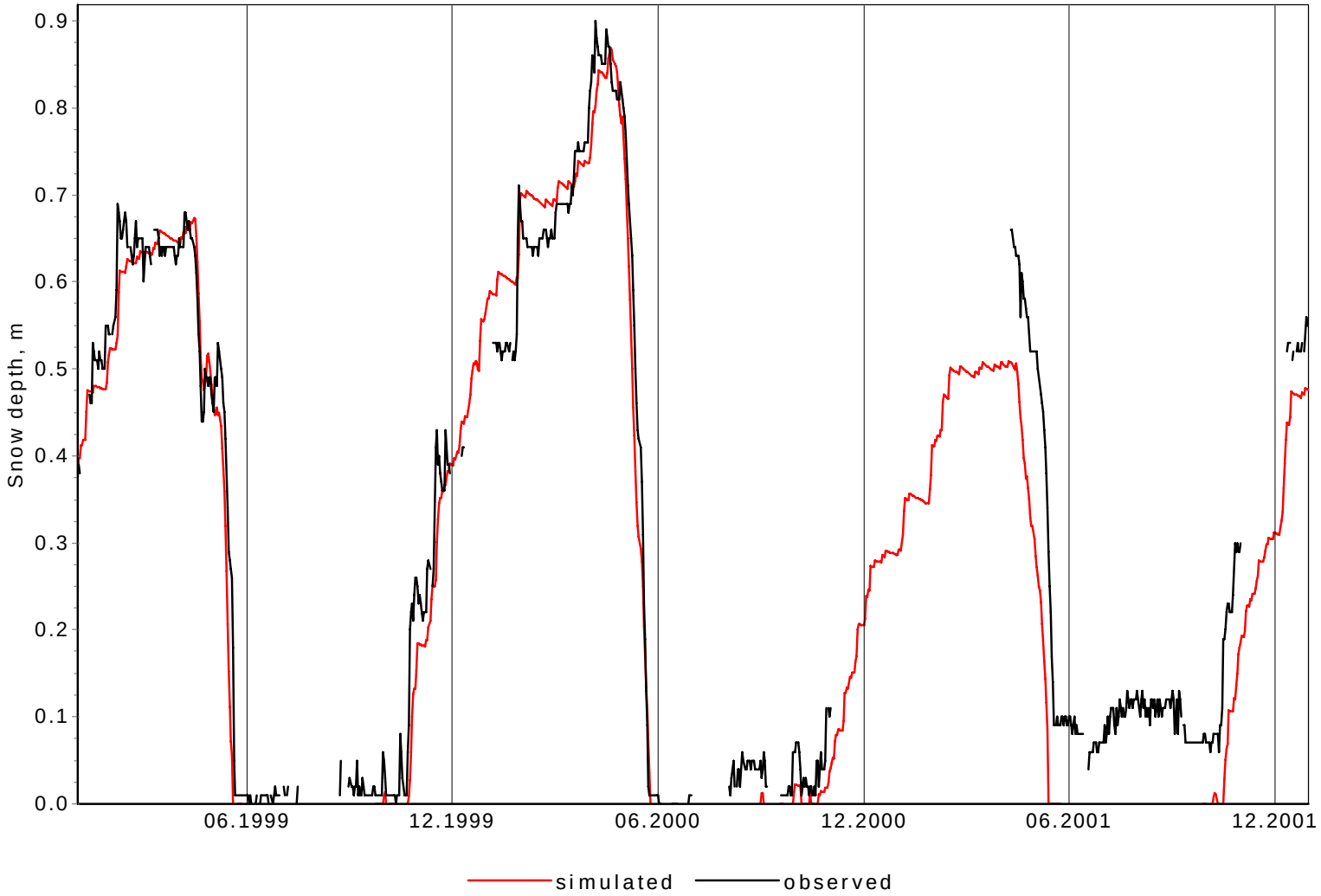

Figure 11. Observed and simulated snow depth at Backrush Taiga site, 1999–2001.

4.3 Conclusions

This section covered the application of the Hydrograph model to the Wolf Creek Watershed in the Yukon Territory, Canada. The procurement of data necessary to run the model proved particularly challenging. Information of precipitation, temperature, streamflow, snow water equivalent and solar radiation had considerable gaps. Some of the missing temperature data had been reconstructed, but there are questions regarding that reconstruction. Computations of snow water equivalent during missing periods also had procedural problems. Soil temperature was observed at a few stations, but at a fairly shallow depth. In spite of these difficulties, we were able to obtain meaningful simulations by approaching the problem from a more conventional path (calibration of parameters), rather than our favoured approach (direct observation of parameters). We will continue to research sources of information, particularly regarding the soils. For the time series, we are hoping to be able to examine the records of temperature soundings from airport observations, including radiosonde information.

4.4 References

Burnash, RJC, Ferral, RL. (1974) Mathematical Models in Hydrology Volume 2; Proceedings of the Warsaw Symposium, July 1971: International Association of Hydrological Sciences Publication No. 101, p 838-847

Carey, S.K., and Woo M.-K. (2001) Spatial variability of hillslope water balance, Wolf Creek basin, subarctic Yukon. Hydrol. Process. 15, 3113–3132

Crawford NH, Linsley RK. (1966) Digital simulation in hydrology: Stanford watershed model IV (Dept. of Civil Engineering Tech Report). Stanford University, Stanford, CA.

Eagleson, P.S. (1978) Climate, Soil, and Vegetation 2. The Distribution of Annual Precipitation Derived From Observed Storm Sequences, *Water Resources Res.*, 14(5), 713–721.

Francis, Sh. Smith, S. and Ric Janowicz (1998) Data Integration and Ecological Zonation of Wolf Creek Watershed. Proceedings of Wolf Creek Research Basin Planning Workshop, Whitehorse, March 1998.

Granger, R.J. (1998) Partitioning of Energy During the Snow-free Season at the Wolf Creek Research Basin. Proceedings of Wolf Creek Research Basin Planning Workshop, Whitehorse, March 1998.

Gardner, W.R. (1960) Soil mater relation in arid and semi-arid conditions. UNESCO Arid Zone Res. Vol 15, p. 37 – 61.

Haillare, M. (1962) Le potential efficace de l'eau dans le sol en regime de dessechement. C.R.Acad.Sci., 254, p. 2047–2049.

Haillare, M. (1960) Le probleme au potentiel de l'eau dans le sol et de la disponibilite de l'eau pour la végétation. Ann. Physiol.Vég., p 119 – 113.

Ivanov, V. Y., E. R. Vivoni, R. L. Bras, and D. Entekhabi (2004), Catchment hydrologic response with a fully distributed triangulated irregular network model, *Water Resour. Res.*, 40, W11102, doi:10.1029/2004WR003218

Kite, G. W., and N. Kouwen (1992), Watershed Modelling Using Land Classifications, Water Resour. Res., 28(12), 3193–3200

Leavesley, G. H., R. W Lichty, B. M. Troutman and L. G. Saindon (1983) Precipitation-Runoff Modeling System: User's Manual, 207 pp., USGS Water Resources Investigations Report 83-4238

Liang, X., D.P. Lettenmaier, E.F. Wood, and S.J. Burges. 1994. A Simple Hydrologically Based Model of Land-Surface Water and Energy Fluxes for General-Circulation Models. Journal of Geophysical Research-Atmospheres 99:14415-14428.

Myshkis, A.D. (1994) *The elements of mathematical models theory*. Nauka, Moscow.

Pomeroy, J., Hedstrom, N., Parviainen, J. (1998) The Snow Mass Balance of Wolf Creek, Yukon: Effects of Snow Sublimation and Redistribution. Proceedings of Wolf Creek Research Basin Planning Workshop, Whitehorse, March 1998.

Seguin, M.-K., Stein, J., Nilo, O., Jalbert, Ch. and Yan Ding (1998) Hydrogeophysical Investigation of the Wolf Creek Watershed, Yukon Territory, Canada. Proceedings of Wolf Creek Research Basin Planning Workshop, Whitehorse, March 1998.

Vinogradov, Yu. B. (2003a) River Runoff Modelling. In Hydrological Cycle, edited by I.A. Shiklomanov, in Encyclopedia of Life Support Systems (EOLSS), Developed under the auspices of the UNESCO, Eolss Publishers, Oxford, UK, [http://www.eolss.net]

Vinogradov, Yu. B. (2003b) Runoff Generation and Storage in Watershed. In Hydrological Cycle, edited by I.A. Shiklomanov, in Encyclopedia of Life Support Systems (EOLSS), Developed under the auspices of the UNESCO, Eolss Publishers, Oxford, UK, [http://www.eolss.net]

Vinogradov, Yu. B. (2003c) Hydrology of Sloping Terrain. In Hydrological Cycle, edited by I.A. Shiklomanov, in Encyclopedia of Life Support Systems (EOLSS), Developed under the auspices of the UNESCO, Eolss Publishers, Oxford, UK, [http://www.eolss.net]

Vinogradov, Yu. B. (2003d) Surface Water Runoff. In Hydrological Cycle, edited by I.A. Shiklomanov, in Encyclopedia of Life Support Systems (EOLSS), Developed under the auspices of the UNESCO, Eolss Publishers, Oxford, UK, [http://www.eolss.net]

Vinogradov, Yu. B. & Vinogradova, T. A. (2010) Mathematical modelling in hydrology. Academia publishers, Moscow (in Russian, in press).

5.0 Conclusions

Test simulations of runoff processes using CRHM and Hydrograph for Wolf Creek Research Basin was undertaken using data archives that had been assembled and cleaned up in a related project by the University of Saskatchewan. The test simulations are a demonstration of model capabilities and a way to gain familiarity with the basin, its characteristics and data and to better compare model features. Both CRHM and Hydrograph were set up on Wolf Creek involving forest, alpine and shrub tundra hydrology zones; CRHM was also set up for the Granger Sub-basin of Wolf Creek to test the alpine and shrub tundra hydrology representations in detail. CRHM was run without parameter calibration and was able to reproduce the basic patterns of snow accumulation, melt and runoff with reasonable water balance reproduction in all environments. This was the first complete physically-based simulation of a cold regions water cycle (blowing snow, intercepted snow, melt, infiltration to frozen soils, runoff) conducted in the Yukon. With calibration the CRHM runs could be further improved and with more basin information the routing aspects can be run using physical characteristics of the basin. Hydrograph was set up with some manual parameter calibration from streamflow where parameters were relatively unknown. This was the first application of Hydrograph to the Canadian North and certain similarities were noticed between Yukon and east Siberian hydrology. The sub-surface hydrology presented a formidable unknown in parameterising the model. Hydrograph performed well in initial simulations of the basin hydrograph for multi-year runs. Several issues with observational data quality created substantial uncertainty in evaluating the model runs.

The results presented in this report should be considered to be preliminary, given the incompleteness of the data required to run the model with directly observable parameters. Both modelling groups will continue to refine the information to take advantage of the best characteristics of the CRHM and Hydrograph models, namely their ability to use parameters that are obtained directly from field observations. The next steps in this project are to use the models in a complementary manner for process representation, parameter estimation and routing so that hydrological modelling can be developed and improved for the Upper Yukon Basin. It is essential that this research be supported to develop over a longer term than this short scoping study, so that the benefits of collaboration between the Canadian and Russian groups with Wolf Creek as the nexus, can be fully realised into a suite of improved cold regions hydrological models that can be run with confidence over large and small basins in the North.

6.0 References Describing Wolf Creek Hydrology

Applied Ecosystems Management. 2000. A users guide to Wolf Creek Terrain mapping. Report carried out for DIAND Water Resources, Whitehorse, YT., 6 pp.

Beatty, K. n.d. The Spatial Distribution of Permafrost in Wolf Creek Basin. B.Sc. Honors Essay, University of Saskatchewan, Saskatoon, Saskatchewan, 21 p.

Bewley, D., J.W. Pomeroy and R.L.H. Essery, 2007. Solar radiation transfer through a sub-arctic shrub canopy. *Arctic, Antarctic and Alpine Research*, 39(3), 365-374.

Bewley, D., J.W. Pomeroy and R. Essery, 2005. Processes of solar radiation transfer through a sub-arctic shrub canopy. *Proceedings of the Eastern Snow Conference*, 62. 109-128.

Boucher JL, Carey SK. 2009. The hydrometric and hydrochemical role of channel icing (aufeis) on streamflow in a subarctic, subalpine watershed. In Proceedings of the 17th International Research Basins Symposium and Workshop, Iqualuit-Pangnirtung-Kuujjuaq, August 2009, 35-46.

Carey S.K. and M.-K. Woo, 1998. Snowmelt hydrology of two subarctic slopes, southern Yukon, Canada. Nordic Hydrology, 29, 331-346.

Carey, S.K and Woo M.K, 1999. Hydrology of two slopes in subarctic Yukon, Canada. Hydrological Processes, 13, 2549-2562.

Carey, S.K. and M.-K. Woo. 2000. The role of soil pipes as a slope runoff mechanism, subarctic, Yukon, Canada. Journal of Hydrology, 233, 206-202.

Carey, S.K. and M.-K. Woo. 2000. Within slope variability of ground heat flux, subarctic Yukon. Physical Geography, 21 (5) 407-417.

Carey, S.K. and M.-K. Woo. 2000. Slope runoff processes and flow generation in a subarctic, subaline catchment. Submitted Journal of Hydrology

Carey, S.K. and Woo, M.K. 2001. Spatial variability of hillslope water balance, Wolf Creek basin, subarctic Yukon. Hydrological Processes, 15, 3113-3132.

Carey, SK. 2003. Dissolved organic carbon fluxes in a discontinuous permafrost subarctic alpine catchment. Permafrost and Periglacial processes, 14, 161-171.

Carey SK, Quinton, WL. 2004. Evaluating snowmelt runoff generation in a discontinuous permafrost catchment using stable isotope, hydrochemical and hydrometric data. Nordic Hydrology, 35: 309-324.

Carey SK, Quinton WL. 2005. Evaluation of runoff generation during summer using hydrometric, stable isotope and hydrochemical methods in a discontinuous permafrost environment. Hydrological Processes, 19: 95-114

Carey SK, Woo MK. 2005. Freezing of subarctic hillslopes, Wolf Creek Basin, Yukon. Arctic, Antarctic and Alpine Research, 37: 1-10.

Carey SK, Quinton WL, Goeller NT. 2007. Field and laboratory estimates of pore size properties and hydraulic characteristics for subarctic organic soils. Hydrological Processes, 21, 2560-2571.

Carey SK, Debeer CM. 2008. Rainfall-runoff hydrograph characteristics in a discontinuous permafrost watershed and their relation to ground thaw. In: Proceedings, Ninth International Conference on Permafrost, Fairbanks, Alaska, 233-238

Carey SK, Boucher JL, Duarte CM. 2009. A multi-year perspective on snowmelt runoff generation in an alpine watershed catchment. In Proceedings of the 17th International

Research Basins Symposium and Workshop, Iqualuit-Pangnirtung-Kuujjuaq, August 2009, 77-87.

Coultish, T. and Lewkowicz, A.G. 20xx, An investigation of palsas and frost mounds in Wolf Creek, Yukon Territory.

Dornes, P.F., Pomeroy, J.W., Pietroniro, A., Carey, S.K., and W. L. Quinton. 2008. Influence of landscape aggregation in modelling snow-cover ablation and snowmelt runoff in a sub-arctic mountainous environment. *Hydrological Sciences Journal*, 53(4), 725-740.

Dornes, P.F, Pomeroy, J.W., Pietroniro, A. and D.L. Verseghy. 2008. Effects of spatial aggregation of initial conditions and forcing data on modelling snowmelt using a land surface scheme. *Journal of Hydrometeorology*, 9, 789-803.

Dornes, P.F., Tolson, B.A., Davison, B., Pietroniro, A., Pomeroy, J.W., and P. Marsh. 2008. Regionalisation of land surface hydrological model parameters in subarctic and arctic environments. *Physics and Chemistry of the Earth*. Doi 10.1016/j/pce.2008.07.007.

Eamer, J. and D. van de Wetering. 1999. Monitoring forest biodiversity at Wolf Creek. In Wolf Creek Research Basin – Hydrology, Ecology, Environment – Proceedings of a workshop held in Whitehorse, Yukon, March 5 – 7, 1998, NHRI publication 37-121/1999E, Saskatoon, Saskatchewan, pp 101-108.

Ednie, M. and A. Lewkowicz. 2002. Preliminary evaluation of the basal temperature of snow method to map discontinuous mountain permafrost, Wolf Creek, Yukon Territory. Presented at the Annual Meeting of the Canadian Association of Geographers - Ontario Division. University of Western Ontario, London, Ontario. October 25-26, 2002. (abstract only).

Ednie, M. 2003. Evaluation of the basal temperature of snow (BTS) method to map permafrost in complex mountainous terrain, Wolf Creek, Y.T. MSc Thesis, University of Ottawa, Ottawa, ON.

Essery, R.L.H. and J.W. Pomeroy. 2004. Implications of spatial distributions of snow mass and melt rate on snowcover depletion: theoretical considerations. *Annals of Glaciology*, 38, 261-265.

Essery, R.L.H., R.J. Granger and J.W. Pomeroy. 2006. Boundary layer growth and advection of heat over snow and soil patches: modelling and parameterization. *Hydrological Processes*, 20, 953-967.

Francis, S., S. Smith and R. Janowicz. 1999. Data integration and ecological zonation of Wolf Creek watershed. In Wolf Creek Research Basin – Hydrology, Ecology, Environment – Proceedings of a workshop held in Whitehorse, Yukon, March 5 – 7, 1998, NHRI publication 37-121/1999E, Saskatoon, Saskatchewan, pp 93-100.

Gartner Lee Limited. 2001a. Upper Yukon River 2000 Surface and Groundwater Inventory Project. Part 2: Wolf Creek and Pineridge Water Well Database Pilot Project. Report prepared for Indian and Northern Affairs Canada, Government of Yukon, and City of Whitehorse. Whitehorse, YT.

Gartner Lee Limited. 2001b. Upper Yukon River 2000 Surface and Groundwater Inventory Project. Part 3: Wolf Creek and Pineridge Subdivisions Groundwater Usage Study. Report prepared for Indian and Northern Affairs Canada, Government of Yukon, and City of Whitehorse. Whitehorse, YT.

Gartner Lee Limited. 2003. Long term monitoring well no. 1 – Wolf Creek Subdivision. Prepared for Indian and Northern Affairs Canada. Whitehorse.

Giesbrecht, M.A and Woo, M.K. 2000. Simulation of snowmelt in a subsrctic spruce woodland:2. Open woodland model. Water Resources Research, 36(8*: 2287-2295.

Granger, R.J**.,** J.W. Pomeroy, N. Bussières and R. Janowicz. 1998. Parameterization of evapotranspiration using remotely-sensed data. In, (ed G. Strong) *Proceedings of the 3rd Scientific Workshop for the Mackenzie GEWEX Study [MAGS]*. Environment Canada, Saskatoon. p69-72.

Granger, R.J. 1999. Partitioning of energy during the snow-free season in the Wolf Creek research basin. In Wolf Creek Research Basin – Hydrology, Ecology, Environment – Proceedings of a workshop held in Whitehorse, Yukon, March 5 – 7, 1998, NHRI publication 37-121/1999E, Saskatoon, Saskatchewan, 33-44.

Granger, R.J., J.W. Pomeroy, N. Bussières and R. Janowicz. 2001. Parameterization of Evapotranspiration using Remotely-sensed data. In: The Mackenzie GEWEX Study (MAGS) Phase 1 Final Reports and Proceedings, 6th Scientific workshop (G.S. Strong, ed.) p120-129.

Granger, R.J., J.W. Pomeroy and J. Parviainen. 2002. Boundary-layer integration approach to advection of sensible heat to a patchy snow cover. Hydrological Processes, 16, 3559-3569.

Granger, R.J., J.W. Pomeroy and R.L.H Essery. 2006. Boundary layer growth over snow and soil patches. *Hydrological Processes*. 20, 943-951.

Gray, D.M., B.Toth, L. Zhao, J.W. Pomeroy and R.J. Granger. 2001. A deterministic approach of modeling and scaling frozen soil infiltration during snow ablation. Hydrological Processes, 15, 3095-3111.

Hamilton, A.S., D.G. Hutchinson and R.D. Moore. 2001. Estimation of winter streamflow using a conceptual hydrological model: a case study, Wolf Creek, Yukon Territory. Proceedings of the 11th Workshop on River Ice, May 14 – 16, 2001, Ottawa, ON.

Hedstrom, N.R. and J.W. Pomeroy. 1998. Measurements and modelling of snow interception in the boreal forest. Hydrological Processes, 12, 1611-1625.

Hedstrom, N.R., R.J. Granger, D.K. Bayne and R. Janowicz. 2002. 'Wolf Creek Data Index Report'. Technical Report' NHRI Contribution Series No. AEI-TN-02-001.

Indian and Northern Affairs Canada. 1993. Wolf Creek Research Basin, Yukon. Whitehorse, YT. Cat. No. R71-51/1993E, 10p.

Indian and Northern Affairs Canada. 1995. Wolf Creek Research Basin, Yukon. Whitehorse, YT. Cat. No. R71-51/1995E, 10p.

Janowicz, J.R., J.W. Pomeroy and R.J. Granger. 1995. A preliminary water balance for a small subarctic mountainous basin. Presented at the Canadian Geophysical Union 21st scientific meeting, Banff, Alberta, May 22 – 26, 1995.

Janowicz, J.R., D.M. Gray and J.W. Pomeroy. 1996. Snowmelt and runoff in a subarctic mountain basin. Proceedings of the Hydro-ecology Workshop on the Arctic Environmental Strategy, Canadian Geophysical Union – Hydrology Section Annual Meeting, Banff, Alberta, May 5 – 10, 1996., NHRI Symposium No. 16., Saskatoon, Saskatchewan, 303 – 320.

Janowicz, J.R. 1997. Wolf Creek Research Basin: A Move Towards Integration. Proceedings of the Northern Research Basins Eleventh International Symposium &

Workshop, Prudhoe Bay to Fairbanks, Alaska, USA, August 18 – 22, 1997. Volume II. Published by The Water and Environmental Research Center, University of Alaska, Fairbanks, Alaska.

Janowicz, J.R., D.M. Gray and J.W. Pomeroy. 1997. Snowmelt and runoff in a subarctic mountain basin. Proceedings of the Hydro-ecology Workshop on the Arctic Environmental Strategy Action on Water, Banff, May, 1996.

Janowicz, J.R. 1999. Wolf Creek Research Basin – an overview. In Wolf Creek Research Basin: Hydrology, Ecology, Environment, Proceedings of a Workshop held in Whitehorse, Yukon, March 5-7, 1998 p121-130.

Janowicz, J.R. 2000. Spatial variability of snowmelt infiltration to frozen soil within the Yukon boreal forest. Proceedings AWRA Conference Water Resources in Extreme Environments, Anchorage, Alaska, May 1-3, 2000. Edited by D.L. Kane, 121-127.

Janowicz, J.R., D.M. Gray and J.W. Pomeroy. 2002. Characterisation of snowmelt infiltration scaling parameters within a mountainous subarctic watershed. Proceedings of 59th Eastern Snow Conference, Stowe, Vermont, June 5-7, 2002. Edited by J. Hardy and S. Frankenstein. p67-81.

Janowicz, R.J, Gray, D.M. and J.W. Pomeroy. 2003. Spatial variability of fall soil moisture and spring snow water equivalent within a mountainous sub-arctic watershed. *Proceedings of the Eastern Snow Conference*, 60. 127-139.

Janowicz JR, Hedstrom N, Pomeroy J, Granger R, Carey SK. 2004. Wolf Creek Research Basin water balance studies. In: Northern Research Basins Water Balance, King DL, Yang D (Eds), IAHS publ. 290, 195-204.

Janowicz, J.R., Hedstrom, N., Pomeroy, J.W., Granger, R., and S.K. Carey 2004. Wolf Creek Research Basin water balance studies. In, (eds Kane, D.L. and D. Yang) *Northern Research Basins Water Balance*, IAHS Publ. No. 290, IAHS Press, Wallingford. 195-204.

Janowicz, J.R., N. Hedstrom, J. Pomeroy, R. Granger and S. Carey. 2004. Wolf Creek Research Basin water balance studies. Northern Research Basins Water Balance, IAHS Publication 290, edited by Douglas L. Kane and Daqing Yang. 195-204

Janowicz, J.R., N. Hedstrom, J. Pomeroy, R. Granger and S. Carey. 2004. Wolf Creek Research Basin – cold region studies 1992 – 2004, Poster prepared for American Geophysical Union Fall Meeting, San Francisco, December, 2004.

Janowicz, J.R. 2004. Wolf Creek Research Basin Study – water balance and related studies – 1992-2004, prepared for Northern Research Basin Water Balance Workshop, Victoria, B.C., March 15 – 19, 2004.

Jasek, M. and G. Ford. 1999. Coal Lake outlet freeze-up, containment of winter inflows and estimates of related outburst flood. In Wolf Creek Research Basin – Hydrology, Ecology, Environment – Proceedings of a workshop held in Whitehorse, Yukon, March 5 – 7, 1998, NHRI publication 37-121/1999E, Saskatoon, Saskatchewan, pp 89.

Johnstone, J. and J. Eamer. 1999. Tools for measuring biodiversity and ecosystem change in the Wolf Creek watershed. In Wolf Creek Research Basin – Hydrology, Ecology, Environment – Proceedings of a workshop held in Whitehorse, Yukon, March 5 – 7, 1998, NHRI publication 37-121/1999E, Saskatoon, Saskatchewan, pp105-120.

Jones, H.G. and J.W. Pomeroy. 1999. The ecology of snow and snow-covered systems:

summary and relevance to Wolf Creek. Wolf Creek Research Basin – Hydrology, Ecology, Environment – Proceedings of a workshop held in Whitehorse, Yukon, March 5 – 7, 1998, NHRI publication 37-121/1999E, Saskatoon, Saskatchewan, pp 1-13.

Kinar, N.J. and J.W. Pomeroy. 2008. Determining snow water equivalent by acoustic sounding. *Hydrological Processes*, 21, 2623-2640.

Kinar, N. and J.W. Pomeroy 2009. Automated determination of snow water equivalent by acoustic reflectometry. *Institute of Electrical and Electronic Engineering, Transactions on Geoscience and Remote Sensing*, in press.

Kinar, N. and J.W. Pomeroy 2009. Operational techniques for determining SWE by sound propagation through snow: I. General theory. *Proceedings of the Eastern Snow Conference,* 65, in press.

Kotoll, R.S. 1999. Subarctic Soils in Yukon Territory, Northwest Canada B Pedological Studies on Their Types, Weathering Intensity Relief and Aspect Dependency. Diploma Thesis, Philipps-Universtät Marburg, Fachbereich Geographie, 69 p.

Lacroix, M, 1995. Wolf Creek precipitation analysis, University of Victoria, Department of Geography Co-op Work Term Report, Spring, 1995, 24 p.

Lacroix, M. and L.W. Martz. 1998. Assessing the impact of varying sub-basin scale on hydrological model response. Abstract Volume, Carrefour in Earth Sciences: A Joint Meeting of Geological Association of Canada, Mineralogical Association of Canada, Association Professionnelle des Géologues et Géophysiciens du Québec, International Association of Hydrologists, Canadian Geophysical Union, May 18-20, 1998, Québec City, Québec, pp. A-99.

Lacroix, M. and L. W. Martz. 1999. The application of digital terrain analysis modeling techniques for the parameterization of a hydrological model in the Wolf Creek Research Basin. In Wolf Creek Research Basin – Hydrology, Ecology, Environment – Proceedings of a workshop held in Whitehorse, Yukon, March 5 – 7, 1998, NHRI publication 37-121/1999E, Saskatoon, Saskatchewan, pp 79-86.

Leenders, E.E. and M-K. Woo. 2002. Modeling a two-layer flow system at the subarctic, subalpine tree line during snowmelt. Water Resources Research, 38:10, 201-208.

MacDonald, M.K., Pomeroy, J.W. and A. Pietroniro. 2009. Parameterising
redistribution and sublimation of blowing snow for hydrological models: tests in a mountainous subarctic catchment. *Hydrological Processes*, OI:10.1002/hyp.7356.

Martz, L.W. 1998. Hydrologic characterization of the surface materials of Wolf Creek Basin. Abstracts, Wolf Creek Research Basin Planning Workshop, March 1998, Whitehorse, Yukon, 15 p.

Martz, L.W., Woo MK, Lacroix, M, Carey, Sk, Giesbrecht, MA, and Leenders, E. 2001. The spatial aspects of the hydrology of subarctic slopes in Wolf Creek Basin. MAGS: Final Reports and Proceedings, 6th Scientific Workshop for MAGS: 15-17 November, 2000, Saskatoon, SK.

McCartney SE, Carey SK, Pomeroy JW. 2006. Intra-basin variability of snowmelt water balance calculations in a Subarctic catchment. Hydrological Processes, 20: 1001-1016.

McCartney, S.E., S.K. Carey and J.W. Pomeroy. 2006. Intra-basin variability of snowmelt water balance calculations in a subarctic catchment. *Hydrological Processes*, 20, 1001-1016.

Palliath, R.U., Martz, L.W. and Woo, M.K. 2000. An evaluation of surface flow patterns across hydrological zone boundaries in Wolf Creek Basin. Presented at the Canadian Geophysical Union, Annual Scientific Meeting, May 23-27, 2000, Banaff, Alberta.

Petrone, R.M., L. Martz, M.-K. Woo, and S.K. Carey. 2000. Statistical Characteristics and Representation of Soil Moisture in a Subarctic Slope. Presented at the Canadian Geophysical Union, Annual Scientific Meeting, May 23-27, 2000, Banff, Alberta.

Pomeroy, J.W. and R.J. Granger. 1999. Wolf Creek Research Basin – Hydrology, Ecology, Environment – Proceedings of a workshop held in Whitehorse, Yukon, March 5 – 7, 1998, NHRI publication 37-121/1999E, Saskatoon, Saskatchewan.

Pomeroy, J.W., N.R. Hedstrom and J. Parviainen. 1999. The snow mass balance of Wolf Creek, Yukon: effects of snow sublimation and redistribution. In Wolf Creek Research Basin – Hydrology, Ecology, Environment – Proceedings of a workshop held in Whitehorse, Yukon, March 5 – 7, 1998, NHRI publication 37-121/1999E, Saskatoon, Saskatchewan, 15-29.

Pomeroy, J.W., D.M Gray, R.J. Granger, P. Marsh, N.R. Hedstrom, J.R. Janowicz, R. Essery and R. Harding. 2001. Biome-scale representation of snow cover development and ablation in boreal and tundra ecosystems. MAGS: Final Reports and Proceedings, 6th Scientific Workshop for MAGS: 15-17 November, 2000, Saskatoon, SK.

Pomeroy, J.W., D.M. Gray, N.R. Hedstrom and J.R. Janowicz. 2002. Prediction of seasonal snow accumulation in cold climate forests. Hydrological Processes, 16, 3543-3558.

Pomeroy, J.P., D.M. Gray, N.R. Hedstrom and R. Janowicz. 2002. 'Physically based estimation of seasonal snow accumulation in the boreal forest'. In: Proceedings of the 59th Annual Meeting Eastern Snow Conference, Stowe, Vermont, p93-117.

Pomeroy, J.P., D.M. Gray, N.R. Hedstrom and R. Janowicz. 2002. 'Physically based estimation of seasonal snow accumulation in the boreal forest'. In: Proceedings of the 59th Annual Meeting Eastern Snow Conference, Stowe, Vermont, p93-117.

Pomeroy, J.W., B. Toth, R.J. Granger, N.R. Hedstrom, and R.L.H. Essery. 2003. variation in surface energetics during snowmelt in a subarctic mountain catchment. Journal of Hydrometeorology, 4, 702-719.

Pomeroy, J.W., D.S. Bewley, R.L.H. Essery, N.R. Hedstrom, T. Link, R.J. Granger, J.E. Sicart, C.R. Ellis, J.R. Janowicz. 2006. Shrub Tundra Snowmelt. Hydrological Processes. 20(4): 923-941 DOI: 10.1002/hyp.6124

Pomeroy, J.W., R.J. Granger, N.R. Hedstrom, D.M. Gray, J. Elliott, A. Pietroniro, and J.R. Janowicz. 2005. The process hydrology approach to improving prediction of ungauged basins in Canada. IN: Prediction in Ungauged Basins: approaches for Canada's Cold Regions (CWRA the Yellowknife workshop March, 2004.) p67-99.

Pomeroy, J., R. Essery, N. Hedstrom, R. Janowicz, R. Granger. 2005. Snowmelt Hydrometeorology over a High Latitude Mountain Catchment .(in press) submitted to IAHS redbook series

Pomeroy, J.W., D.S. Bewley, R.L.H. Essery, N.R. Hedstrom, R.J. Granger, J.E. Sicart, T. Link, C.R. Ellis, J.R. Janowicz and D. Marks. 2005. Shrub Tundra Snowmelt. Poster presentation to the AGU meeting, Dec. 2005.

Pomeroy, J., R. Granger, N. Hedstrom, J. Elliot, A. Pietroniro, R. Janowicz and D. Gray. 2004. The process hydrology approach to designing instrumented research basins in western Canada. Proceeding of International Instrumented Watershed Symposium, Edmonton, June 2004. Centre for Hydrology Report No. 1, University of Saskatchewan, Saskatoon.

Pomeroy, J.P., D.M. Gray, N.R. Hedstrom and R. Janowicz. 2002. 'Prediction of seasonal snow accumulation in cold climate forests', *Hydrological Processes*, 16 (18), p3543-3558.

Pomeroy, J.W., D.M. Gray, R.J. Granger, P. Marsh, N. Hedstrom, R. Janowicz, R.S.L. Essery and R. Harding, 2001. Biome-scale representation of snow cover development and ablation in boreal and tundra ecosystems. In: The Mackenzie GEWEX Study (MAGS) Phase 1 Final Reports and Proceedings, 6th Scientific workshop (G.S. Strong, ed.) p70-80.

Pomeroy JW, Gray DM, Brown T, Hedstrom NR, Quinton WL, Granger RJ, Carey SK. 2007. The cold regions hydrological model, a platform for basing process representation and model structure on physical evidence. Hydrological Processes, 21, 2650-2667.

Pomeroy, J.W., B. Toth, R.J. Granger, N.R. Hedstrom, R.L.H Essery, 2003. Variation in surface energetics during snowmelt in complex terrain. *Journal of Hydrometeorology*, 4(4), 702-716.

Pomeroy, J.W., Gray, D.M. and P. Marsh. 2008. Studies on snow redistribution by wind and forest, snow-covered area depletion and frozen soil infiltration. In, (ed. M-K Woo) *Cold Region Atmospheric and Hydrologic Studies, the Mackenzie GEWEX Experience, Vol. 2: Hydrologic Processes.* Springer-Verlag, Berlin, Germany. 81-96.

Pomeroy, J.W. 2007. Cold regions hydrology, snow and PUB. In, *Predictions in Ungauged Basins: PUB Kick-off*. IAHS Publ. No. 309. IAHS Press, Wallingford, UK. 85-91.

Pomeroy, J.W. R. J. Granger, N. R. Hedstrom, D. M. Gray, J. Elliott, A. Pietroniro and J. R Janowicz. 2005. The process hydrology approach to improving prediction to ungauged basins in Canada. In, (eds. C. Spence, J. Pomeroy and A. Pietroniro) *Prediction in Ungauged Basins, Approaches for Canada's Cold Regions*. Canadian Water Resources Association, Cambridge, 67-95.

Pomeroy, J.W., Rowlands, A. Hardy, J., Link, T., Marks, D., Essery, R., Sicart, J-E., and C. Ellis. 2008. Spatial Variability of Shortwave Irradiance for Snowmelt in Forests. Journal of Hydrometeorology, 9(6), 1482-1490.

Pomeroy, J.W., Gray, DM, Brown, T., Hedstrom, N.H., Quinton, W.L., Granger, R.J. and S.K. Carey. 2007. The cold regions hydrological model: a platform for basing process representation and model structure on physical evidence. *Hydrological Processes*, 21, 2650-2667.

Pomeroy, J.W., D.S. Bewley, R.L.H. Essery, N.R. Hedstrom, T. Link, R.J. Granger, J.E. Sicart, C.R. Ellis, and J.R. Janowicz. 2006. Shrub tundra snowmelt. *Hydrological Processes*, 20, 923-941.

Pomeroy, J.W., R.L.H. Essery and B. Toth. 2004. Implications of spatial distributions of snow mass and melt rate on snow-cover depletion: observations in a subarctic mountain catchment. *Annals of Glaciology*, 38, 195-201.

Quick, M.C., A. Loukas and E. Yu. 1999. Calculating the runoff response of the Wolf Creek watershed. In Wolf Creek Research Basin – Hydrology, Ecology, Environment – Proceedings of a workshop held in Whitehorse, Yukon, March 5 – 7, 1998, NHRI publication 37-121/1999E, Saskatoon, Saskatchewan, pp 91.

Quilty, E.J. and Whitfield, P.H. 2001. Assessing continuous water quality data from Wolf Creek, Yukon Territory. Proceedings Canadian Water Resoucres Association British Columbia Branch 2001 Conference, 11-19.

Quinton, W.L., T. Shirazi, S.K. Carey and J.W. Pomeroy, 2005. Soil water storage and active layer development in a sub-alpine tundra hillslope, southern Yukon Territory, Canada. *Permafrost and Periglacial Processes*, 16, 269-382.

Quinton WL, Bemrose RK, Zhang Y, Carey SK. 2009. The influence of spatial variability in snowmelt and active layer thaw on hillslope drainage for an alpine tundra hillslope. Hydrological Processes. 23, 2628-2639DOI: 10.1002/hyp 7327.

Quinton WL, Hayashi M, Carey SK. 2008. Peat hydraulic conductivity in cold regions and its relation to pore size and geometry. Hydrological Processes, 22, 2829-2837.

Quinton WL, Sharizi T, Carey SK, Pomeroy JW. 2005. Soil Water Storage and active layer development in a subalpine tundra hillslope, southern Yukon Territory, Canada. Permafrost and Periglacial Processes, 16: 369-382.

Quinton WL, Carey SK, Goeller NT. 2004. Snowmelt runoff from northern alpine tundra hillslopes: major processes and methods of simulation. Hydrology and Earth System Sciences, 8: 877-890.

Rouse, W.R., E.M. Blyth, R.W. Crawford, J.R. Gyakum, J.R. Janowicz, B. Kochtubajda, H.G. Leighton, P.Marsh, L.Martz, A. Pietroniro, R. Ritchie, W.M. Schertzer, E.D. Soulis, R.E. Stewart, G.S. Strong, and M.K. Woo. 2003. Energy and water cycles in a high-latitude, north-flowing river system – summary of results from the Mackenzie GEWEX study – phase 1. American Meteorological Society, January, 2003, p73-87.

Seguin, M. 1998. Regolith Profiles and Permafrost Distribution of the Wolf Creek Watershed, Yukon Territory, Canada. Presented at the Institut National de la Recherche Scientifique, INRS-EAU. Québec.

Seguin, M-K., J. Stein, O. Nilo, C. Jalbert and Y. Ding. 1999. Hydrogeophysical investigation of the Wolf Creek watershed, Yukon Territory, Canada. In Wolf Creek Research Basin – Hydrology, Ecology, Environment – Proceedings of a workshop held in Whitehorse, Yukon, March 5 – 7, 1998, NHRI publication 37-121/1999E, Saskatoon, Saskatchewan, pp 55-78.

Shirazi, T., Allen, D., Quinton, W., and J.W. Pomeroy 2009. Estimating soil thaw energy in sub-Alpine tundra at the hillslope scale, Wolf Creek, Yukon Territory, Canada. *Hydrology Research*, 40.1, 1-18.

Sicart, J-E, J.W. Pomeroy, R.L.H. Essery and D. Bewley. 2006. Incoming longwave radiation to melting snow: observations, sensitivity and estimation in northern environments. *Hydrological Processes*, 20, 3697-3708.

Sicart, J.E., Pomeroy, J.W., Essery, R.L.H., Hardy, J.E., Link T. and D. Marks 2004. A sensitivity study of daytime net radiation during snowmelt to forest canopy and atmospheric conditions. *Journal of Hydrometeorology*, 5. 774-784.

Sicart, J.E., J.W. Pomeroy, R.L.H. Essery, and J.Hardy. 2003. Snowmelt in a Canadain spruce forest: a sensitivity study to the canopy cover. Proccedings of the 60th Eastern Snow Conference, June 4 – 6, 2003, Sherbrooke, PQ, 99-110.

Sicart, J.E., Pomeroy, J.W., Essery, R.L.H. and J. Hardy. 2003. Snowmelt in a Canadian spruce forest: a sensitivity study to canopy cover. *Proceedings of the Eastern Snow Conference*, 60. 99-110.

Spence, C., Pomeroy, J.W. and A. Pietroniro. 2005. *Prediction in Ungauged Basins, Approaches for Canada's Cold Regions*. Canadian Water Resources Association, Cambridge, Ontario. 218 p.

Stein, J. and Martz, L.W. 1997. Physical hydrological modelling approaches for the Wolf Creek Research Basin. Procs. 2nd Scientific Workshop for the Mackenzie GEWEX Study (MAGS), 23-26 March, 1997.

Woo, M-K. and S.K. Carey. 1999. Permafrost, seasonal frost and slope hydrology, central Wolf Creek basin, Yukon. In Wolf Creek Research Basin – Hydrology, Ecology, Environment – Proceedings of a workshop held in Whitehorse, Yukon, March 5 – 7, 1998, NHRI publication 37-121/1999E, Saskatoon, Saskatchewan, pp 45-54.

Woo, M-K., L.W. Martz, S.K. Carey, M.A. Giesbrecht, E. Leenders and M. Lacroix. 2001. Effects of frost and organic soils on the hydrology of subarctic slopes. MAGS: Final Reports and Proceedings, 6th Scientific Workshop for MAGS: 15-17 November, 2000, Saskatoon, SK.

Woo, M-K. and M.A. Geisbrecht. 2000. Simulation of snowmelt in a subarctic, spruce woodland: Scale considerations. Nordic Hydrology, 31, 301-316.

Woo, M-K. and M.A. Geisbrecht. 2000. Simulation of snowmelt in a subarctic, spruce woodland: 1. Tree model. Water Resources Research, 36(8): 2275-2285.

Zhang Y, Carey SK, Quinton WL, Janowicz JR, Flerchinger GN. 2009. Comparison of algorithms and parameterizations for infiltration into organic-covered permafrost soils. Hydrological and Earth System Science - Discussions, 6, 5705-5752.

Zhang Y, Carey SK, Quinton WL. 2008. Evaluation of the algorithms and parameterizations for ground thawing and freezing simulation in permafrost regions. Journal of Geophysical Research - Atmospheres, 113, D17116, doi:10.1029/2007JD009343.